1971

Application of Remote Sensing Techniques to Monitoring Soil Moisture

Hal D. Werner

APPLICATION OF REMOTE SENSING TECHNIQUES TO MONITORING SOIL MOISTURE

BY

HAL DAVID WERNER

A thesis submitted
in partial fulfillment of the requirements for the
degree Master of Science, Major in
Agricultural Engineering, South Dakota
State University

1971

APPLICATION OF REMOTE SENSING TECHNIQUES

TO MONITORING SOIL MOISTURE

This thesis is approved as a creditable and independent investigation by a candidate for the degree, Master of Science, and is acceptable as meeting the thesis requirements for this degree, but without implying that the conclusions reached by the candidate are necessarily the conclusions of the major department.

Victor L. Myers — May 14, 1971

Thesis Advisor — Date

Dennis L. Moe — May 14, 1971

Head, Agricultural Engineering Department — Date

ABSTRACT

Application of Remote Sensing Techniques

To Monitoring Soil Moisture

Hal David Werner

B.S., South Dakota State University

During the 1970 growing season, research was conducted to investigate the relationship between remote sensing imagery and soil moisture. Extensive aerial and ground truth data were collected and studied in order to evaluate the moisture supply and water use. The three hectare study site, located on the South Dakota State University James Valley Research and Extension Center, contained irrigated and non-irrigated sorghum and two fallow treatments. Results indicate that remote sensing is a feasible method for monitoring available soil moisture.

Thirteen aerial missions were conducted between June 17 and October 5 at altitudes between 305 meters (1,000 feet) above ground level and 1525 meters (5,000 feet) above ground level. Photography was collected each flight with color reversal infrared film and three black and white films filtered for the green, red, and near infrared bands of the spectrum. A thermal infrared scanner and a precision radiation thermometer recorded earth-emitted radiation and temperature anomalies. Solameters measured both incoming and outgoing radiation.

Imagery analyses were performed by three methods: (1) visual interpretation, (2) use of a closed circuit television color

encoding system specifically designed for imagery interpretation and overall film density analysis, and (3) film density measurements. Film densities were corrected to account for seasonal changes in incoming radiation, amount of plant canopy, and reflectances of the crop and soil. Final analysis was accomplished by correlation of the soil moisture data with the film densities and corrected film densities.

The results revealed that the soil-plant system viewed by the sensors provided information on the different soil moisture treatments. While the soil itself seemed to indicate only surface soil moisture, the crop related the available moisture conditions of the soil profile. Of the three reflected radiation bands, the red band provided the best results for determination of soil moisture; the green band gave reasonable results throughout most of the season; and near infrared photography did not provide helpful indications of available soil moisture.

ACKNOWLEDGMENTS

It is hardly possible in this short space to express appreciation to everyone who had a share in this investigation. The author is especially indebted to Dr. Fred A. Schmer for his guidance and assistance and for his unending encouragement during the research.

The author expresses sincere gratitude to Mr. Victor I. Myers, Director, and Dr. Frederick Waltz, Data Specialist, of the Remote Sensing Institute, and Dr. John L. Wiersma, Professor of Agricultural Engineering, for the technical assistance, suggestions, and encouragement which made possible the completion of this investigation.

Appreciation is extended to the other members of the Remote Sensing Institute and the Agricultural Engineering Department, and to Dr. Tamlin C. Olson and Dr. Maurice L. Horton, Associate Professors of Plant Science, for counsel during planning and conducting the research. The author is grateful to Larry Thompson for his help in collecting and processing the field data.

Sincere appreciation is acknowledged to Mrs. Lynda Schmer for typing the final manuscript. The author is indebted to his wife, LeAnn, for her patience and understanding, and for time spent in reviewing this manuscript.

Funds for this research were provided in part by the Remote Sensing Institute, South Dakota State University, and the United States Geological Survey, United States Department of the Interior, under contract Number 14-08-0001-12510.

HDW

TABLE OF CONTENTS

LIST OF FIGURES

FIGURE PAGE

FIGURE PAGE

FIGURE PAGE

LIST OF TABLES

Chapter I

INTRODUCTION

Conservation and management of earth resources is a problem today and promises to be a larger problem in the future. In the field of water resources for the United States alone, the estimated consumptive water use for the year 2000 is over 484 billion liters (128 billion gallons) daily. In the area of agriculture, the consumptive water supply needed daily will be nearly 340 billion liters (90 billion gallons) (28). The ever-changing and ever-increasing demands on the world's water resources have created the need for new methods of evaluation and management of water resources. Because of the very nature of remote sensing, it is feasible to apply its principles to agricultural and hydrologic management.

Remote sensing is a commonly used term in today's scientific terminology. Actually remote sensing is as old as man himself. From the very beginning, man has used his eyes as remote sensors. The principle of the camera obscura dates back to Aristotle (384-322 BC). This camera provided for development of photography where images could be retained for later use. Until the early 1800's remote detection of the environment was still limited to the human senses. Then in 1822 the first permanent photograph was obtained by Niepce (5). The photographic methods improved and developed throughout the years with Vogel obtaining the first color works in 1873 (5).

New methods of photography and of measuring radiation and temperature were discovered in the first half of this century. Possibly the most beneficial research achievements were the discovery of radar and infrared detection capabilities. Infrared photography was first used for military purposes. Interest in the infrared portion of the electromagnetic spectrum after World War II stimulated development of new equipment and techniques to aid in remote sensing research. Photographic equipment and films, scanner detectors, and temperature measuring instruments have been developed and are being continually improved at the present time.

Remote sensing research in agriculture and hydrology is in its infancy, and most of the research to date has allowed application only in limited cases. Monitoring of water resources should be possible in the future for extensive geographical areas. Hopefully, research will be able to provide basic remote sensing techniques to improve our environmental management ability.

Purposes and Objectives

The ability to evaluate soil moisture and to detect and relate soil moisture stress to crop production are of special concern to agriculture and hydrology. Based on the above need, the general objective of this research was to develop a method for estimating soil moisture by using remote sensing techniques. Specific objectives were:

1. To investigate the relationship between remote sensing imagery and soil moisture by detecting the crop and soil parameters; and
2. To determine the remote sensing measurements which are most valuable to soil moisture research by correlation between the aerial data and the existing conditions on the ground.

Chapter II

LITERATURE REVIEW

The basic principles of remote sensing, though used for many years, have just recently been expanded for use in resource evaluation and management. An area of widespread concern today is the application of remote sensing techniques to agriculture and hydrology. Increased present and future demands require the development of usable methods of evaluating resource capabilities. Water resources assessment and planning are needed to determine the allotment and distribution of the water supply. Of special concern to hydrology and agriculture is the monitoring of soil moisture. Knowledge of the soil moisture status over a large geographical region would provide information for forecasting agronomic production, managing water supplies and irrigation, managing cropland and rangeland, and predicting runoff after rainfalls (2, 17, 30).

Remote sensing is the measurement of some property of an object without physically contacting the object (22). Every object or body known to man possesses certain energy properties associated with the electromagnetic spectrum. Remote sensing detects or measures the radiation or energy properties of the electromagnetic spectrum. Figure 2.1 (a) shows most of the spectrum (4). Radioactive materials comprise the shortest wavelengths. These materials emit radioactive particles such as gamma rays and X-rays. Thermal emitted radiation, commonly recognized as heat and light, is predominant from the ultraviolet to microwaves. All bodies radiate heat as a result of

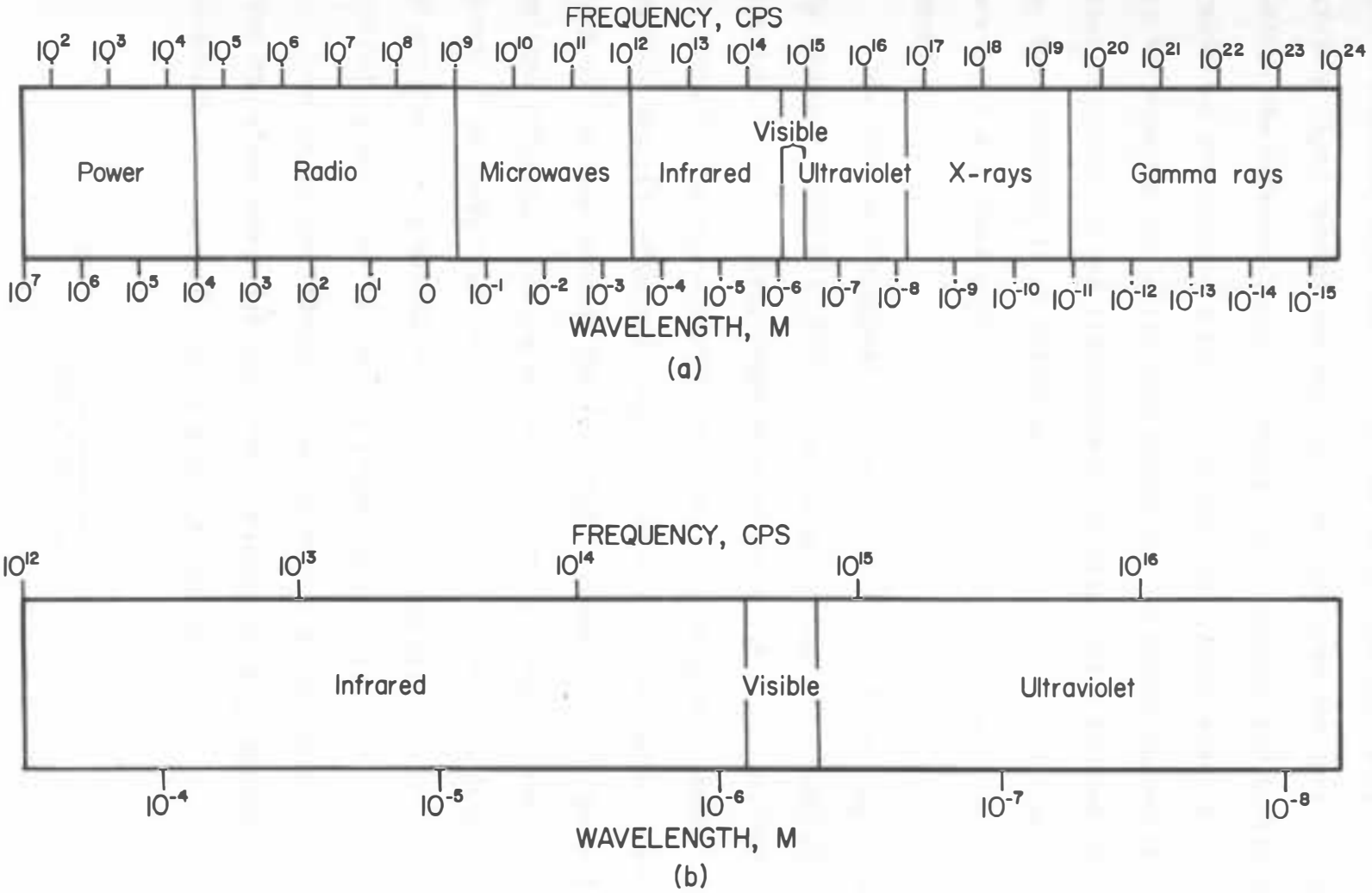

Figure 2.1 - (a) The electromagnetic spectrum; and (b) a portion of the electromagnetic spectrum commonly associated with remote sensing measurements in agriculture and hydrology (4).

their absolute temperature. Maximum solar radiance falls within the visible light region, and emitted radiation from the earth is greatest within the infrared spectral region (26). Emitted and reflected solar radiation are monitored by passive sensing systems where a passive system measures radiation from a source. An active system is one that provides its own illuminating radiation which is then sampled by the sensor as it is reflected back (22). The longest wavelengths are radio and power waves. Radar uses radio waves with an active sensing system.

The principal spectral region of concern to hydrology is shown in Figure 2.1 (b) (11, 18). This region includes the portion of the spectrum from the ultraviolet through the visible and the infrared. In the ultraviolet, visible, and near infrared bands, remote sensing usually detects reflected solar radiation from the earth's surface. Much of the remainder of the infrared is concerned with thermal emitted radiation from bodies on the earth's surface. For each specific wavelength within a spectral band, a body possesses values of emittance, transmittance, reflectance, and absorptance which completely describe the radiant properties of the body.

Wavelength and frequency characterize a given spectral value from the electromagnetic spectrum. Wavelength and frequency are inversely proportional (31) as given by the equation

$$1 \text{ cps} = \frac{1}{2.998 \times 10^{10} \text{ cm}}, \qquad 2.1$$

where

cps = cycles per second, and

cm = centimeters.

Wavelength is sometimes designated as the inverse of wave number. The measurement of wavelength can be expressed in a variety of terms (11) as shown by

$$1 \text{ m} = 10^2 \text{ cm} = 10^6 \ \mu\text{m} = 10^{10} \text{ A}, \qquad 2.2$$

where

m = meters,

cm = centimeters,

μm = micrometers, and

A = angstroms.

Application of the properties of spectral radiation involves the understanding of certain basic laws. The first important law is Kirchoff's Law which states that the emissive power divided by the absorptivity of a body in equilibrium with blackbody radiation is a universal constant (15). This constant is equal to the emissive power of a blackbody at the same temperature. For a blackbody (31)

$$\rho = \tau = 0, \qquad 2.3$$

and

$$\varepsilon = \alpha = 1, \qquad 2.4$$

where

ρ = reflectance,

τ = transmittance,

ε = emissivity or emissive power, and

α = absorptance.

Kirchoff's Law can also be stated for any body. The emissivity of that body at a particular temperature can be expressed as a fraction of the emissivity of a blackbody at the same temperature (23). For an opaque material or where τ is equal to zero (31),

$$\varepsilon = \alpha = 1 - \rho. \qquad 2.5$$

This equation can be applied to many radiation studies of the earth's surface.

Planck's Radiation Formula is the fundamental radiation law which describes the radiation emitted by a blackbody at a certain wavelength and absolute temperature. Sutton (26) gives this formula as

$$E(\lambda,T) = c_1\lambda^{-5}\,(e^{c_2/\lambda T} - 1)^{-1}\,, \qquad 2.6$$

where

E = energy,

λ = wavelength,

T = absolute temperature,

e = exponential function, and

c_1 and c_2 = constants.

Integration of Planck's Law over all wavelengths provides another very useful relationship known as the Stefan-Boltzmann Law for a blackbody (15), which is written as

$$E = \sigma T^4 , \qquad 2.7$$

where

E = energy,

T = absolute temperature, and

σ = Stefan-Boltzmann universal constant.

In the general case for a given body, the Stefan-Boltzmann Law (27) from equation 2.5 becomes

$$E = \varepsilon\sigma T^4. \qquad 2.8$$

A fourth helpful law in remote sensing endeavors is Wien's Displacement Law which approximates a value of the wavelength at which radiance from a body is maximum (31) by the equation

$$\lambda_{max} T = 2897.9. \qquad 2.9$$

The absolute temperature (T) of the body is measured in degrees Kelvin, and λ_{max} is expressed in micrometers.

The nature of reflected and emitted radiation dictates certain spectral band selections in remote sensing operations. Solar shortwave radiation is contained in the spectral region from 0.15μm to 4.0μm; therefore, reflected shortwave radiation from terrestrial surfaces would be restricted to that spectral region. Thermal emitted

radiation by virtue of absolute temperature of the earth would range between 3μm and 80μm (26). A limitation in band selection is encountered due to various atmospheric attenuations. Van Lopik, et. al., (27) and Holter (14) specify that there are essentially three types of attenuation. The first is due to water vapor, carbon dioxide, ozone, and other gases with absorption predominant above 1.3μm in the infrared. Atmospheric windows or regions of minimum absorption are present at 3.5μm to 5.5μm and 8μm to 13μm. Since all of these bands lie within the region of maximum emitted radiation from the earth's surface, each could be band selections for thermal detectors. A second important attenuation is Rayleigh scattering or scattering by air molecules. Rayleigh scattering occurs within the ultraviolet and blue portion of the visible band and, therefore, generally limits remote sensing to regions above 0.45μm. Within the atmospheric windows additional attenuation from atmospheric particles such as haze, smoke, dust, clouds, and fog are present.

The type of research determines the selection of smaller bands within either reflected or emitted radiation. Soil moisture investigations by remote sensing are feasible using both reflected and thermal radiation (20) where the principal methods of data collection are photography, television, and scanning devices (12, 14). Photography, using black and white and color film, measures reflected radiation within the visible and near infrared to about 1.0μm. In general, two types of color film are used. Conventional color film produces nearly the same image that the eye would perceive and has

three-layer sensitivity in the blue, green, and red portions of the visible spectrum. Color infrared film, or "false color" film, is not totally an infrared film as is commonly believed. The three formative layers are in the near infrared and in the green and red parts of the visible portion of the spectrum with sensitivity from 0.35μm to 0.9μm (12, 16). Black and white films used for remote sensing research are usually filtered for some specific spectral band such as blue, green, red, or near infrared (12).

Television systems do not provide the same high resolution as photographic methods (14). Their usefulness is found in space application because the electrical signals from television systems are more easily transmitted to earth than data from a processed photograph. A system of three filtered television cameras is currently planned for the National Aeronautics and Space Administration Earth Resources Technological Satellite (ERTS) program.

Optical mechanical scanners are common equipment in remote sensing. The principle used most often is the object plane scan where a line scan image of a surface is recorded either electronically or photographically as the aircraft proceeds along the flight line. The heart of the optical mechanical scanner is the detector (14). Each detector has a certain spectral range to which it is sensitive. In this way, band-pass data collection can be obtained by using various detector-filter combinations. Optical mechanical scanners can be used through a wide range from ultraviolet to far

infrared but are most commonly used to record thermal emitted radiation between 3.5μm and 14μm from the earth's surface.

Soil moisture studies involve looking at the complicated soil-plant interface. Gates (7) has presented a comprehensive method of studying the problem. Energy budget relationships involving thermal and reflected solar radiation are developed from the theoretical viewpoint. Specific attention is given to the study of varying field conditions where degrees of crop cover versus exposed soil occur. Detailed analysis of the soil moisture problem involves looking at the energy budget of the soil and crop.

The energy balance of the soil is not nearly as complicated as the plant. Incoming radiation is either reflected or absorbed by the soil surface. Radiation that is absorbed is lost by conduction, convection, evaporation of moisture, and reradiation to the surroundings (8). The processes of conduction, convection, and condensation of moisture are reversed in certain cases and provide energy to the soil. The reflected and emitted radiations are two properties of soil surfaces of principal interest in remote sensing (20).

The energy balance for plant surfaces involves nearly the same processes encountered for soil surfaces. Incoming solar radiation is reflected, transmitted, and absorbed. The plant then maintains its environmental balance by reradiation, convection, and transpiration (8). This balance is complex due to the physiological properties in the plant. Gates, et. al., (9) described how the plant

maintains an energy balance. In the ultraviolet and visible regions of the spectrum, the plant absorbs a large amount of the incoming radiation. Chlorophyll absorption is predominant with maximums in the blue and red spectral bands (8). Here the plant needs energy for photosynthesis. Above 0.7μm in the near infrared, the plant absorption becomes small; and transmittance and reflectance greatly increase because the plant does not need the high amount of incoming energy from this region. Beyond 2.5μm where atmospheric attenuation is high and incoming solar radiation is low, the plant becomes a good absorber. Since good absorbers are good emitters, the plant can therefore reradiate a large portion of the energy that is not needed and is neither convected nor transpired. This band of high emittance in the infrared is within the spectral region where earth-emitted radiation is maximum. Gates, et. al., (9) summarized this process by saying:

> "Hence, plants absorb efficiently where they require the energy, absorb poorly the near infrared to keep from becoming overheated, and absorb the far infrared in order to be efficient radiators."

The problem of soil moisture monitoring can be approached by application of the basic principles of plant physiology to remote sensing where reflected and thermal emitted radiation are measured. The soil-plant-water relationship closely relates to a transpirational demand. The structure of the plant cell controls the transpirational moisture loss. As moisture supplies to the plant decrease, the stomatal opening restricts the transpiration; and a potential gradient is transferred from the air to the soil in the

root zone (24). This morphological change in leaf structure affects the reflectance characteristics of the plant (13). Variations in pigmentations associated primarily with chlorophyll can also result from plant stress due to a changing moisture status. Therefore, a change in reflectance due to pigmentation can be valuable in determining plant condition (7).

The temperature of the plant is increased by restricted transpiration because of the loss of evaporative cooling (20). The temperature rise results in higher thermal radiation from the plant surface. Remote sensing measurements would thereby closely correlate with plant stress resulting from decreased transpirational cooling caused by a soil moisture deficit.

Remote sensing studies have been conducted to determine relationships between remote sensing data collected and soil moisture (19, 20, 21, 29). Other plant stress conditions relating to soil salinity, evapotranspirational demands, or insect and disease damage might possess the same symptom signatures as a soil moisture deficit. The desirable approach would be to choose spectral bands which could isolate specific causal conditions. Myers, et. al., (20) studied the infrared reflectance of crops under moisture stress using color infrared film and found that a decrease in reflectance was a result of increased moisture stress. Gates (7) has indicated that certain visible bands where pigment absorption is predominant may be just as useful for plant studies as the near infrared region because of the combination of variables contributing to near infrared reflectance.

Chlorophyll absorption bands at 0.445μm in the blue region and at 0.645μm in the red region would be of principal concern (9). Selected water absorption bands may also be useful in remote sensing investigations (13). These bands at 0.96μm, 1.2μm, and 1.95μm relate the moisture contents of the leaves.

Remote sensing research should determine which spectral bands would be the best detectors of certain conditions. Selection of these bands and development of the proper equipment to conduct the research should provide valuable assistance in future resource management.

Chapter III

RESEARCH METHODOLOGY AND THEORY

Energy Balance

Remote Sensing is generally the measurement of radiant flux from a given body relating the energy status or the condition of that body. Detection and analysis of agriculture-related variables by remote sensing can be approached almost entirely by use of the conservation of energy law or the energy balance for the soil-plant surface. A radiation energy balance relationship is defined as incoming energy equals outgoing energy plus the energy stored in the system. Application of this principle to a soil-plant interface results in the following equation (23, 26)

$$R_S = R_\rho \pm R_L \pm E_S \pm E_H \pm E_L \ , \qquad 3.1$$

where

R_S = total shortwave radiation received by the ground surface from the sun and sky,

R_ρ = reflected shortwave radiation,

R_L = net longwave radiation at the surface,

E_S = energy stored by the plant or soil,

E_H = sensible energy gain or loss, and

E_L = latent energy gain or loss.

Looking at a surface such as a plant canopy, an equation can be (23)

$$\alpha + \rho + \tau = 1 \ , \qquad 3.2$$

where

α = absorptance,

ρ = reflectance, and

τ = transmittance.

Assuming that with the overall soil-plant surface total transmittance of incident radiation is equal to zero; then the above equation becomes

$$\alpha + \rho = 1, \qquad 3.3$$

which is equivalent to equation 2.5.

In agricultural environments, the physical and chemical properties of the soils and plants are closely interrelated with each quantity of the energy balance. Remote sensing measures the radiant flux terms from equation 3.1. The remaining terms interact with and contribute to the radiation terms. The terms of equation 3.1 in turn are functions of many factors within the soil-plant environment. The following discussion takes each of the terms in equation 3.1 and develops the functional relationships that govern their variability.

Incoming Radiation

Incoming shortwave radiation, R_S, is comprised of solar radiation and skylight. R_S is a function of radiant flux at the outer edge of the atmosphere, atmospheric attenuation, latitude, season, and time of the day. The spectral distribution and intensity of the incoming

radiation are controlled by all of these factors. The latitude, season, and time of the day determine the geometry of illumination.

The radiant flux at the outer edge of the atmosphere is the result of the absolute temperature of the sun. With the sun's surface temperature as approximately 6,000°K, the wavelength at which the solar radiance is maximum (λ_{max}) can be approximated by utilizing Wien's Displacement Law to obtain

$$\lambda_{max} = \frac{2897.9}{6{,}000} = 0.483\mu m. \qquad 3.4$$

The solar spectral emission is almost entirely contained between 0.15μm and 4.0μm (26). However, atmospheric attenuation is predominant at both ends of this range, resulting in a narrowed range for shortwave radiation at the earth's surface. The remote sensing measurement of incoming radiation can be obtained with solameters or radiometers sensitive to the desired spectral region.

Reflected Radiation

Reflected shortwave radiation is the product of incoming radiation, R_S, times the fractional reflectance, ρ, or albedo of the surface. Causes of variation in incoming radiation were discussed in the previous section. Albedo is also a complex function of many variables. A functional equation for soil and plant reflectance is

$$\text{Reflectance} = F\ (\text{exposed soil or crop cover, plant and soil type, soil surface condition, crop canopy geometry, plant maturity and physiological condition, soil moisture, and evapotranspirational demands}). \qquad 3.5$$

The problem of analysis of each of these controlling factors becomes huge. Remote sensing investigations have generally taken measurements which would identify key features pertinent to a specific study.

For the soil-plant regime, the reflected radiation was described by Gates (8) as

$$R_\rho = f\rho_g R_S + (1-f)\ \rho_c R_S\ , \qquad 3.6$$

where

f = fraction of exposed soil,

ρ_g = fraction reflectance of the ground or soil, and

ρ_c = fraction reflectance of the crop or plant.

The above equation assumes certain quantities negligible such as the transmission of incoming radiation through the crop canopy and resulting reflection from the ground surface.

Multispectral sensing is the measurement of monochromatic radiation using specific bands of the spectrum. Band-pass filtering of reflected radiation is commonly used today in remote sensing. Multispectral sensing capabilities using band-pass filters involves modification of equation 3.6. Variations in spectral distribution and intensity of the incoming radiation are largely the result of atmospheric attenuation and the position on the earth's surface in

relationship to the sun. Selection of band-pass filters requires the knowledge of the spectral intensity of each band. If the spectral radiance within a specific band is R_{Sband}, the relation between R_{Sband} and incoming shortwave radiation, R_S, is described by the following equation

$$R_{Sband} = RF\ (R_S), \qquad 3.7$$

where

RF = fraction of the total incoming radiation from a spectral band.

The above equation provides band correction for incoming radiation. After correction for incoming radiation, a difference observed between two values of reflected radiation for a band would indicate a change in reflectance of the soil-plant surfaces. Equation 3.6 can be expanded to give

$$\begin{aligned} R_{\rho band} &= f\rho_{gband}\ R_{Sband} + (1-f)\rho_{cband}\ R_{Sband} \\ &= R_{Sband}\ [\ f\rho_{gband} + (1-f)\rho_{cband}\ ], \end{aligned} \qquad 3.8$$

where

$R_{\rho band}$ = reflected radiation from a spectral band,

f = fraction exposed soil,

ρ_{gband} = fraction reflectance of the soil for a spectral band,

ρ_{cband} = fraction reflectance of the plant for a spectral band, and

R_{Sband} = incoming radiation within a spectral band.

Application of equation 3.8 to soil moisture studies requires determination of all terms in the equation. The resultant, $R_{\rho band}$, can be measured by photography, scanner-detectors, and solameters. The values for f and 1-f need to be assessed on the ground. $R_{S band}$ can be measured from either an aerial or a ground location by a spectrometer or a bank of filtered solameters. The remaining terms in equation 3.8 are the reflectance terms. One variable that controls reflectance is soil moisture as given by equation 3.5. Accounting for several of the remaining factors affecting reflectance by multispectral sensing and spectral analysis of the crop and soil should make monitoring of soil moisture possible.

Thermal Radiation

Thermal emitted radiation is characterized by the emissivity and the absolute temperature of a body. Looking specifically at a soil-plant surface, thermal emitted radiation is the residual from the other terms of the energy balance. If possible, the soil and plant remain in energy equilibrium. The absorbed radiation that is neither stored nor lost by convection and evaporation must be reradiated because of the change in absolute temperature. In this way emitted radiation from a soil-plant surface is related to the soil moisture status.

Deriving an expression for the net longwave radiation, R_L, using the Stefan-Boltzmann Law (equation 2.8) and considering the amount of plant cover and exposed soil, an equation can be written as follows

$$R_L = (1-f)\,[\varepsilon_c \sigma T_c^{\,4} + (\rho_c - 1)\,R_a] + f\,[\varepsilon_g \sigma T_g^{\,4} + (\rho_g - 1)\,R_a]$$

$$= (1-f)\,(\varepsilon_c \sigma T_c^{\,4} + \rho_c R_a) + f\,(\varepsilon_g \sigma T_g^{\,4} + \rho_g R_a) - R_a, \qquad 3.9$$

where

f = fraction of exposed soil,

$1-f$ = plant cover,

ε_c = emissivity of the crop surface,

σ = Stefan-Boltzmann universal constant,

T_c = absolute temperature of the crop,

ρ_c = reflectance of the crop surface,

ε_g = emissivity of the soil surface,

T_g = absolute temperature of the soil,

R_a = downward longwave radiation from the atmosphere, and

ρ_g = reflectance of the soil surface.

The thermal scanning system used in most remote sensing research measures only the outgoing thermal radiation. Equation 3.7 can be modified to give the outgoing thermal radiation (R_{Lout}) as

$$R_{Lout} = (1-f)\,(\varepsilon_c \sigma T_c^{\,4} + \rho_c R_a) + f\,(\varepsilon_g \sigma T_g^{\,4} + \rho_g R_a). \qquad 3.10$$

Applying Wien's Displacement Law to approximate the wavelength at which maximum radiance is emitted from the earth, the following equation can be written

$$\lambda_{max} = \frac{2897.9}{300} = 9.66\mu m\ , \qquad 3.11$$

where λ_{max} is for an average absolute temperature of the earth of approximately 300°K. The practical limits of earth-emitted radiation are from 3.0μm to 80μm (26); and just as with incoming solar radiation, atmospheric attenuations further limit measurement of thermal radiation to certain spectral bands specified in Chapter II.

Both thermal line scanners and radiation thermometers are used in remote sensing to measure the temperature of given surfaces. When the variables contributing to changes in emissive power or absolute temperature are analyzed, deductions concerning soil moisture may be possible.

Stored Energy

The stored energy, E_S, in a soil-plant system should be considered from the standpoint of both plants and soils where it can be either positive or negative. The plant stores energy in two ways, by a change in temperature and by photosynthesis or assimilation of carbohydrates. Photosynthesis, which is the basis for plant growth, depends on the type of plant, the incident light, the available nutrients, and the available soil moisture (23).

E_S for the soil involves actual heat stored in the ground surface and heat flux downward or conduction into the earth. Controlling factors for energy stored in the soil are soil type, heat capacity, thermal conductivity, and energy available. Heat capacity (specific heat) and thermal conductivity are directly dependent upon the water

content of the soil (26). Therefore, it can be assumed that E_S is affected largely by the available soil moisture supply.

The stored energy, E_S, cannot be measured directly by a remote sensor. The change in temperature due to E_S, however, can be monitored indirectly by using the thermal radiation term, R_L. Photosynthetic changes cause a change in plant reflectance which can be detected by the reflected radiation term, R_ρ. Ground truth monitoring of the stored energy can be accomplished by recording soil heat flux, soil temperature, and crop condition.

Sensible Energy

The sensible heat exchange, E_H, involves the convection and conduction of energy from the soil-plant surface to the surrounding air. These two terms closely interact but it is believed that in the field the convection term is larger than the conduction term for the total energy exchange because convection involves mixing large volumes of air. Conduction is the transfer of energy between molecules and for air is dependent upon the absolute humidity or, specifically, the moisture content of the air.

Convection is the exchange of energy by mass transfer of the air and can be either free or forced convection. As the air in the lower layers becomes heated by conduction from the plant and soil surfaces, it begins to overturn, and the cooler air from above replaces it. The cooler air then becomes heated, and the process is repeated. Free convection is convection when the atmosphere is at rest. Forced

convection occurs during a wind or breeze and usually is greater than free convection. Strong winds, however, may have a sealing effect and decrease convection (23). The dependence of the sensible energy exchange, E_H, upon soil moisture is generally related only through the other terms of the energy balance equation. No remote sensing measurement can be made for E_H. Wind profile and air temperature profile measurements on the ground would help to describe the conductive and convective heat losses from the plant canopy.

Latent Energy

The latent energy term, E_L, is pertinent to a soil moisture study. This term relates to evapotranspiration and describes the heat lost by evaporation and transpiration of liquid water from a soil-plant surface. Heat may also be gained by condensation of moisture onto the surface in the form of dew or frost since E_L is either positive or negative. However, latent energy is usually positive in a semiarid climate because condensation is less than total evaporation.

Separating the latent energy term into soil and plant components gives

$$E_L = \pm LE_g \pm LE_\ell \ , \qquad 3.12$$

where

L = latent heat of vaporization of water,

E_g = moisture evaporated or condensed at the soil surface, and

E_ℓ = moisture transpired or condensed at the plant surface.

The amount of water that is evaporated from the soil, E_g, is not as difficult to evaluate as the transpiration term, E_ℓ. E_g is a function of available soil moisture, soil type and surface condition, available energy for exchange, and vapor pressure deficit of the atmosphere. When the available moisture on the soil surface is low, evaporative heat exchange from the soil is decreased; and the surface temperature rises. The rise in temperature causes increased thermal radiation which can be detected by remote sensors.

Similar to evaporation from soils, transpirative moisture losses, E_ℓ, from plants depend on available soil moisture, plant type, incoming radiation, and vapor pressure deficit of the surrounding air. Plant type, incoming radiation, and vapor pressure deficit of the air designate a potential transpiration rate for a given crop. The actual transpiration is limited only by the available soil moisture. In order to understand transpiration, the complex mechanism of plants should be discussed. If the water supply is insufficient, the plant's temperature will rise due to the lack of transpirational cooling. A change in the complex stomatal and cell structure of the plant associated with wilting may be a combination of both low available moisture and high evapotranspirational demand. High evapotranspirational demands are commonly a result of a large vapor pressure deficit and high incoming radiation.

Under normal conditions, transpiration is an equilibrium soil-water-plant system that originates in the root zone and terminates in the atmosphere. The potential gradient developed at

the leaf surface by evaporation of water from the mesophyll cells is transferred through the plant to the soil (24). The leaf cells actually control the stomatal opening; and as long as a sufficient quantity of soil moisture is available, evaporation rate is not greatly altered. Loss of moisture due to transpiration from the leaf surface produces a potential gradient which is the driving force through the system. If there is no water available at a given gradient level due to high soil potential, increased gradient is developed until the plant potential reaches either the soil potential where moisture is accessible or a maximum plant potential where permanent wilting occurs.

The increase in temperature due to the lack of transpirational cooling can be detected by remote sensing in the form of thermal radiation. The structural and chemical changes within moisture stressed plants result in a change in the spectral reflectance characteristics of the plants (8, 19). The reflectance properties are evaluated by the reflected radiation term, R_ρ.

The measurement of reflected radiation by photography and thermal emitted radiation are primary methods of collecting remote sensing data. Incoming radiation is also easily recorded. Reflected radiation, R_ρ, thermal radiation, R_L, and incoming radiation, R_S, are three terms of the energy balance equation (equation 3.1). As can be seen by the preceding discussion, the remaining terms of the energy balance equation interact to contribute to R_L and R_ρ. Changes in stored energy, E_S, latent energy, E_L, and sensible energy, E_H, are

the principal causes for changes in R_L and R_ρ. Since soil moisture is an important factor contributing to stored and latent energy exchange, monitoring of soil moisture should be feasible by sensing R_L and R_ρ. For an accurate analysis of soil moisture, the variables, not directly related to soil moisture such as plant and soil type that affect R_L and R_ρ, should be considered and eliminated by multispectral sensing techniques and data analysis.

Chapter IV

EQUIPMENT AND DATA COLLECTION

Field Layout

The 1970 soil moisture study was conducted at the South Dakota State University James Valley Research and Extension Center. This experimental station is located one mile north of Highway 212, five miles east of Redfield, South Dakota. Figure 4.1 is a color print from color infrared film (#8443) of the entire farm. The farm is managed by the South Dakota State University Agricultural Experiment Station. The farm is within the Oahe Unit, James Division, Missouri River Basin Project. The ground truth data for this research was collected cooperatively with Water Resources Project A-018-SDAK, conducted by Dr. Maurice Horton, Plant Science Department, South Dakota State University.

The research plots are near the James River, and the river serves as a water supply for irrigation at the center. The entire region is within the bed of the extinct glacial Lake Dakota. This provides an explanation for the flat terrain and the soil formation in the area. The soil type in the plots is Beotia silt loam which is a reasonably heavy textured soil but still adaptable to irrigation. The irrigated parts of the plots were sufficiently level so that no gradework was needed to facilitate use of a surface irrigation system. Irrigation has been practiced on the plots for several years.

Figure 4.1 Print from color infrared film, #8443 with G15/30m filter, showing an aerial view of the entire James Valley Research and Extension Center near Redfield, S. D., 1525m (5,000 ft) agl, 4X enlargement, scale: 1 cm = 62m, north is toward the top of the print.

The climate of the area falls within semiarid classification. National Oceanic and Atmospheric Administration (NOAA) records for South Dakota (1, 3) show that the average annual precipitation for the area is near 46 cm with over 75 percent of the rainfall coming during the growing season from April through September. The average temperature for the growing season is about 18^{o}C with the highest monthly average of 24.1^{o}C in July. Growing season pan evaporation is nearly 100 cm, and the wind throughout the summer averages more than 16.1 kilometers per hour, generally southerly in direction. Temperature in the summer can reach over 38^{o}C with winds up to 50 kilometers per hour. An average of 65 to 70 percent of the possible sunshine can be expected during the growing season. July can have nearly 80 percent of the possible sunshine.

The experimental study area consisted of a three hectare field which included irrigated and non-irrigated grain sorghum and two fallow plots. Figure 4.2 shows the arrangement of the plots within the test site. The plots were of sufficient size so that they could be identified on the aerial imagery at the altitudes to be flown. The field layout was chosen to minimize labor and time needed for data collection. The relatively small plot sizes were selected in order to reduce the variability of the experimental study area.

The differential soil moisture levels within the sorghum plots were of primary concern to the soil moisture research. The fallow was useful as a reference plot. The treatments for the two fallow plots were planned for cooperative study with the Plant Science Department.

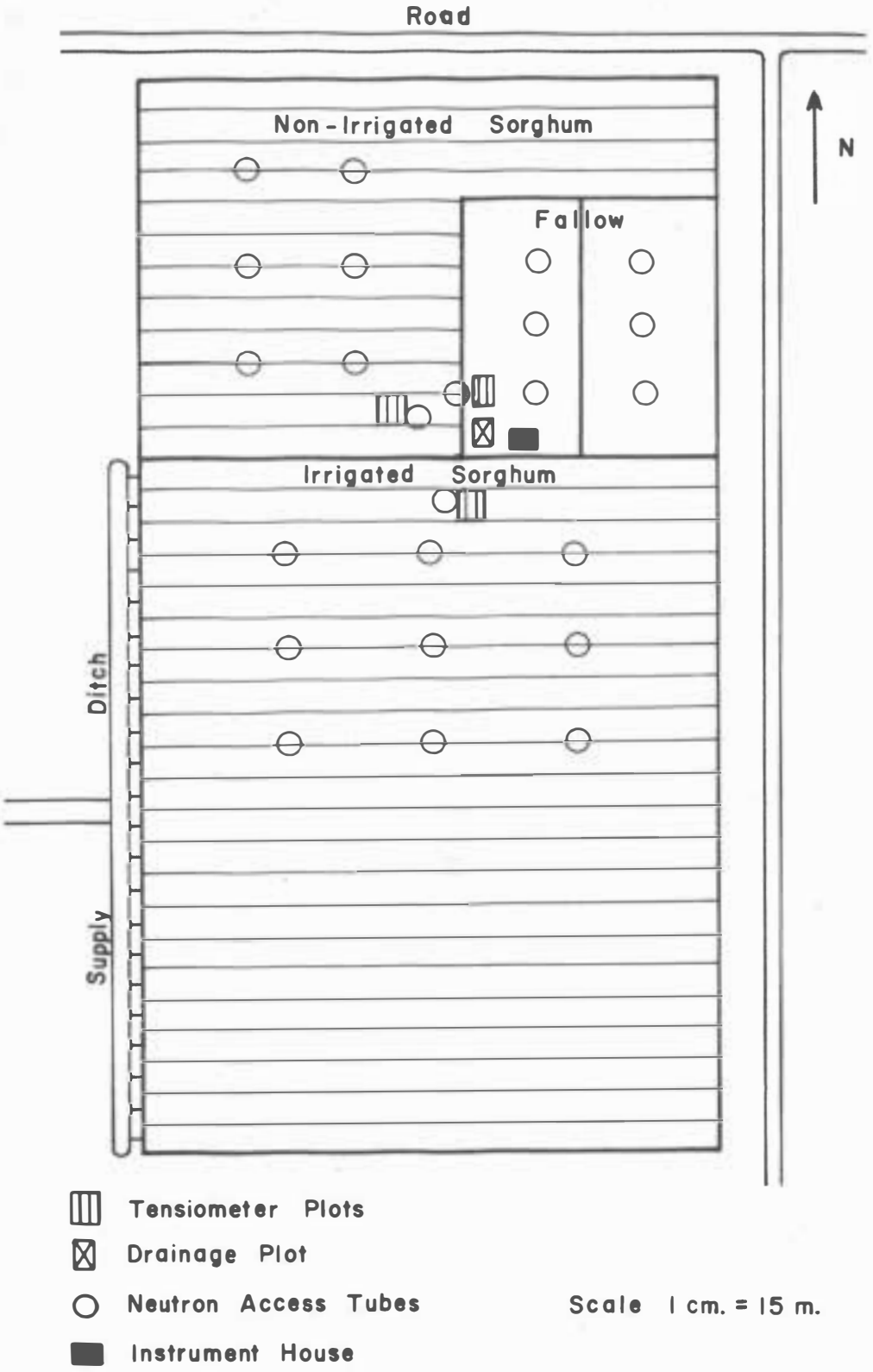

Figure 4.2 - Field layout for the soil moisture study at Redfield.

A conventional tillage fallow and a chemical fallow were used. On Figure 4.2, the chemical fallow is on the left side with the tilled fallow on the right. The grain sorghum was divided into non-irrigated and irrigated parts as shown by Figure 4.2. It was planted in 54.2 cm rows at a plant population of 261,250 plants per hectare (104,500 plants per acre). The variety of sorghum was Sokota 503. Fertilizer applied to the plots was 182 kilograms per hectare of nitrogen (160 pounds per acre) and 32 kilograms per hectare of phosphorus (28 pounds per acre).

Ground Truth Data Collection

In remote sensing research, ground truth data are needed to provide verification of the results obtained from the remote sensors. Ground truth is the basis for correlation and evaluating results in soil moisture research. Table 4.1 lists the ground truth variables collected during 1970. It also lists the method in which each variable was collected and the approximate frequency of collection. Appendix D lists the instrument designation and description of the collection equipment used.

Some ground truth data listed in Table 4.1 are not used directly in the soil moisture analysis. The variables including temperatures, wind, humidity, net radiation, and soil tension were collected primarily for the cooperative research program of the Plant Science Department. The tensiometer plots as shown in Figure 4.2 were used to record lateral movement of water through the soil. The tensiometer

TABLE 4.1. GROUND TRUTH VARIABLES FOR THE SOIL MOISTURE STUDY AT REDFIELD, 1970.

Variable	Method of Collection	Frequency of Collection
Crop and Variety	Record	Seasonal
Row Spacing and Direction	Measure	Seasonal
Plant Population	Measure	Seasonal
Soil Bulk Density	Soil Samples - Lab Analysis	Seasonal
Ground Truth Photos	35 mm Nikon	Periodic
Gravimetric Soil Moisture	Soil Samples - Lab Analysis	Weekly
Volumetric Soil Moisture	Neutron Probe	Weekly
Crop Condition	Evaluate	Weekly
Plant Maturity	Evaluate	Weekly
Plant Height	Measure	Weekly
Ground Cover (%)	Estimate	Weekly
Surface Soil Condition	Evaluate	Weekly
Cultivation Condition	Evaluate	Weekly
Irrigation Log	Record and Estimate	As Occurring
Precipitation Log	Measure	As Occurring
Pan Evaporation	Measure	Daily
Haze Condition and Visibility	Evaluate	Weekly
Cloud Type and Condition	Evaluate	Weekly
Cloud Cover (%)	Estimate	Weekly
Weather Condition	Evaluate	Weekly
Soil Tension	Tensiometers	Daily
Soil and Air Temperatures	Thermocouples	Continuous
Wind Speed and Direction	Anemometer	Continuous
Humidity	Dew Probe	Continuous
Net Radiation	Miniature Net Radiometer	Continuous
Incoming Radiation	Solameter	Continuous

data and the microclimate measurements of temperature, wind, humidity, and net radiation were collected for cooperative water resources research.

The researcher needs to assess general condition variables as accurately as possible to facilitate the analysis of the remote sensing imagery and the remaining ground truth data. The qualitative variables are crop condition, plant maturity, soil surface and cultivation condition, haze and cloud condition, and weather condition. Precise numerical measurements are difficult to obtain for these variables. Experience and judgment are required in order to appraise the field conditions consistently from mission to mission. The condition analysis code that was used in 1970 is presented in Appendix C. Table 4.2 is a summary of several crop and soil conditions that were collected. This table relates the conditions as they were recorded by using the ground truth code from Appendix C.

The condition variables and many other variables from Table 4.1 were utilized in the remote sensing imagery analysis. The type of crop and type of soil specified the spectral signature. Imagery interpretation of the relative soil-plant environment was accomplished by studying the row direction, plant population, and percent crop cover.

The ground truth data that were specifically utilized in this research include soil moisture, soil bulk density, irrigation and precipitation log, pan evaporation, soil tension, and several of the condition variables. Two methods of collecting soil moisture data

TABLE 4.2. SUMMARY BY DATE OF GROUND TRUTH DATA FOR CROP AND SOIL CONDITION VARIABLES IN THE IRRIGATED AND NON-IRRIGATED SORGHUM AT REDFIELD, 1970.*

Julian Date	Plant Height - cm		Plant Maturity		Plant Condition		Crop Cover - %		Surface Soil Condition	
	Irr.	Non-Irr.	Irr.	Non-Irr.	Irr.	Non-Irr.	Irr.	Non-Irr.	Irr.	Non-Irr.
168	10	10	28	28	50	50	10	10	72	72
176	16	16	35	35	58	58	20	20	25	22
182	40	40	37	37	68	68	70	70	24	24
188	51	53	40	40	70	70	70	70	15	16
195	80	75	47	47	88	80	85	80	82	45
199	96	88	48	48	85	70	98	95	72	24
205	108	95	54	53	80	50	100	98	64	34
211	130	115	57	57	78	70	98	95	73	63
223	160	125	60	60	80	60	98	90	63	22
231	160	130	65	65	85	60	98	95	35	24
237	160	130	68	68	80	55	98	95	25	14
243	160	130	72	72	85	55	95	90	15	14
251	160	130	78	78	85	60	95	90	15	15
259	160	130	84	84	85	70	95	90	75	66
278	160	130	89	89	80	65	90	85	26	15

* The code for analysis of the condition variables is found in Appendix C.

were employed. The older of these methods of soil moisture measurement is the use of soil samples. This method known as the gravimetric method results in a soil moisture relationship giving weight of water per unit weight of dry soil. It involves taking a soil sample, weighing it at field moisture conditions, oven drying it, and finally weighing the oven dry soil. Computation of the gravimetric moisture content, θ_g, is by the following equation

$$\theta_g = \frac{WW - DW}{DW} \times 100\% , \qquad 4.1$$

where

WW = wet weight of the soil, and

DW = dry weight of the soil.

The neutron probe method is a newer method of soil moisture determination. The probe is a radioactive device which is lowered into the ground through a previously installed access tube. The radioactive particles or neutrons emitted by the probe penetrate into the soil. Due to the composition of the water molecule, the rate at which the particles are deflected in the soil is proportional to the soil moisture content. A detector in the probe measures the rate at which the neutron particles are deflected, and transmits this value to a ratemeter or counter. Used properly, the neutron probe can provide representative values of existing soil moisture conditions. The radioactive source has a sphere of influence in the soil up to a radius of 30 cm. It is, therefore, reasonable to assume that the

soil moisture values obtained from the neutron method are more reliable than data from a spot measurement source such as a soil sample since the moisture in a larger area is measured or sampled.

The raw soil moisture data was first processed by computer. Gravimetric moisture data were processed by using equation 4.1. Neutron probe data is in terms of neutron counts per standard counts. When the probe is correctly calibrated, the volumetric soil moisture content can be obtained by use of an equation or read directly from a computed table. The equation used to determine the volumetric moisture percent, θ_v, from neutron data is

$$\theta_v = 61.576 \left(\frac{C}{C_s}\right) - 5.676, \qquad 4.2$$

where

C = counts, and

C_s = standard counts.

In order to obtain comparable values for θ_v and θ_g, θ_g may be converted by using

$$\theta_v = \theta_g \left(\frac{BD_s}{BD_w}\right), \qquad 4.3$$

where

BD_s = bulk density of the soil, and

BD_w = density of water.

The bulk density of the soil is the dry weight of the soil per unit volume of soil, and the density of water is usually equal to one gram per cubic centimeter.

The field arrangement for the ground truth data collection is shown in Figure 4.2. As previously mentioned, two grain sorghum plots and two fallow plots were in the experimental design. Within the non-irrigated sorghum plots, seven neutron access tubes were used. Six were placed evenly throughout the field, and one was placed close to a tensiometer plot where a bank of tensiometers recorded soil tension at several depths. Of the six access tubes in the non-irrigated field, four were positioned in the sorghum rows and two were positioned between successive rows. The larger field of irrigated sorghum had ten access tubes with one tube next to a tensiometer plot. The nine remaining tubes were placed evenly across the field with three between the rows and six in the rows. The chemical and mechanical fallow each contained three access tubes with one additional tube located at the tensiometer plot in the fallow. A total of 24 neutron access tubes were in the overall design. Neutron readings were obtained at five depths within the soil profile. Readings were made at depths of 15.24 cm, 30.48 cm, 60.96 cm, 91.44 cm, and 121.92 cm. Soil samples for soil moisture were collected at the surface, 15.24 cm, and 30.48 cm levels.

Besides obtaining soil moisture percentages, the depth of water for each successive 30.48 cm depth and the total depth of water for accumulated depths up to 121.92 cm were calculated. Available soil

moisture for given depths was then computed. Available soil moisture is the soil moisture that is accessible for use by the plant. The maximum suction or tension that a plant can withstand in relation to the water supply is called the permanent wilting point. The permanent wilting point of many crops is near 15 bars tension. Therefore, for this study all moisture that is held in the soil at less than 15 bars was considered to be available soil moisture. Moisture tension data available for Beotia silt loam is very limited. From the data available, the amount of water held in the soil in the top 121.92 cm (four feet) between zero and 15 bars is 35.26 cm. The amount of water held between 1/3 bar and 15 bars is 27.82 cm. Figures 4.3, 4.4, 4.5 and 4.6 show the available soil moisture for accumulated depths of 30.48 cm, 60.96 cm, 91.44 cm, and 121.92 cm, respectively. To relate the water input into the soil-plant system, a log of the rainfall and irrigations is plotted above the available moisture graphs on each of the figures.

Aerial Data Collection

Remote sensing research is characterized by data collection from a platform where the platform can be satellite, aircraft, or ground location. In 1970 the aerial data were collected by use of a twin Beechcraft, RC45J. Flight altitudes were 610m (2,000 ft) and 1525m (5,000 ft) above ground level with supplementary flights at 305m (1,000 ft) above ground level. All components of the sensor systems were installed in the aircraft during each flight mission. The

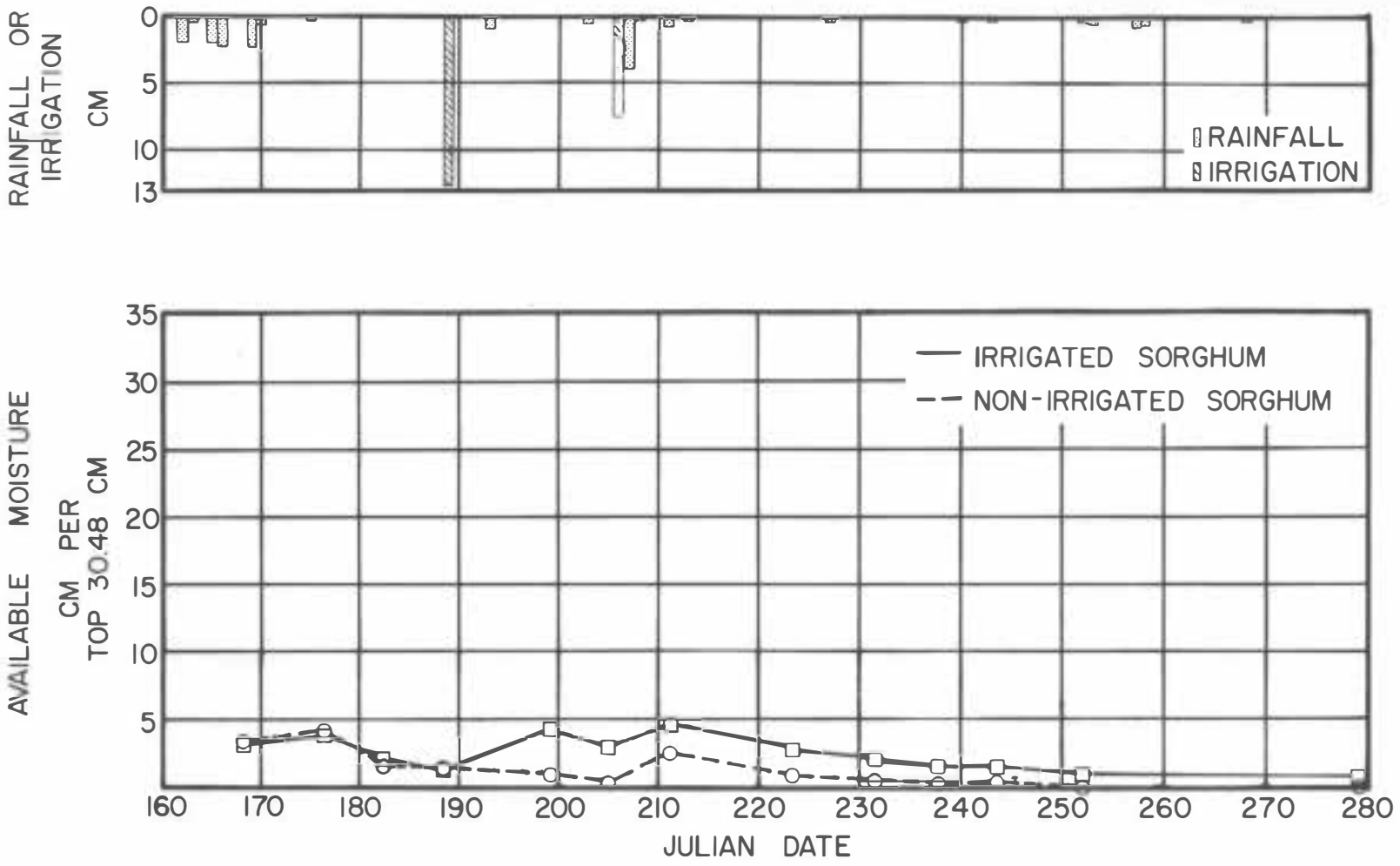

Figure 4.3 - Available soil moisture in the top 30.48 cm and the rainfall and irrigation input plotted versus time.

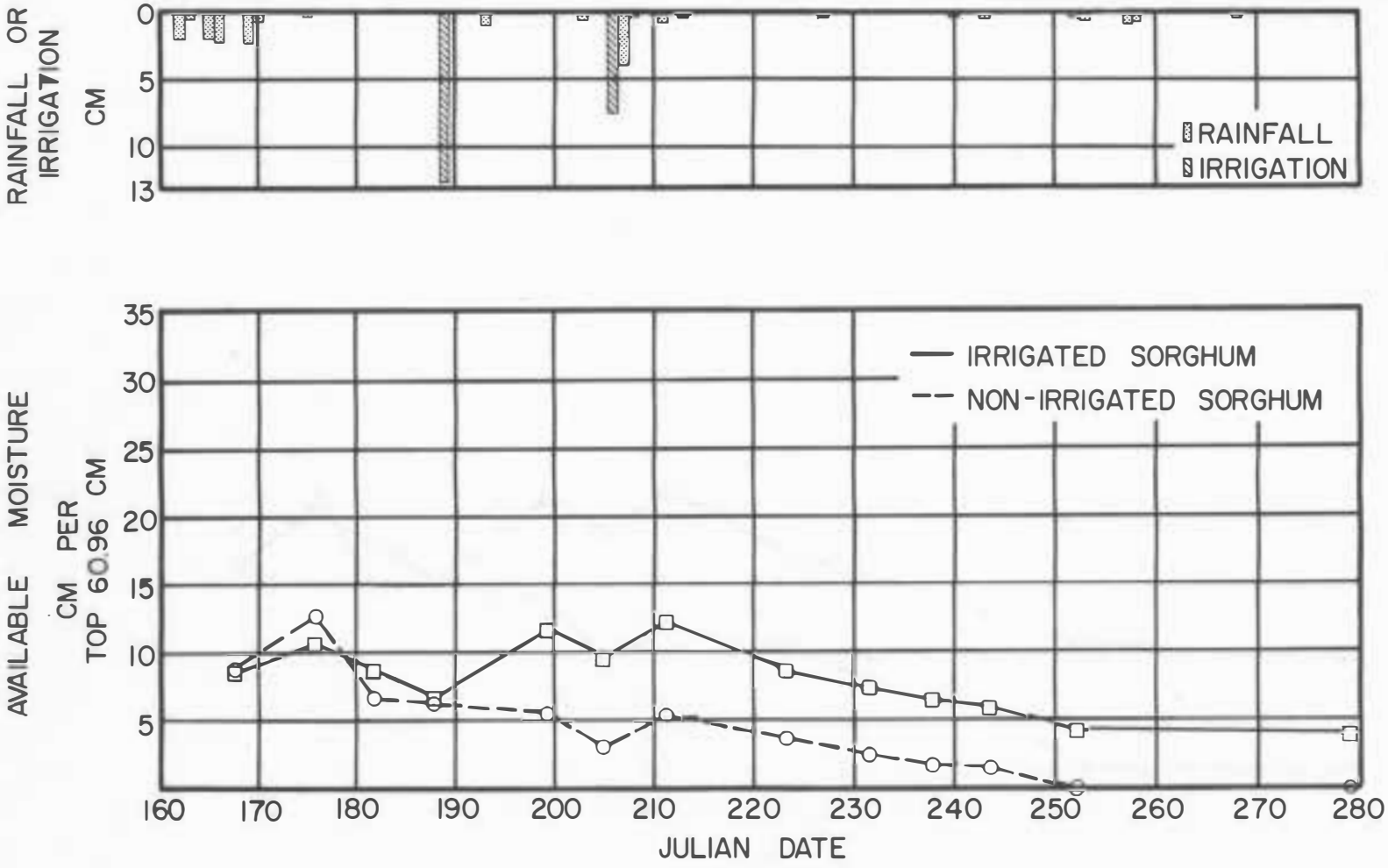

Figure 4.4 - Available soil moisture in the top 60.96 cm and the rainfall and irrigation input plotted versus time.

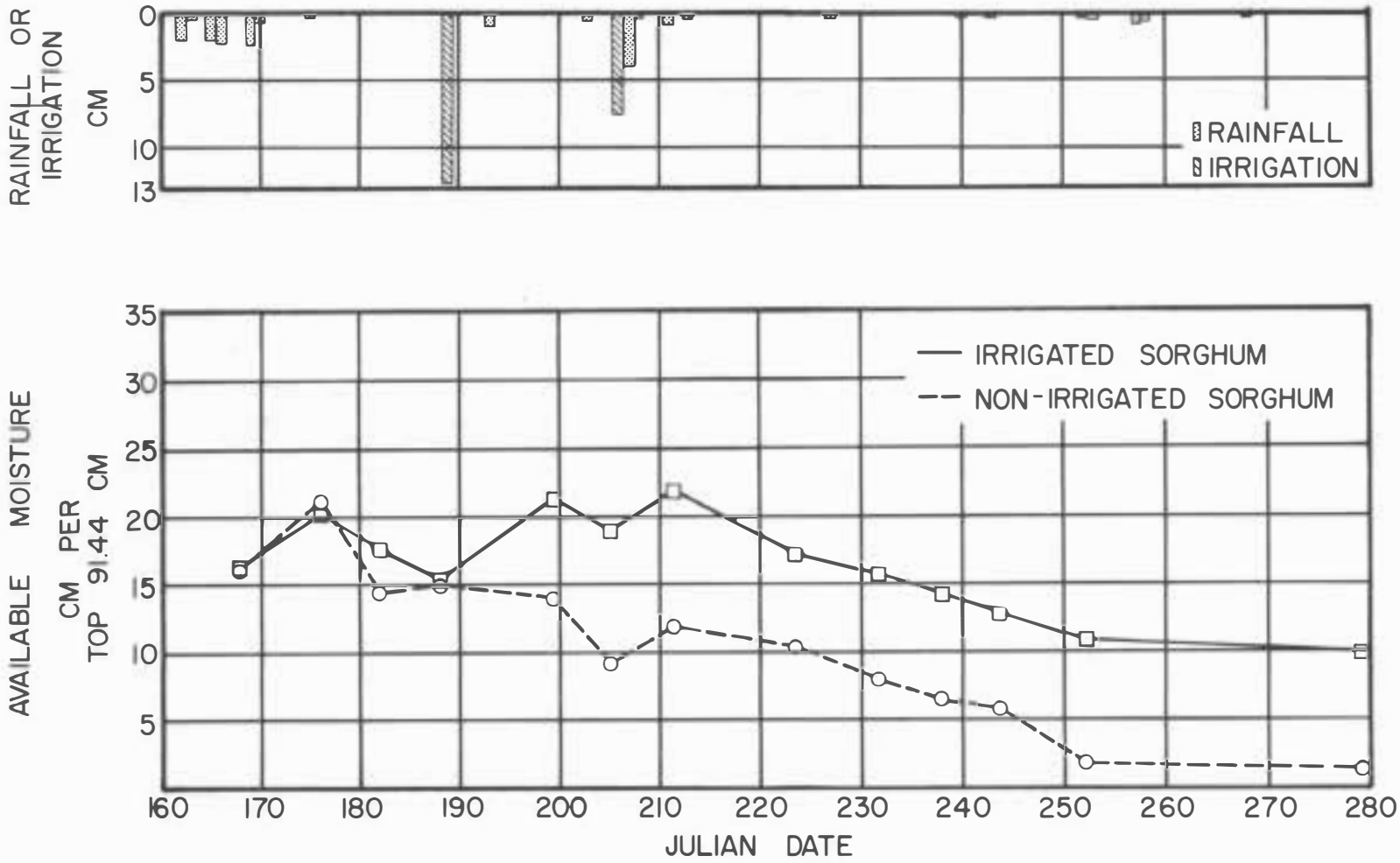

Figure 4.5 - Available soil moisture in the top 91.44 cm and the rainfall and irrigation input plotted versus time.

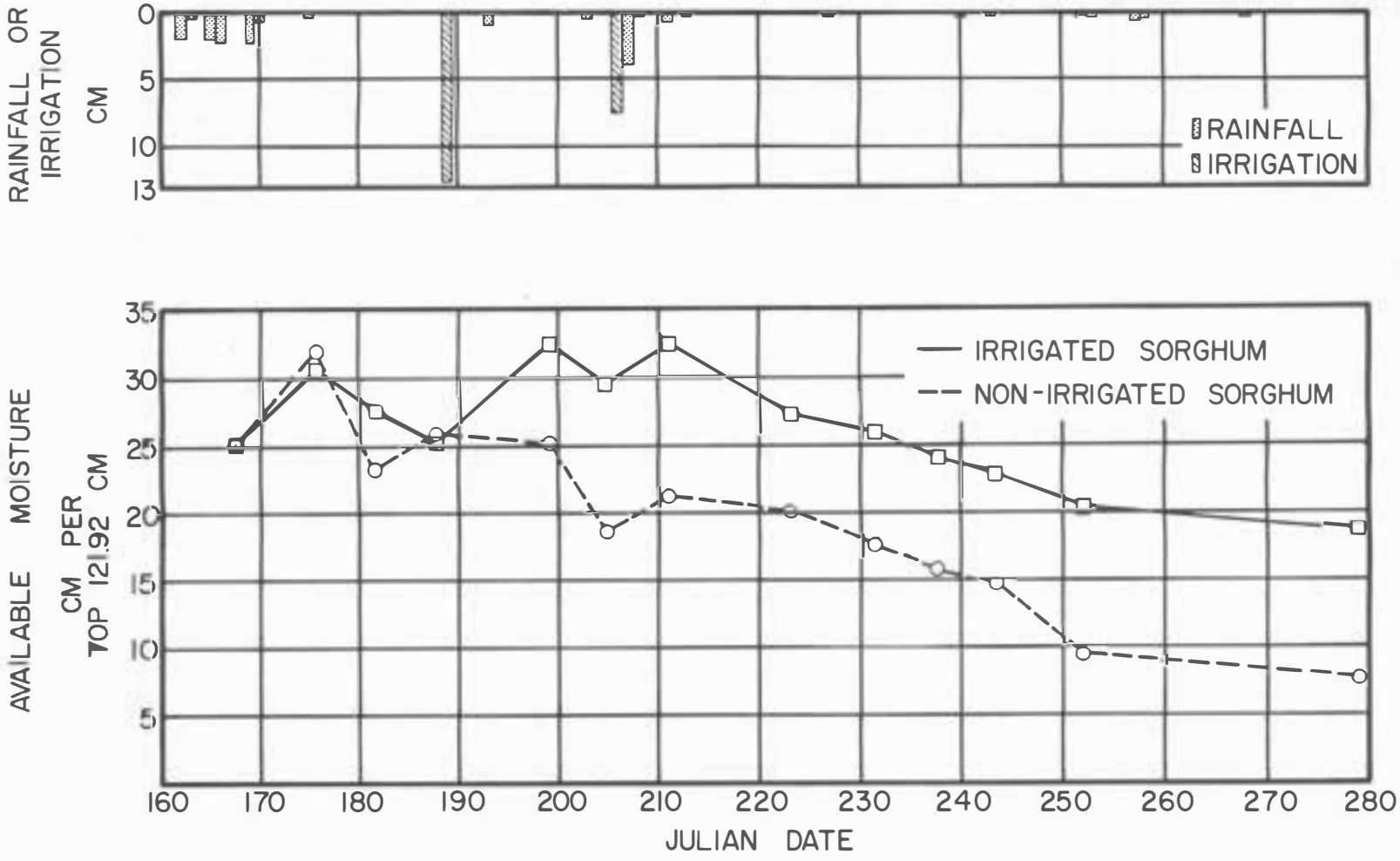

Figure 4.6 - Available soil moisture in the top 121.92 cm and the rainfall and irrigation input plotted versus time.

variables for which data were collected from the aircraft are listed in Table 4.3 along with a brief description of the equipment used to collect the data. Appendix D provides a complete description of all sensors and instrumentations used for the project. The frequency of the aerial missions was approximately once per week. The photographic sensors measuring reflected radiation were operated throughout the season, but the thermal scanner was not used the first five missions. Functional problems also limited the capabilities of the scanner during the remainder of the data collection period. The actual principles of sensor detection were discussed in detail in Chapters II and III.

Mission Planning

The final task associated with the remote sensing data collections was mission planning and execution. Flight lines were chosen to give complete coverage of the study areas. Two flight lines were planned for the lower altitudes. Referring to Figure 4.1, flight line number one passed directly over the soil moisture plots. The plots are in the upper center of Figure 4.1. Flight line number two passed over the other half of the farm. A third flight line was flown at 1525 meters above ground level (5,000 ft agl) over the center of the farm.

One requirement of the project plan which was strictly followed was that of having simultaneous aerial and ground truth missions. It was realized from previous work in the Remote Sensing Institute that

TABLE 4.3. REMOTE SENSING DATA COLLECTED, 1970.

Variables	Spectral Range	Method of Collection
Photography - Four Cameras		70 mm Hasselblads
Black and White Film - Filtered		
Green - #58	0.47μm → 0.61μm	8403 Film
Red - #25A	0.59μm → 0.70μm	8403 Film
Near Infrared - #89B	0.68μm → 0.90μm	2424 Film
Color Reversal Infrared Film		
Dark Yellow Filter - #15G + 30 Magenta	0.51μm → 0.90μm	8443 Film
Incoming Radiation	0.35μm → 1.15μm	Solameter
Outgoing Radiation - Three Bands		Solameters
Green - #58	0.47μm → 0.61μm	
Red - #25A	0.59μm → 0.70μm	
Near Infrared - #89B	0.68μm → 0.90μm	
Thermal Infrared Radiation	4.5μm → 5.5μm	Daedalus Line Scanner
Surface Temperature	8.0μm → 14.0μm	Precision Radiation Thermometer
Haze Condition		Evaluate
Cloud Type and Condition		Evaluate
Cloud Cover (%)		Estimate

the separation of aerial missions from ground truth missions introduces uncontrollable variability. This variation might be the result of rainfall, high evapotranspirational demands, or other environmental changes.

A total of 16 ground truth missions were conducted during the season. On each of these missions, soil moisture and crop-soil-weather condition data were collected. Thirteen aerial missions were flown throughout the growing season, concurrent with 13 of the ground truth missions. The sorghum was ten centimeters high at the time of the first mission. The last mission was conducted just prior to harvest. Table 4.4 gives the aerial missions by date, mission number, altitude, and time of flight. Also included in Table 4.4 are average values of incoming radiation and the predominant weather conditions at the time of each overflight. Besides the dates given in Table 4.4, ground truth missions were conducted on June 30, July 14, and September 16.

The scheduling of data collection missions for research purposes is difficult due to variable weather conditions. For the purposes of our research, no clouds were permissible overhead during an overflight. This flight requirement was difficult to achieve since, on occasion, more than one week would pass with no clear days. Another problem that was encountered throughout August was extremely heavy haze conditions. This problem, besides causing a spectral shift in the incoming radiation, substantially decreased the intensity of the radiation.

TABLE 4.4. AERIAL MISSION DATA GIVING FLIGHT CONDITIONS FOR EACH DATE, REDFIELD, 1970.

Flight No.	Julian Date	Date	Mission No.	Altitudes m agl	Time cds	Incoming Radiation cal cm^{-2} min^{-1}	Weather Condition
1	168	June 17	108	610 1525	1223→ 1250	1.10	50% Cum. Cl. Mod. Haze Light Wind
2	176	June 25	112	610 1525	1018→ 1030	1.04	Cirrus Cl. Heavy Haze Light Wind
3	182	July 1	114	610 1525	1204→ 1247	1.28	Clear Heavy Haze Light Wind
4	188	July 7	118	610 1525	1628→ 1639	1.00	Lt. Cirrus Cl. V. Heavy Haze Strong Wind
5	199	July 18	119	610 1525	1222→ 1235	1.27	Clear V. Heavy Haze Light Wind
6	205	July 24	125	610 1525	1240→ 1310	1.40	50% Cum. Cl. Mod. Haze Light Wind

TABLE 4.4. Continued.

Flight No.	Julian Date	Date	Mission No.	Altitudes m agl	Time cds	Incoming Radiation cal cm^{-2} min^{-1}	Weather Condition
7	211	July 30	128	305 610 1525	1129→ 1151	1.17	Clear Heavy Haze Light Wind
8	223	Aug. 11	136	305 610 1525	1306→ 1327	1.13	Heavy Cum. Cl. V. Heavy Haze Light Wind
9	231	Aug. 19	143	610 1525	1243→ 1321	1.23	Lt. Cirrus Cl. Mod. Haze Strong Wind
10	237	Aug. 25	146	305 610 1525	1340→ 1424	1.18	Clear Mod. Haze Calm
11	243	Aug. 31	150	305 610 1525	1331→ 1410	1.15	Clear Mod. Haze Light Wind
12	251	Sept. 8	155	305 610 1525	1320→ 1358	1.14	Clear Heavy Haze Strong Wind

TABLE 4.4. Continued.

Flight No.	Julian Date	Date	Mission No.	Altitudes m agl	Time cds	Incoming Radiation cal cm^{-2} min^{-1}	Weather Condition
13	278	Oct. 5	162	305 610 1525	1152→ 1323	0.94	Clear Mod. Haze Light Wind

Missions were planned to coincide, where possible, with critical soil moisture conditions in the field. Flights were planned for periods immediately before irrigations and soon after irrigations and rainfall.

Chapter V

ANALYSIS AND RESULTS

The objective of this research effort was to evaluate the capabilities of remote sensing to monitor soil moisture conditions. In Chapter III the complete theoretical energy balance approach was discussed (equation 3.1). In this analysis only the incoming radiation data, the reflected radiation data (photographic imagery), and the soil moisture data were utilized. Instrumentation and time limitations restricted the analyses to these variables. The remaining factors in the energy balance were assumed constant.

Imagery Analysis

In the imagery analysis, visual, laboratory and statistical analyses were utilized. The first step in the analysis was to visually interpret the data. Visual interpretation included using ground truth data to explain some of the anomalies that appeared on the imagery.

Thirteen aerial data collection missions were flown between June 17 and October 5, 1970. Four of these missions, June 25 (Julian Date 176), July 30 (211), August 25 (237), and October 5 (278), have been chosen as representative. Figure 5.1 is a print from the color infrared film (#8443) exposed on June 25 (176), 1970, showing the soil moisture plots. The sorghum fields are easily distinguished from the fallow. The tilled fallow also appears much darker than the chemically treated fallow because of the difference in the surface soil condition. The tilled fallow had been very recently disked. The

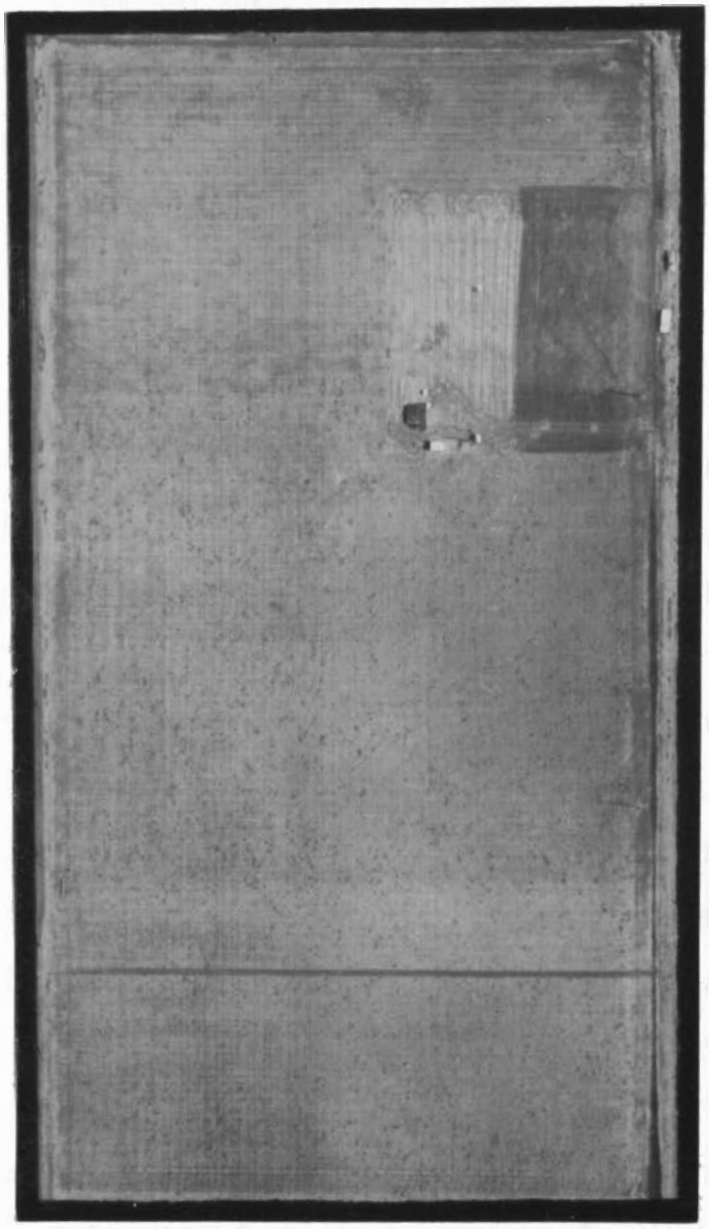

Figure 5.1 Print from color infrared film, #8443 with G15/30m filter, showing the soil moisture plots for June 25, 1970, 610m (2,000 ft) agl, 6X enlargement, scale: 1 cm = 16.5m.

near infrared reflectance of the sorghum appearing red on the film was very small since there was only 20 percent crop cover of the soil. The brighter red specks dispersed throughout the sorghum field were caused by infrared reflectance from clusters of volunteer corn plants that had more growth than the sorghum. The dark strip through the field in the same direction as the rows is assumed to be the result of the farm manager making one cultivation swath through the field. Three black and white films filtered in the green, red, and near infrared spectral bands were exposed simultaneously together with the color infrared film. The black and white film counterparts of Figure 5.1 are Figures E.1, E.2, and E.3 in Appendix E.

Figure 5.2 is a color infrared print exposed on July 30 (211), 1970. It was the seventh data collection flight and was three days after the second irrigation and a 3.94 cm rainfall. A slight contrast is apparent between the irrigated and non-irrigated sorghum, but considerable difference would not be expected because of the recent irrigation and rainfall. The cause of the longitudinal lines with the lighter red tone in the sorghum cannot be explained. A ground search for the anomaly was not successful. The only clue to its cause was that the field was fertilized in the north and south direction, and the feature may have been from a difference in fertilizer application rate. On the left of Figure 5.2 the irrigation supply ditch can be seen. A distinctive feature found in the tilled fallow is the division through the center. The upper half had just been disked at the time of overflight whereas the tilling in the lower half was

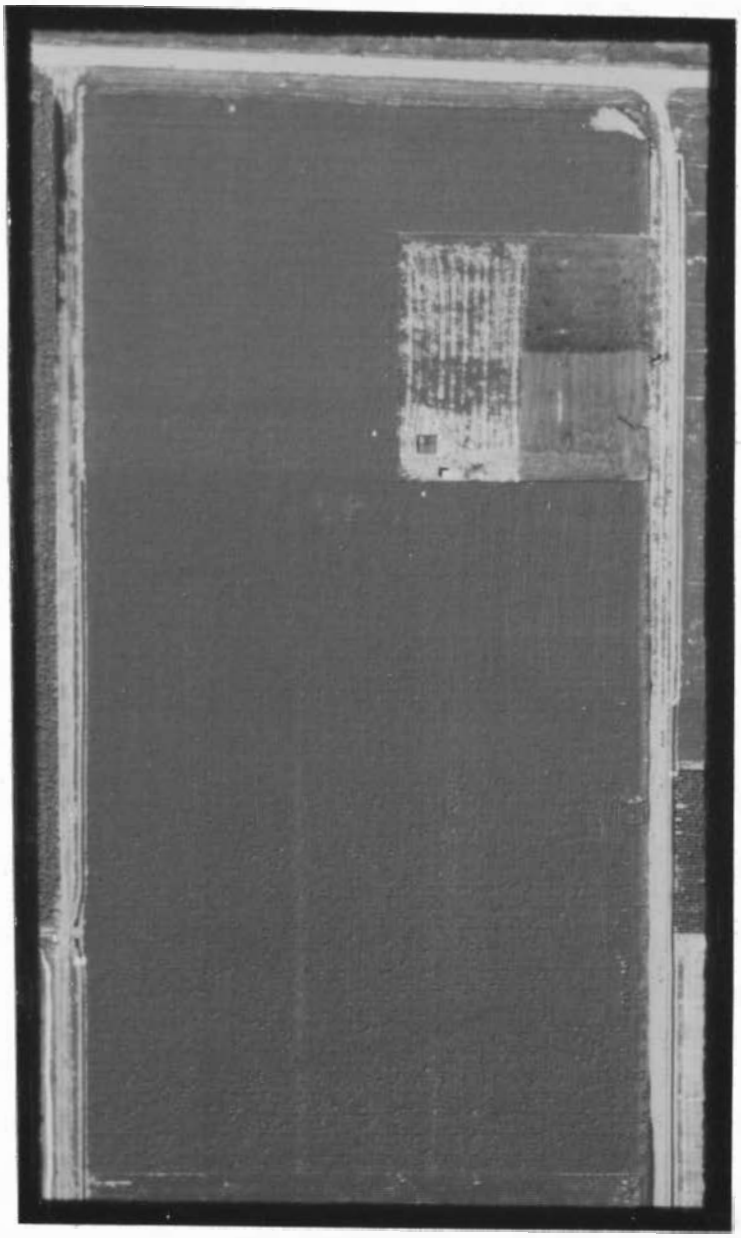

Figure 5.2 Print from color infrared film, #8443 with G15/30m filter, showing the soil moisture plots for July 30, 1970, 610m (2,000 ft) agl, 7X enlargement, scale: 1 cm = 17.8m.

incomplete. The black and white counterpart prints for Figure 5.2 are Figures E.4, E.5, and E.6 in Appendix E.

Figure 5.3 is a color infrared print of the imagery exposed on August 25 (237), 1970. No appreciable precipitation was received between the July 30th (211) flight and this one. A marked difference is evident between the two moisture treatments. Less color IR reflectance is evident in the irrigated sorghum as shown in the lower portion of the print. It should be noted that even after the long, dry period neither soil moisture data nor the condition of the sorghum indicated a stress condition for the non-irrigated sorghum. However, a substantial difference in available soil moisture was observed as indicated in Figures 4.3 through 4.6. The black and white prints exposed at the same time as Figure 5.3 are shown by Figures E.7, E.8, and E.9 in the appendix.

The last data collection mission was after the sorghum was completely mature on October 5 (278), 1970. As can be seen from Figure 5.4, maturation of the plant makes detection of stress conditions difficult. Little information is available on the soil moisture status. By close interpretation of the print, the pathways used by the researchers through the sorghum between the neutron access tubes are easily discernable. The last three figures in Appendix E are black and white counterparts of Figure 5.4 for the October 5, 1970, mission.

Thermal imagery was obtained for all aerial missions between July 24 (205) and October 5 (278), 1970. Instrument malfunction

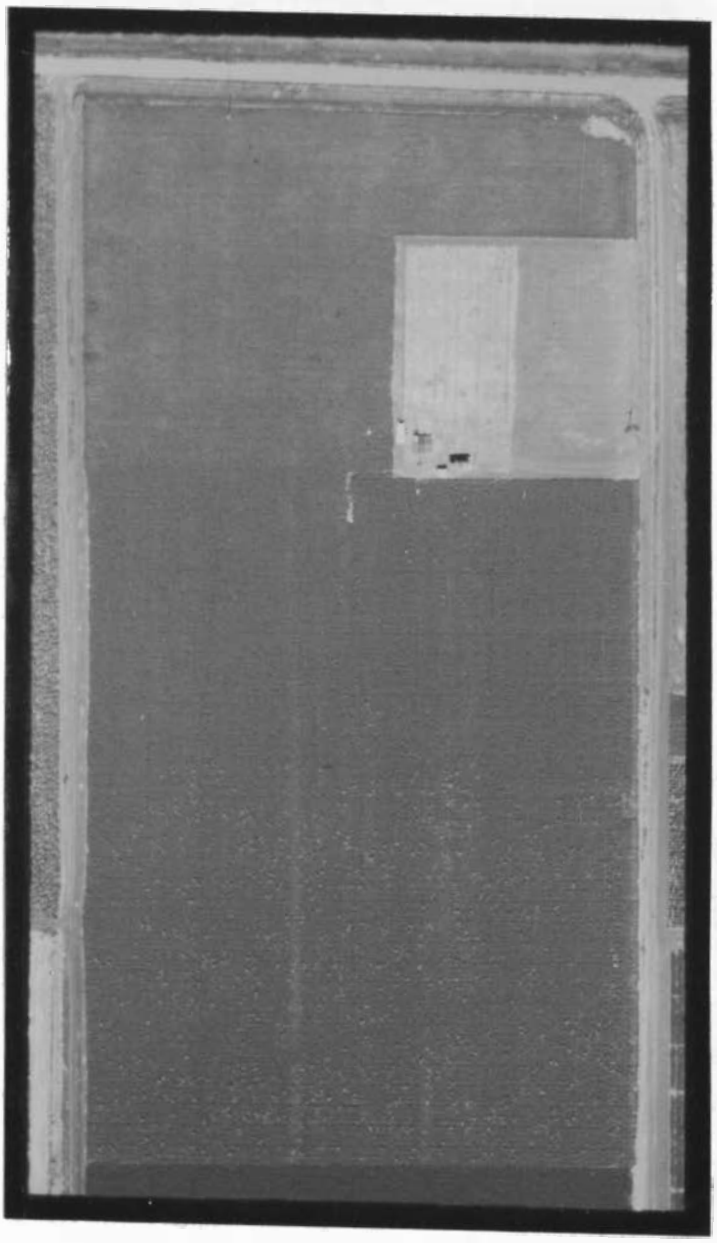

Figure 5.3 Print from color infrared film, #8443 with G15/30m filter, showing the soil moisture plots for August 25, 1970, 610m (2,000 ft) agl, 6.1X enlargement, scale: 1 cm = 18.3m.

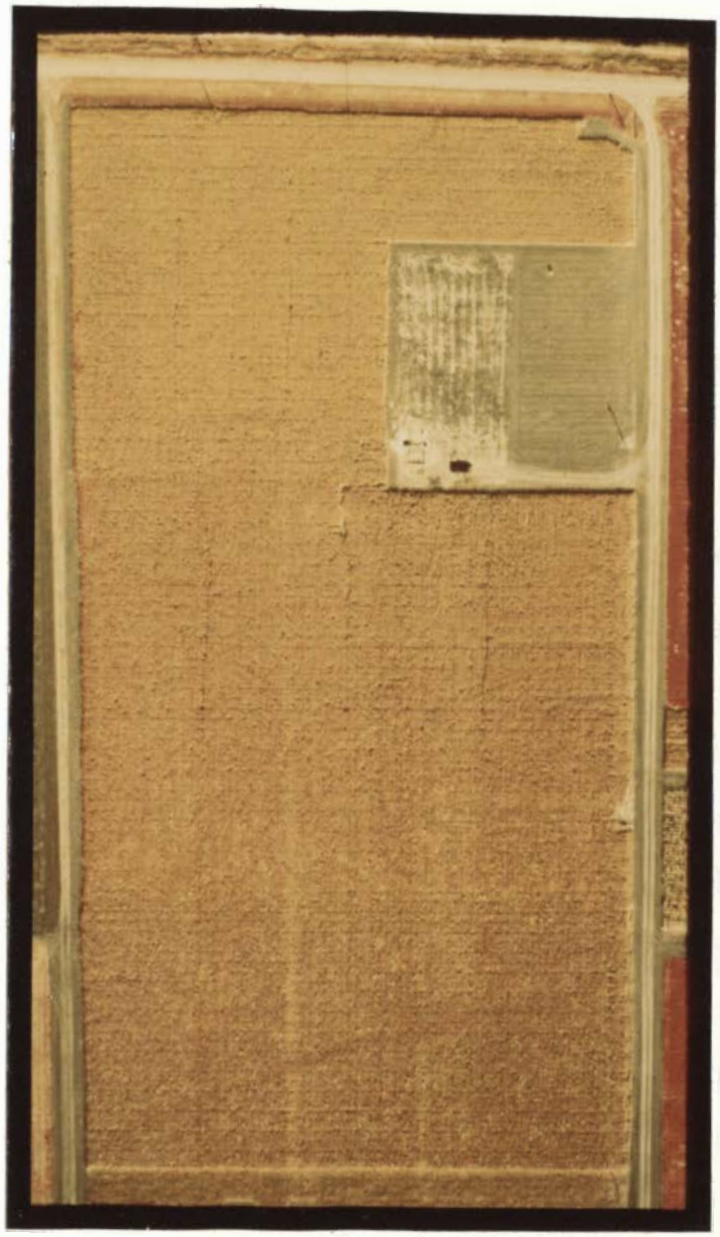

Figure 5.4 Print from color infrared film, #8443 with G15/30m filter, showing the soil moisture plots for October 5, 1970, 610m (2,000 ft) agl, 6.3X enlargement, scale: 1 cm = 17.8m.

caused much of the thermal imagery to be useless. The two best scans are exhibited by Figures 5.5 and 5.6. The first thermal scan in Figure 5.5 was collected July 24, 1970, and relates reasonable distinction between the irrigated and non-irrigated sorghum. The July 24th mission was 12 days after the first irrigation and one day before the second irrigation. Figure 5.6 is a thermal scan obtained on September 8 (251), 1970. The resolution of the imagery in Figure 5.6 is poorer than that for Figure 5.5, but does show a temperature difference between the two sorghum treatments. None of the other thermal imagery was usable because of the equipment problem.

The use of a color encoding film density analysis system, specifically designed for imagery interpretation, was the second method of imagery analysis. A technical description of this equipment is contained in Appendix D. The equipment consists of a black and white television camera, electronics, and a color television monitor. A photographic image is placed between the camera and a light source. The signal from the camera is processed by an electronic analyzer that separates the shades of gray on the image into as many as 32 film density levels and encodes color video signals for each level. A keyboard permits the operator to select any number of encoded levels for viewing on the color monitor. In the analysis of these data, five and two color levels were used. The two colors were sufficient for separation of the two soil moisture treatment effects in the sorghum. The electronic signal relating any number of density levels also lends itself to an automatic analysis system. In future studies within the

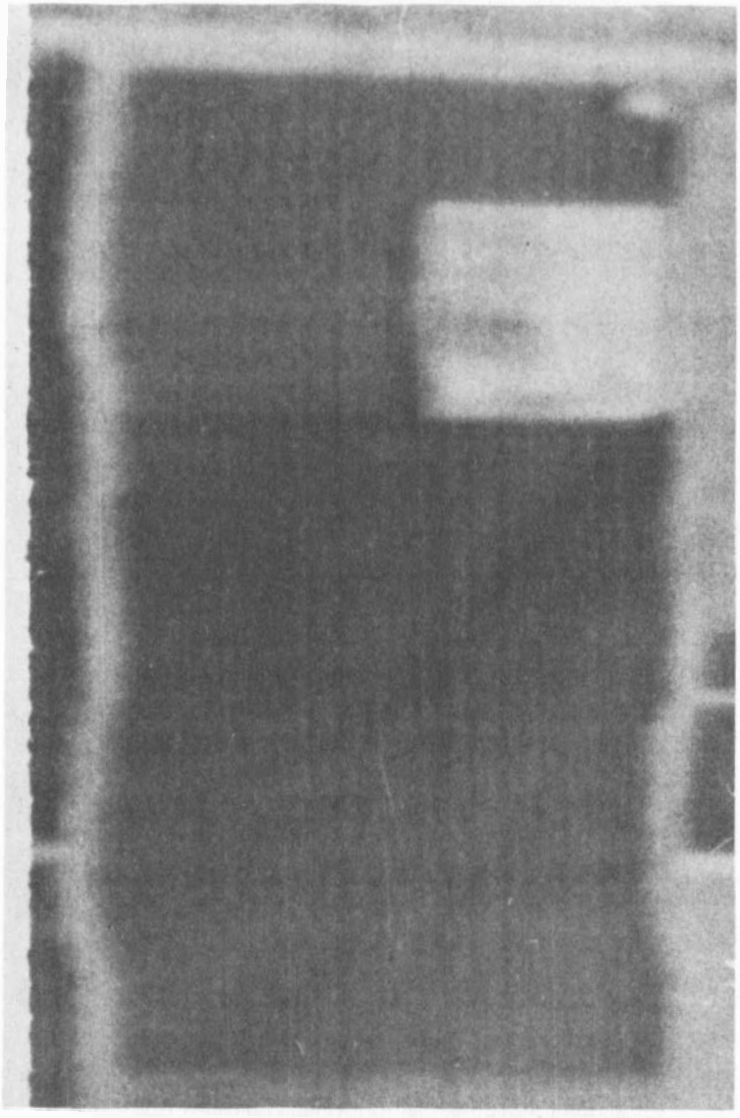

Figure 5.5 Print from thermal scan showing the soil moisture plots for July 24, 1970, 610m (2,000 ft) agl, scale: 1 cm = 18.6m.

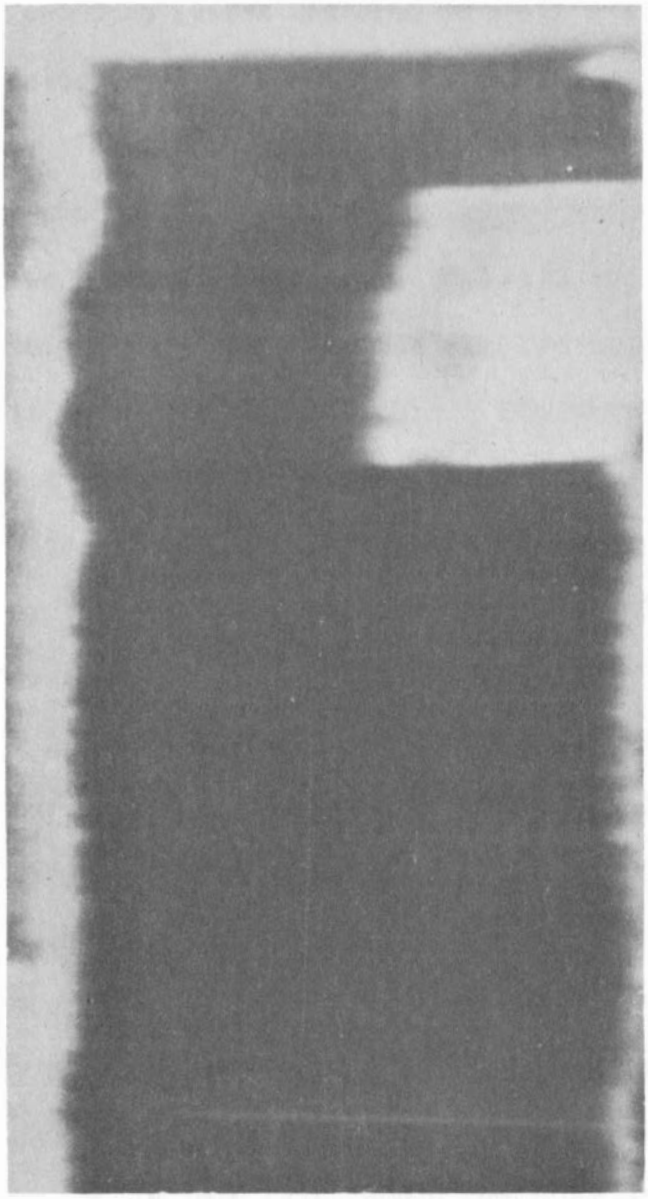

Figure 5.6 Print from thermal scan showing the soil moisture plots for September 8, 1970, 610m (2,000 ft) agl, scale: 1 cm = 18.6m.

Institute, a computer processing system will be available for this type of analysis.

The color encoding system was used to analyze all black and white imagery. The color infrared imagery was not analyzed on the color encoding system. The color encoding television camera is black and white. Density processing of the color imagery was attempted, but no better results were obtained than with the black and white imagery. Filtering the television camera so that only one layer of the color infrared film is viewed is also possible. This method was unsatisfactory because the available filters were too dense, and television viewing results in a severe loss of resolution. Future color encoding of color film by layers will require the obtaining of suitable filters adaptable to the system.

Figure 5.7 presents the data analysis of the green filtered film for the same four dates previously discussed. The color prints are obtained from 35 mm transparencies taken of the two-color image on the color monitor. The dates are June 25 (176), July 30 (211), August 25 (237), and October 5 (278), 1970. A, B, C, and D of Figure 5.7 are encoded density analyses of Figures E.1, E.4, E.7 and E.10 respectively. The blue areas have a higher film density than do the yellow areas. Blue, in this case, would therefore indicate greater reflectance within the green spectral bands since the black and white film is negative type. Slide A does not indicate any substantial soil moisture difference between treatments which is logical since there had been no irrigations. B, taken after the second irrigation,

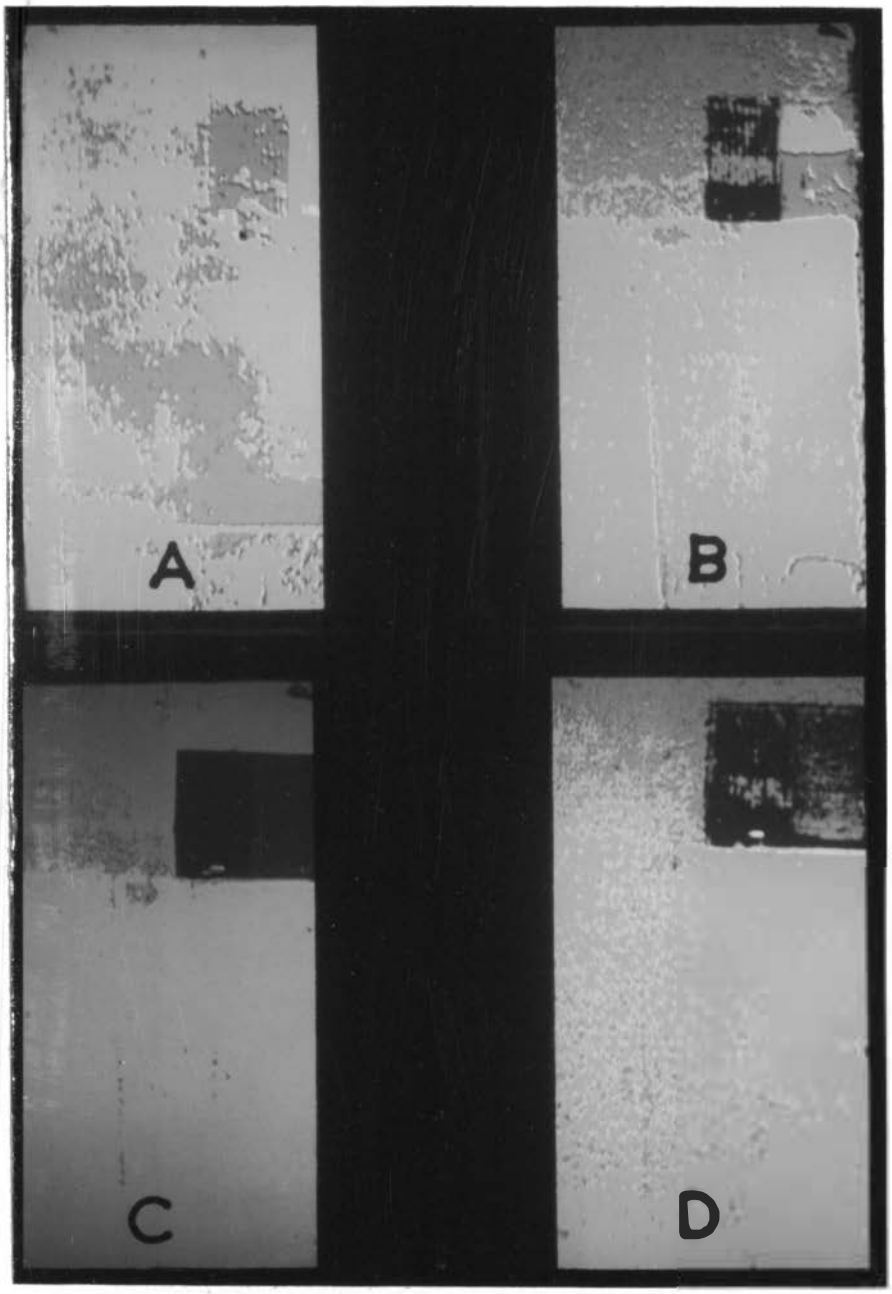

Figure 5.7 Spatial Data density analysis in two colors for the green filtered black and white film, #58, A is June 25, B is July 30, C is August 25, and D is October 5, 1970, (#1 is yellow and #2 is blue).

shows the treatment effects, and C shows treatment effects even more. D, from October 5, shows that differences are less prominent due to senescing of the plant and loss of green color.

The red filtered film as portrayed in Figure 5.8 by the color encoding system has nearly the same results as the green filtered films for June 25, but the results are much better throughout the remainder of the season. The A, B, C, and D parts of Figure 5.8 are respectively the density analyses of Figures E.2, E.5, E.8 and E.11. By both visual and color encoding analysis, the red filtered film relates the soil moisture conditions better than the other band-pass data.

Figure 5.9 is a two-color representation of the black and white infrared film on the same four missions. Likewise, parts A, B, C and D are the analysis of the imagery shown by Figures E.3, E.6, E.9 and E.12, respectively. Interpretation reveals that the infrared filtered film discloses very little information concerning the soil moisture conditions.

The third method of imagery analysis was the use of the film densitometers. Densitometers measure the spot film density of a transparency. The densitometer has four internal filter selections -- neutral, red, green, and blue. For the black and white films only the neutral filter was used because no colors are present in the film. All four filter readings were recorded and used with the color infrared film because of the multilayer response of that film. The color infrared film has three layer response. The near infrared

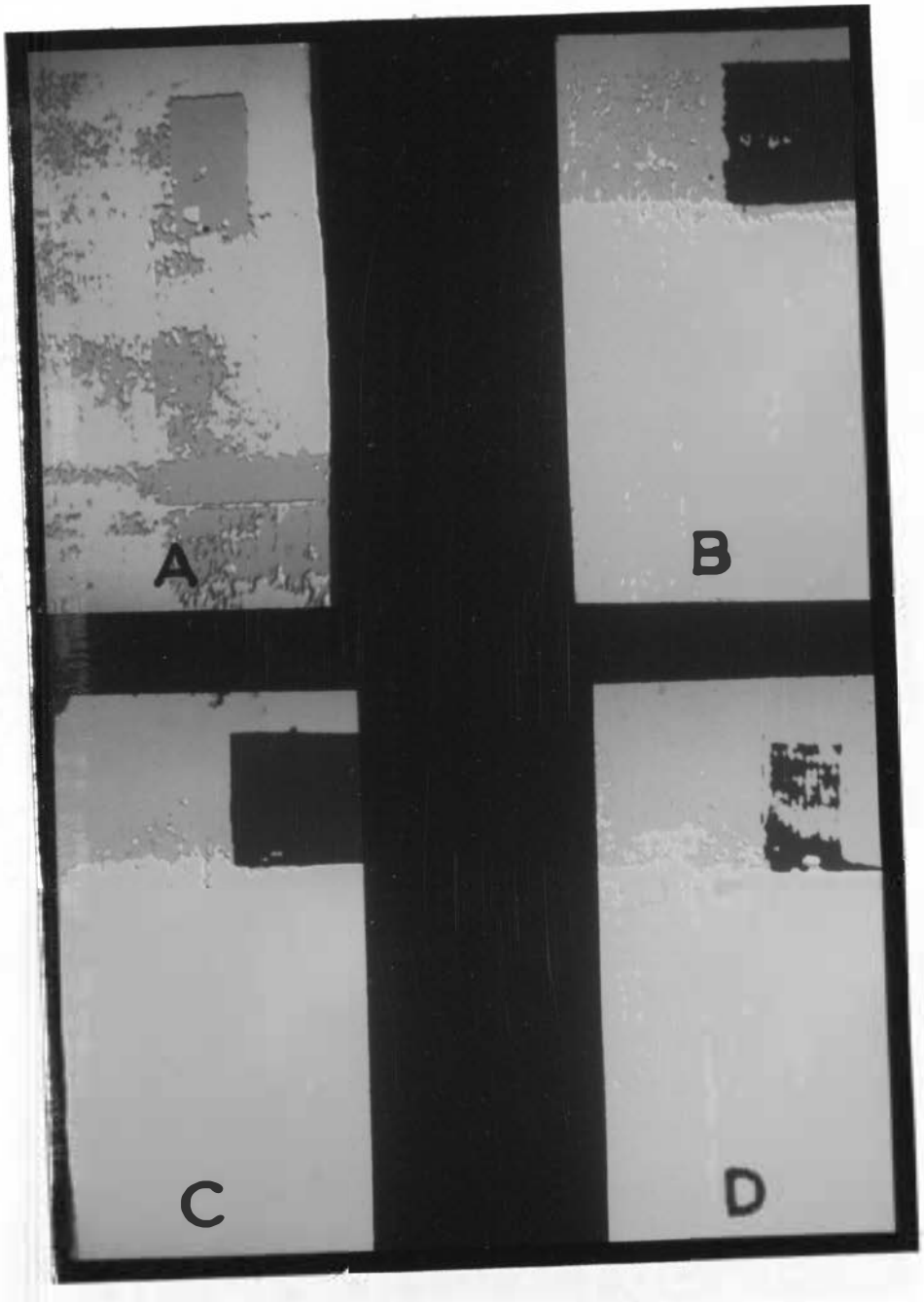

Figure 5.8 Spatial Data density analysis in two colors for the red filtered black and white film, #25A, A is June 25, B is July 30, C is August 25, and D is October 5, 1970, (#1 is yellow and #2 is blue).

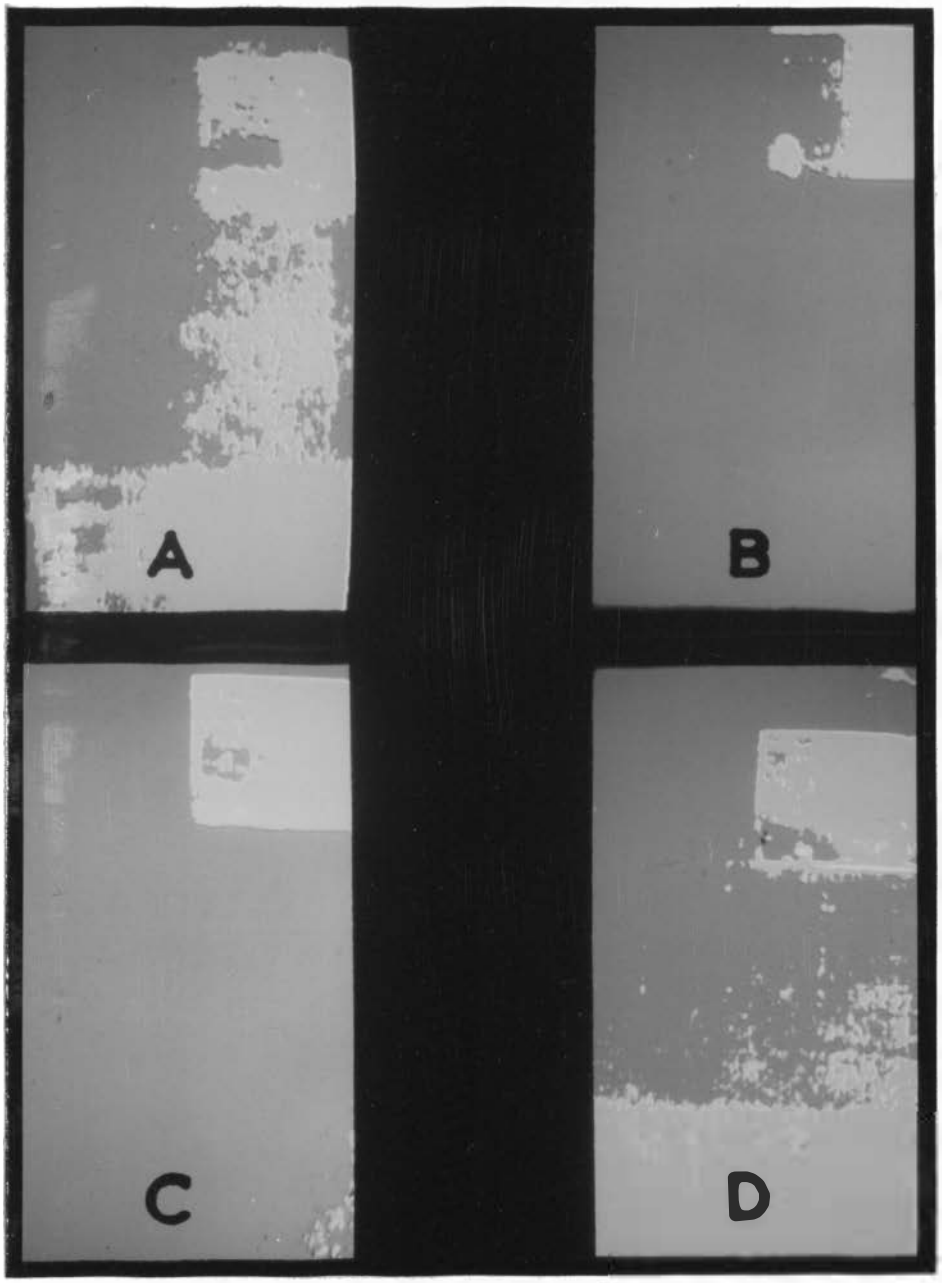

Figure 5.9 Spatial Data density analysis in two colors for the infrared filtered black and white film, #89B, A is June 25, B is July 30, C is August 25, and D is October 5, 1970.

radiation exposes the red layer, the red spectral band radiation exposes the green layer, and the green spectral band radiation exposes the blue layer. The red, green, and blue filters on the densitometer pass only the approximate spectral bands corresponding to the respective layers of the color infrared film. The neutral densitometer filter measures the total density, the red densitometer filter measures the near infrared spectral band density, the green densitometer filter measures the red spectral band density, and the blue densitometer filter measures the green spectral band density. Density values for the soil moisture study were read from the photos at points corresponding to the location of neutron access tubes on the ground. These film densities were then punched onto computer cards for use in computer analysis.

Density-Soil Moisture Analysis

Even though the film densities were taken from the imagery at the same location as the soil moisture reading, interpretation was difficult between the raw soil moisture and film density data. Performing a statistical analysis improved the ability to interpret results. The statistical method chosen was the linear correlation analysis. Correlation is a measure of the degree to which variables vary together (25), and therefore determines the similarities that exist between variables. The equation for the product-moment correlation, r, is

$$r = \frac{\Sigma(X-\bar{x})\ (Y-\bar{y})}{[\Sigma(X-\bar{x})\ \Sigma(Y-\bar{y})]^{\frac{1}{2}}} \qquad 5.1$$

where

X = value of the first variable,

Y = value of the second variable,

$\bar{x}$ = mean of the first variable, and

$\bar{y}$ = mean of the second variable.

Correlations were run on a seasonal and mission basis for sorghum and fallow at all soil moisture levels. Separate correlations were obtained for each flight altitude. Table 5.1 relates the seasonal correlation coefficients for respective film-filter combinations between altitudes of 610m (2,000 ft) above ground level (agl) and 1525m (5,000 ft) agl. The number of observations (n) are 195. All correlations are significant at the .01 level. The seasonal correlations in Table 5.1 between the 610m and 1525m altitudes are quite high, showing that nearly the same field conditions were sensed.

TABLE 5.1. SEASONAL CORRELATION COEFFICIENTS BETWEEN ALTITUDES OF 610m (2,000 ft) agl AND 1525m (5,000 ft) agl.

Variables	r
Black and White, #58, Green Spectral Band	0.887
Black and White, #25A, Red Spectral Band	0.951
Black and White, #89B, Infrared Spectral Band	0.973
Color IR Total	0.826
Color IR Green Spectral Band	0.846
Color IR Red Spectral Band	0.883
Color IR Infrared Spectral Band	0.933

Correlation coefficients were computed between all combinations of the film densities and soil moisture in the two sorghum treatments. After the calculation of the correlations, the significance of each value was determined. The mission correlation coefficients were plotted versus time for accumulated soil moisture depths to 121.92 cm at increments of 30.48 cm. Separate graphs were drawn for each film-densitometer-filter combination. The algebraic signs of the correlation coefficients were changed for the black and white films since they are negative type films. This allows comparison of correlations for the same spectral bands; for example, the red band from the black and white film and from the color infrared film. On each graph, lines connecting the surface 30.48 cm points and the 91.44 cm points are drawn. The sorghum roots penetrated to about the 91 cm depth. Curves connecting the 60.96 cm and 121.92 cm depths were omitted to simplify the figures.

Figure 5.10 is a plot of the correlations of data from the color infrared film with the neutral densitometer filter. Points above the line marked * are correlations significantly different from zero at the .05 level where the number of observations (n) are equal to 15. The line ** shows significance at the .01 level. A correlation of zero means that variation of one variable has no affect on the other variable. A correlation of positive one means that as one variable changes, the other changes identically. A positive one value occurs when a variable is correlated with itself. The correlations were much lower at the start of the season before the crop canopy fully

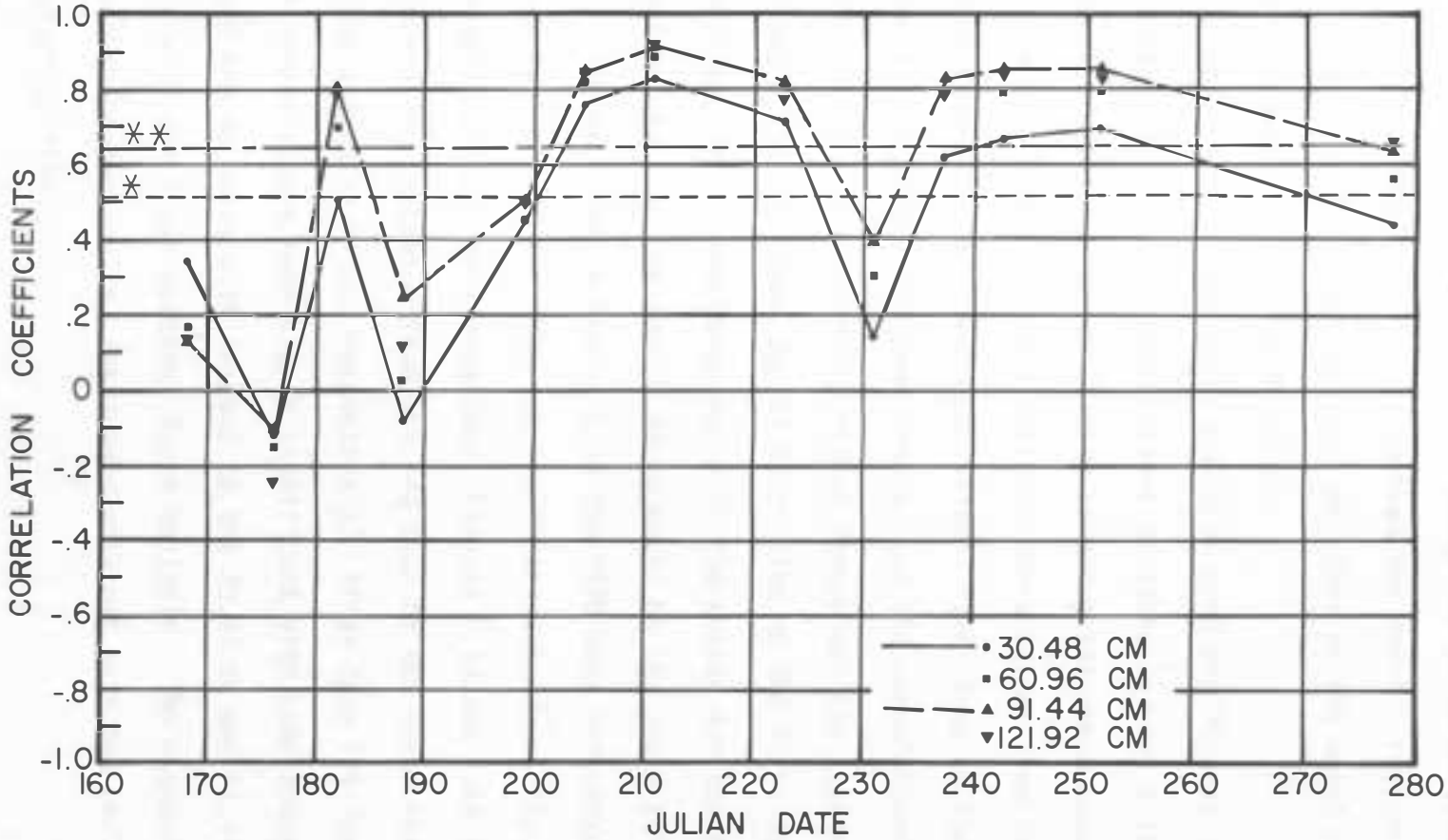

Figure 5.10 - Mission correlation coefficients plotted against time for the available soil moisture in the sorghum versus film density from the color infrared film with the neutral filter.

developed. The 30.48 cm line is below the 91.44 cm line throughout all but one mission, indicating that the overall response of the color infrared film describes the soil moisture of the total root zone better than it does the surface 30.48 cm.

The graphs of the green spectral band are Figures 5.11 and 5.12. Figure 5.11 shows the correlations obtained between soil moisture and the layer from the color IR film relating the green spectral band. Figure 5.12 shows the soil moisture correlations from the black and white film with the green band filter. The lines on the two graphs generally disclose the same trends, and the correlations from the color IR film are generally higher throughout the season. The 30.48 cm depth line is above the 91.44 cm line on the first two dates. The small amount of crop cover early in the season and the higher relative soil moisture in the top 30.48 cm would be the cause for this.

The correlation analysis of the 1970 data indicated just as the imagery analysis did that the red filtered band was the most valuable in soil moisture determination. Figures 5.13 and 5.14 are graphs of correlations obtained from the red band of the color infrared and black and white films, respectively. After date 199 (July 18), almost all correlations were highly significant with some above 0.90. The same trends exist with respect to the 30.48 cm and 91.44 cm curves as did with the green spectral layer analysis. The highest correlations throughout the entire season were obtained with the red filtered black and white film.

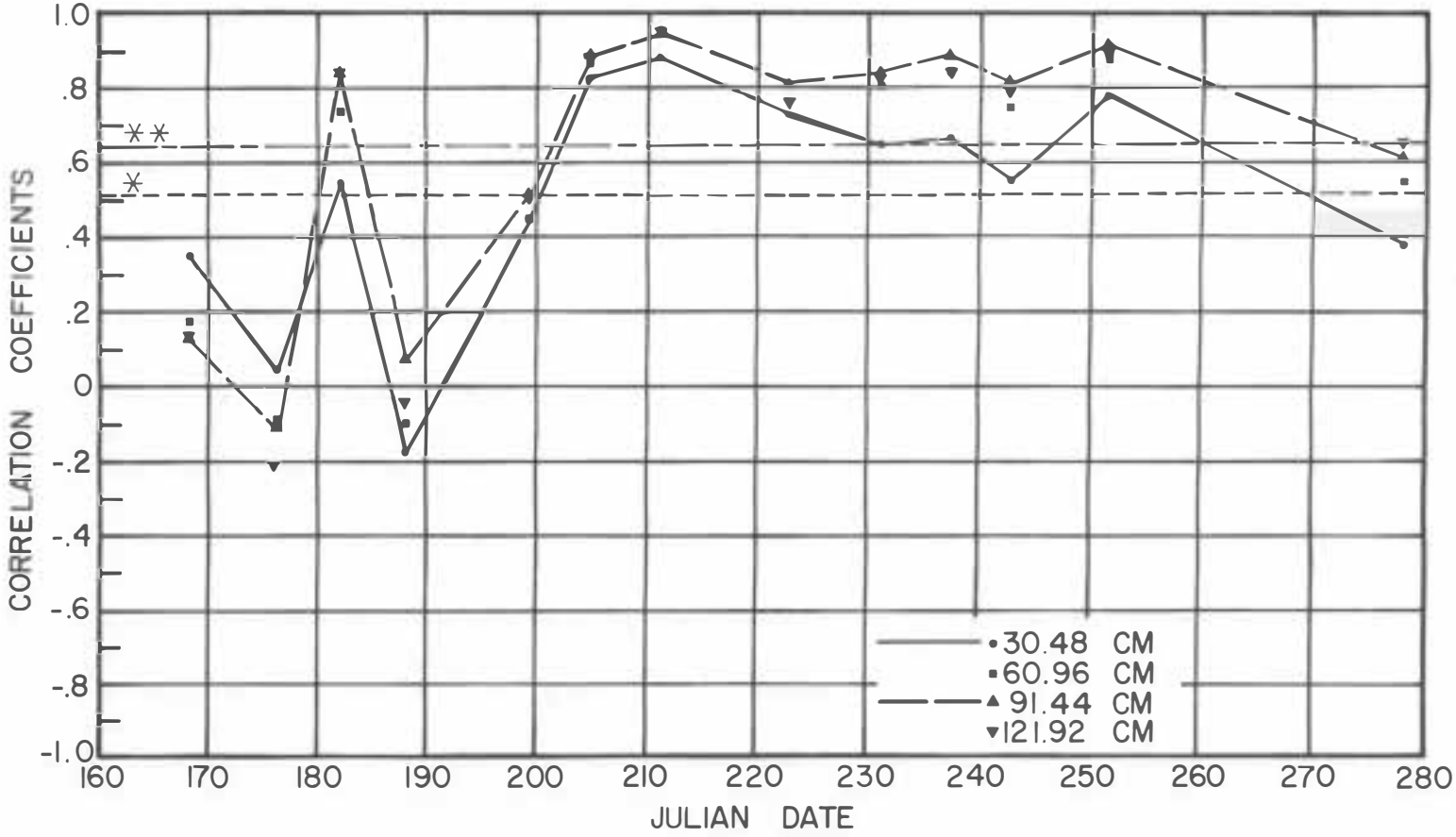

Figure 5.11 - Mission correlation coefficients plotted against time for the available soil moisture in the sorghum versus film density from the green band of the color infrared film.

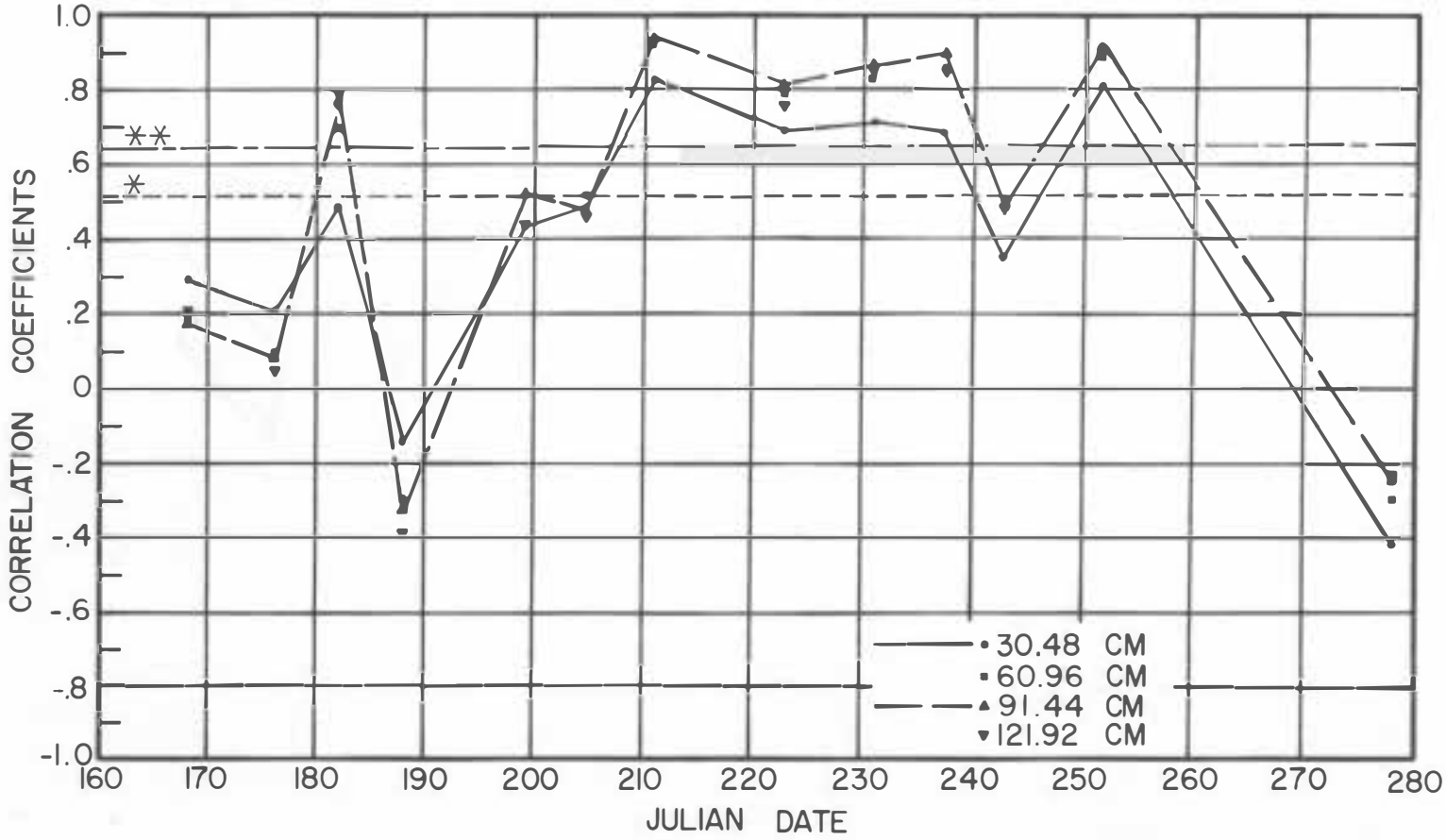

Figure 5.12 - Mission correlation coefficients plotted against time for the available soil moisture in the sorghum versus film density from the green filtered black and white film, #58.

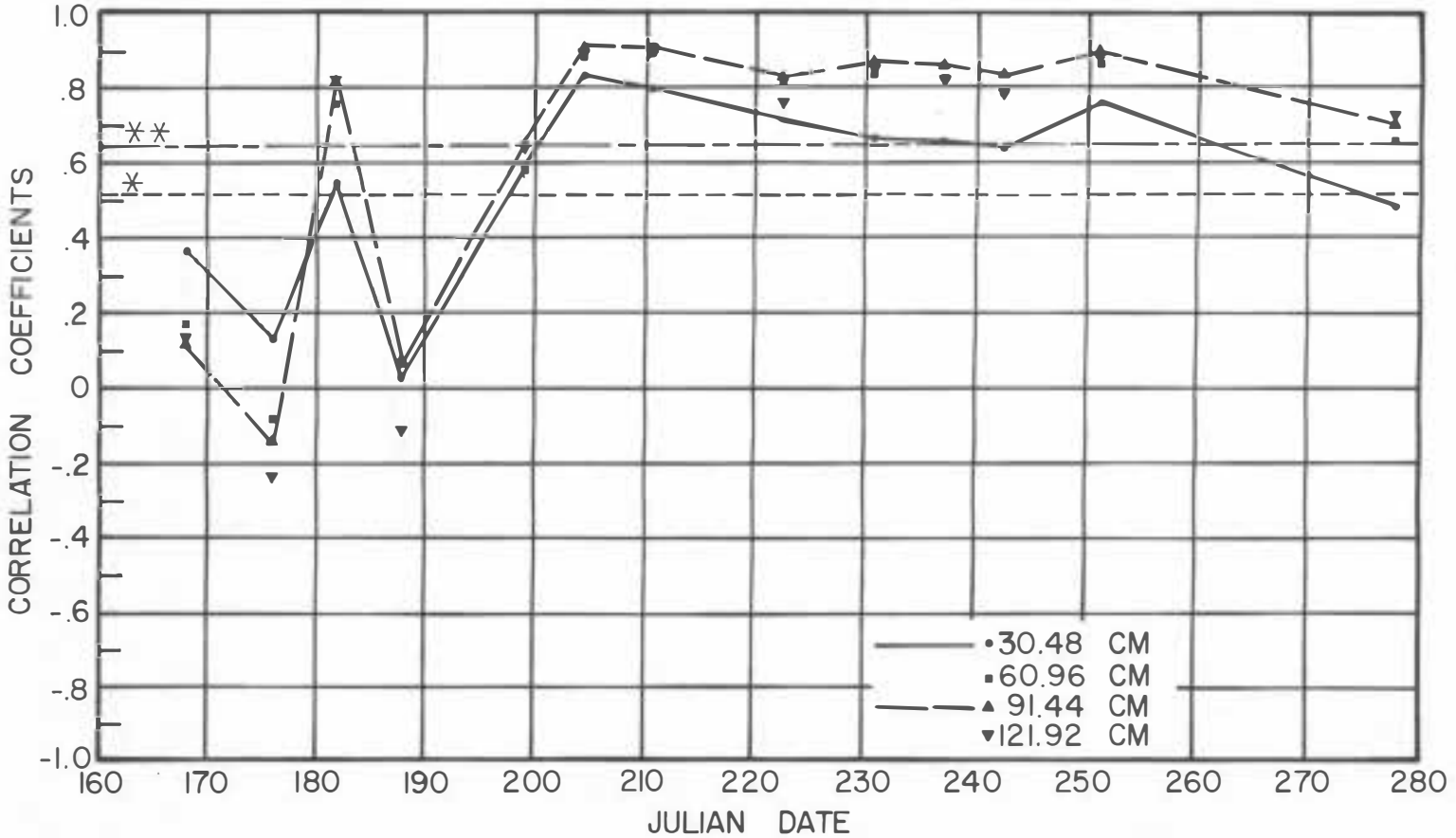

Figure 5.13 - Mission correlation coefficients plotted against time for the available soil moisture in the sorghum versus film density from the red band of the color infrared film.

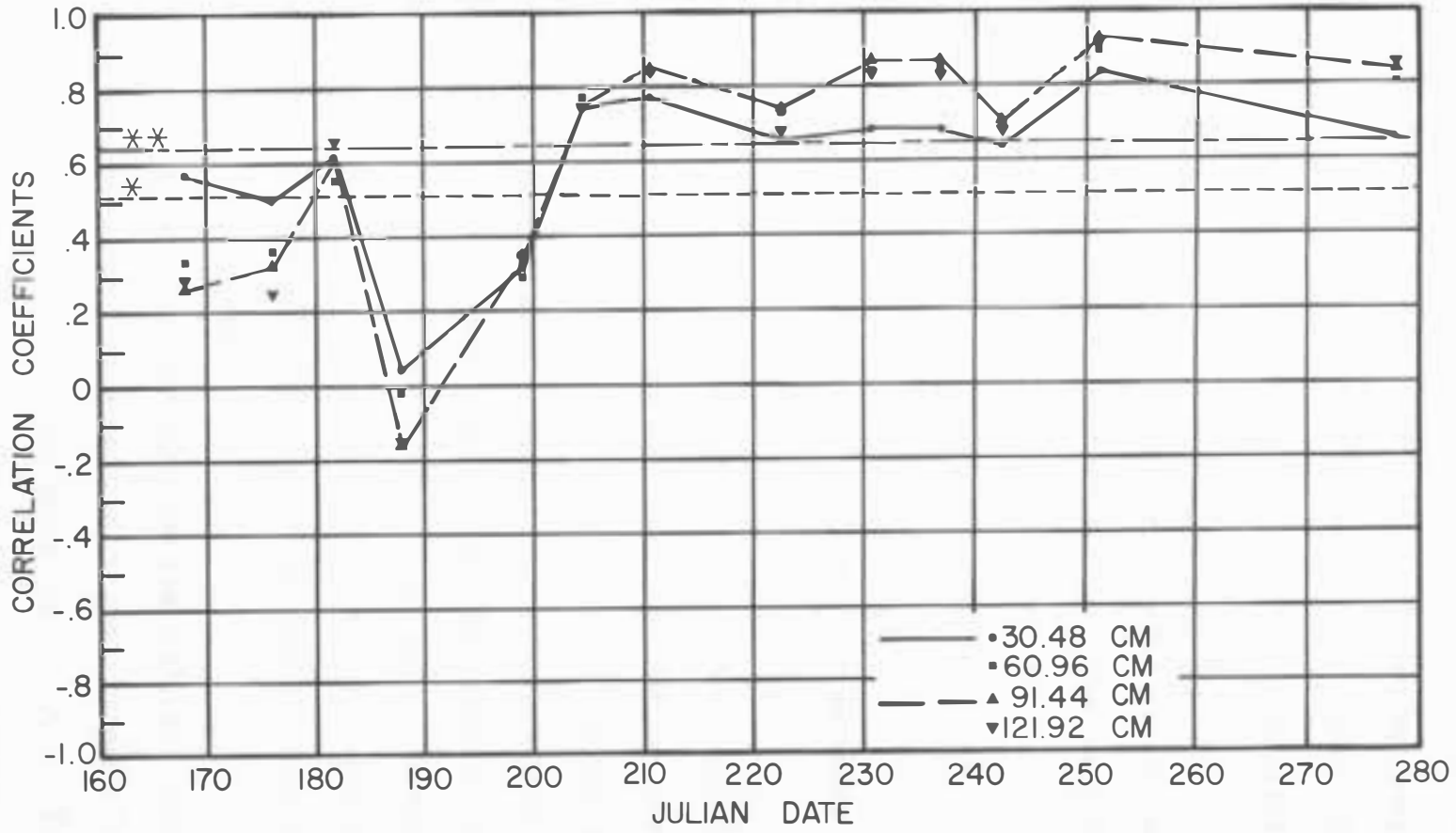

Figure 5.14 - Mission correlation coefficients plotted against time for the available soil moisture in the sorghum versus film density from the red filtered black and white film, #25A.

Figures 5.15 and 5.16 are the correlations from the infrared filtered bands. The values are so inconsistent and erratic that no definite or well-explained conclusions could be made. These results verify the previous indications that no conclusive relationship exists between infrared reflectance and soil moisture.

The curves in Figures 5.10 through 5.16 have various dips as a result of low correlations for a given day. The low correlations on each figure for Julian date 188 (July 7) may be explained by the time of the flight. The flight time was between 1628 and 1639 (Table 4.5), which is much later in the afternoon than the other missions. Decreased radiation and change in illumination geometry would result from the late flight time.

Certain other low correlations are not consistent between film-densitometer-filter combinations. For example, the low correlations shown on Figure 5.10 for date 231 (August 19) are not evident on the other graphs except for Figures 5.15 and 5.16 showing the infrared filtered band. Overlap of layer sensitivity and instability of the color infrared film may have contributed to these low correlations. Low correlations for the total density data of the color infrared film are caused by a combination of one or more of the three layers in the film.

The discrepancy between the same spectral band, such as green, red, or near infrared, where one figure was obtained from the color infrared film and the other from the black and white film, may be the result of the difference in spectral sensitivity between the two films.

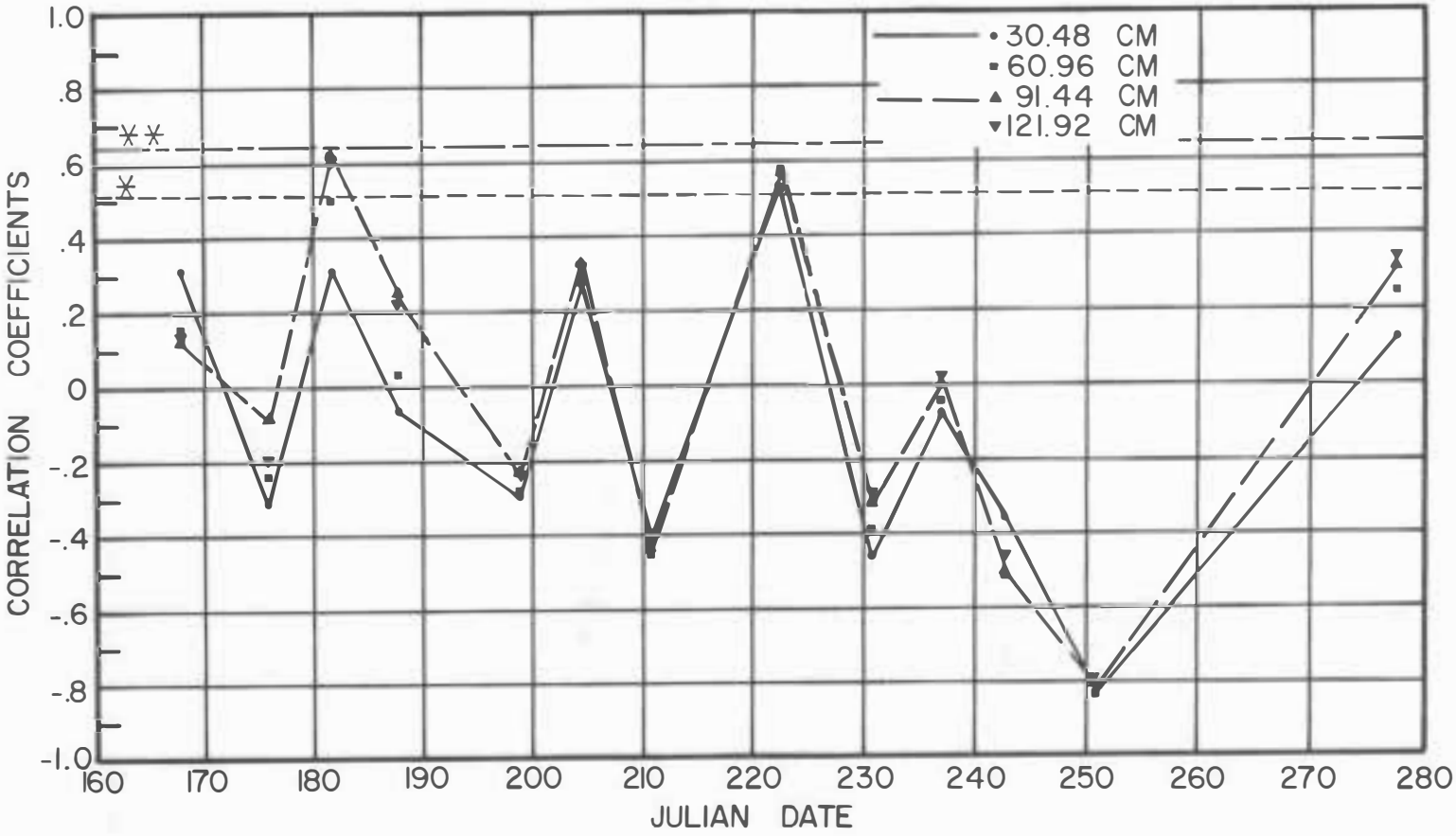

Figure 5.15 - Mission correlation coefficients plotted against time for the available soil moisture in the sorghum versus film density from the infrared band of the color infrared film.

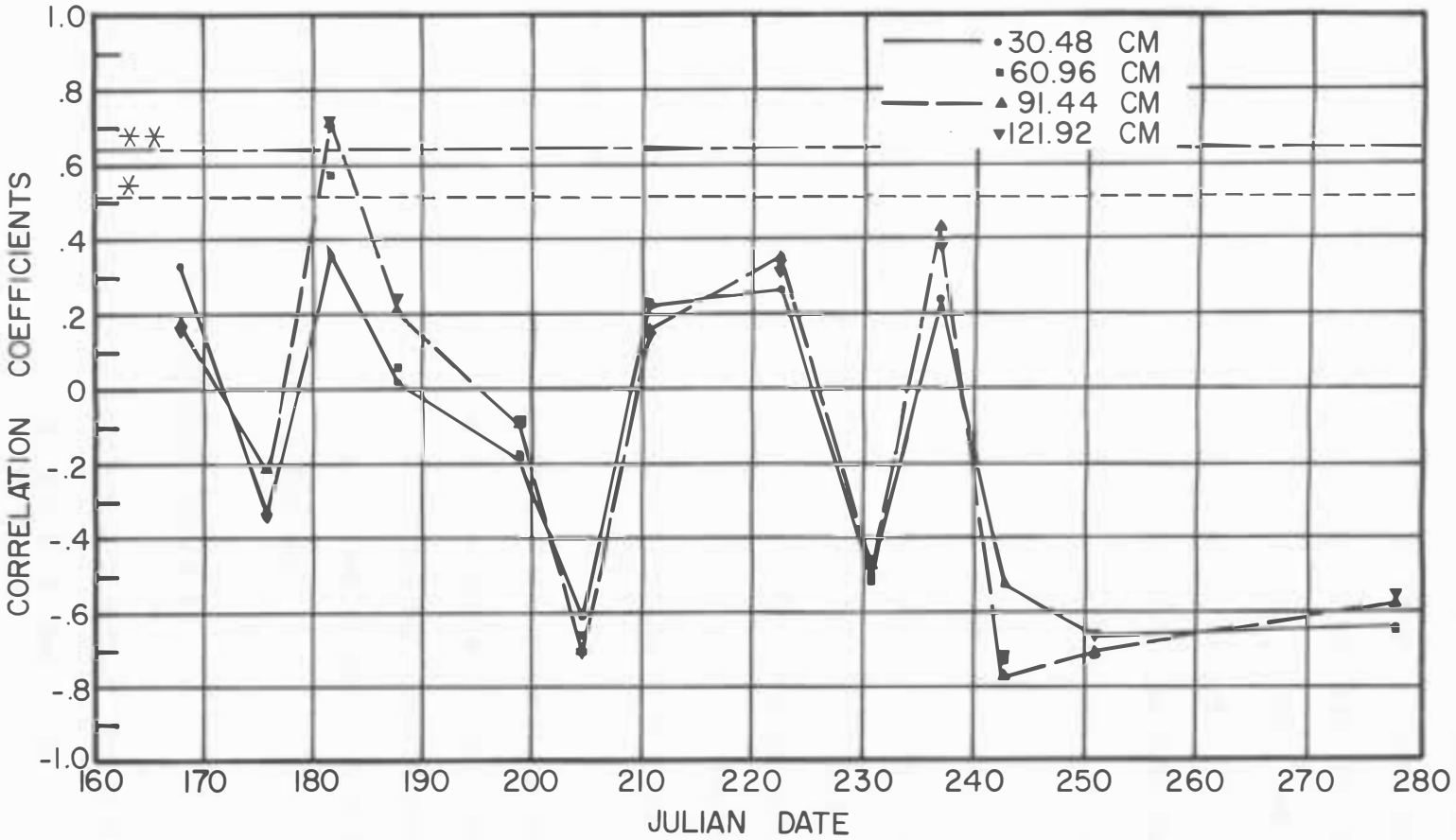

Figure 5.16 - Mission correlation coefficients plotted against time for the available soil moisture in the sorghum versus film density from the infrared filtered black and white film, #89B.

The layers of the color infrared film are not precisely sensitive to given spectral bands (16). A certain amount of band overlap is encountered for color layer formation. The black and white films, however, are filtered for specific spectral bands, and filtering is limited only by the choice of available filters. This theory may explain the difference between Figures 5.11 and 5.12 for the date 278 (October 5). On Figure 5.12 the low correlations for date 278 are related to the loss of green reflectance or color of the sorghum with complete maturity. The correlations in Figure 5.11 from the green layer of the color film are affected somewhat due to overlap in sensitivity. This may explain why the correlations in Figure 5.11 remain higher than those from Figure 5.12 for date 278. The low correlation coefficients for date 243 (August 31) shown on Figures 5.11, 5.12, and 5.14 cannot be explained by either the aerial or ground truth data.

A detailed study of the correlation differences between various film-densitometer-filter combinations was not within the scope of this research effort. However, future detailed study of these observations is indicated and may provide considerable insight into more sophisticated and valuable analysis techniques.

Corrected Density-Soil Moisture Analysis

In order to obtain a complete analysis of the film density as it might relate to soil moisture, the variables other than soil moisture that contribute to the variation in density need to be considered.

This was discussed in Chapter III. Determination of the incoming radiation within given spectral bands, the reflectances of the surfaces, and the relative crop cover make the use of equation 3.8 possible.

At the Research Center, the percent of ground cover by the sorghum was evaluated at the time of overflights; therefore, f and (1-f) are readily available for equation 3.8. Methods for determining spectral distribution of the incoming radiation and the surface reflectance were not available in the 1970 study. Therefore, two assumptions had to be made in order to continue the analysis. They are as follows:

1. the spectral distribution of the incoming radiation was constant throughout the season, and
2. the spectral reflectance responses of the crop and soil were constant throughout the season with the exception of variation primarily caused by changes in soil moisture.

With these assumptions, equation 3.8 can be used. The values for the spectral intensity for incoming radiation were obtained from Figure 5.17 taken from Gates (7). The radiation factor, RF, from equation 3.7 is obtained by integrating the area under the curve within each band for each film-filter combination and dividing this value by the total area under the curve.

The soil and crop reflectance values were obtained by use of Figures 5.18 (a) and (b) (13, 19) which show the percent reflectance for a soil similar to that on the Redfield Farm and for grain sorghum.

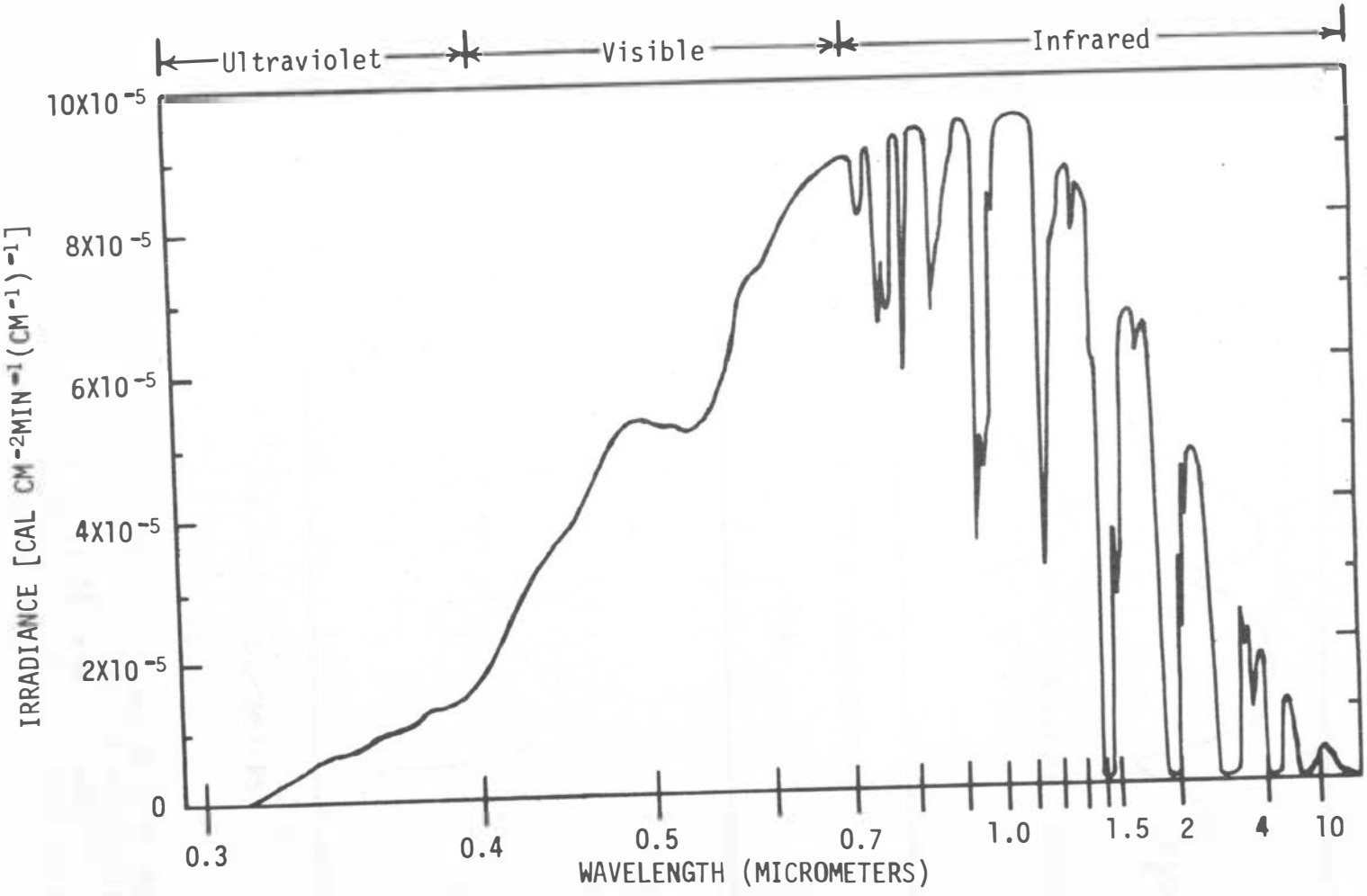

Figure 5.17 - Spectral distribution of solar radiation at sea level for a clear day from Gates (7).

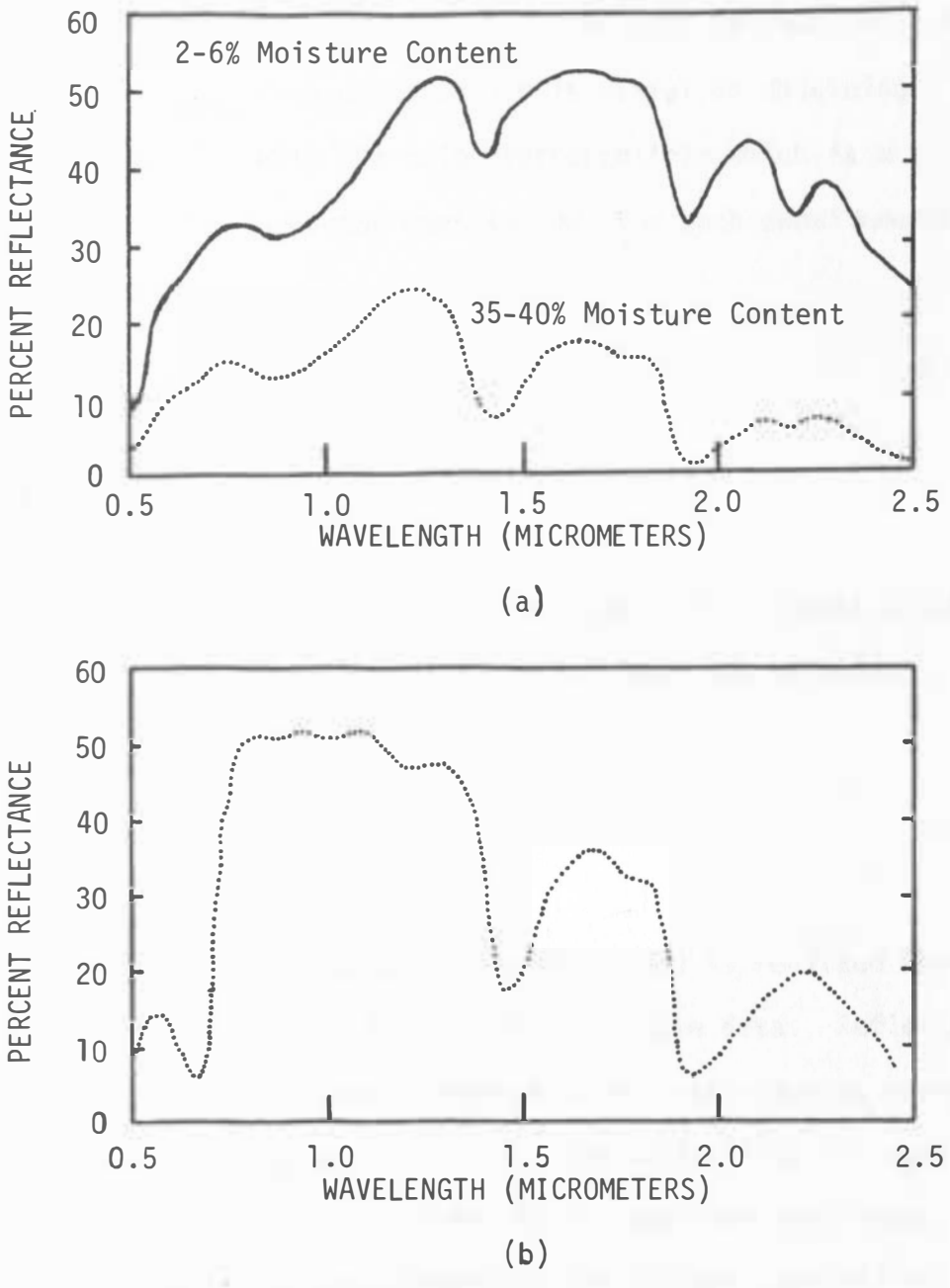

Figure 5.18 - (a) Spectral reflectance of clay soils at two moisture contents as a function of wavelength from Hoffer, et.al.,(13), and (b) Spectral reflectance of grain sorghum as a function of wavelength from Myers (18).

The average reflectance values within the ranges of given film-filter combinations were obtained from Figure 5.18 and used in equation 3.8.

The value of $R_{\rho band}$ from equation 3.8 is useful in obtaining a corrected film density. With the color infrared film which is a positive type film, the corrected density, DC, for each densitometer filter is obtained by

$$DC = R_{\rho band}\ (D), \qquad 5.2$$

where

D = film density.

For the negative type black and white films, the density needs to be inverted to obtain the proper relationship and then the corrected density is

$$DC = R_{\rho band}\ \left(\frac{1}{D}\right). \qquad 5.3$$

The advantage of a procedure such as the above is realized when performing analysis upon seasonal or highly variable data. Reflected radiation is a function of incoming radiation and reflectance, where reflectance is described by equation 3.5. The variability of incoming radiation can be measured and accounted for by applying equations 3.7 and 3.8. In the future the measurement of the factors controlling reflectance by detailed ground truth data collection and improved instrumentation may make isolation and analysis of soil moisture possible. Eliminating the necessity for the two assumptions by

additional instrumentation and measurements may make the procedure quite effective in analyzing a multitude of agriculture and hydrologic parameters.

A complete correlation analysis was run on the corrected densities for the season and for all individual missions. Since no correction was performed between data for a given mission, the correlations by missions for the corrected densities are essentially the same correlations as shown in Figure 5.10 through 5.16. The seasonal correlations are, however, quite different between the corrected and uncorrected densities. Table 5.2 gives the seasonal correlations between five soil moisture readings and the seven film-densitometer-filter combinations for film density. Table 5.3 is similar except for the substitution of corrected density correlations in place of the regular density correlations. Comparison of the two tables reveals that the correction procedure has made the film densities more reliable for predicting soil moisture. Certain correlations more than doubled. The significance is shown by * for the .05 level and by ** for the .01 level where the number of observations (n) are 195.

Another method of illustrating the benefit of correcting densities is to plot the available soil moisture versus both corrected and uncorrected densities. Figures 5.19 through 5.22 are plots of the available soil moisture in the top 91.44 cm versus each film-filter combination. The top 91.44 cm was used because it encompasses most of the sorghum root zone. Figure 5.19 represents the black and white

TABLE 5.2. SEASONAL CORRELATION COEFFICIENTS FOR FILM DENSITIES FROM 610m (2,000 ft) agl AND SOIL MOISTURE ACCUMULATED DEPTHS TO 121.92 cm FOR GRAIN SORGHUM.

	1 Gravimetric Soil Moisture Top 30.48 cm	2 Neutron Soil Moisture Top 30.48 cm	3 Neutron Soil Moisture Top 60.96 cm	4 Neutron Soil Moisture Top 91.44 cm
1 Gr. Soil Moist. Top 30.48 cm	1.000 **			
2 Soil Moist. Top 30.48 cm	.647 **	1.000 **		
3 Soil Moist. Top 60.96 cm	.641 **	.946 **	1.000 **	
4 Soil Moist. Top 91.44 cm	.611 **	.899 **	.987 **	1.000 **
5 Soil Moist. Top 121.92 cm	.579 **	.883 **	.972 **	.993 **
6 Density B&W #58 Green	-.017	.044	-.024	-.024
7 Density B&W #25A Red	-.181 -*	-.114	-.247 -**	-.360 -**
8 Density B&W #89B Infrared	.249 **	-.024	-.002	.045
9 Density Color IR Neutral	.238 **	.299 **	.273 **	.270 **
10 Density Color IR Green	.067	.027	.081	.119
11 Density Color IR Red	.393 **	.290 **	.351 **	.399 **
12 Density Color IR Infrared	.004	.130	.037	.013

TABLE 5.2. Continued.

	5 Neutron Soil Moisture Top 121.92 cm	6 Density B&W #58 Green	7 Density B&W #25A Red	8 Density B&W #89B Infrared
1 Gr. Soil Moist. Top 30.48 cm				
2 Soil Moist. Top 30.48 cm				
3 Soil Moist. Top 60.96 cm				
4 Soil Moist. Top 91.44 cm				
5 Soil Moist. Top 121.92 cm	1.000 **			
6 Density B&W #58 Green	-.023	1.000 **		
7 Density B&W #25A Red	-.360 -**	.477 **	1.000 **	
8 Density B&W #89B Infrared	-.096	.239 **	-.543 -**	1.000 **
9 Density Color IR Neutral	.259 **	.070	.093	-.018
10 Density Color IR Green	.150 *	-.366 -**	-.576 -**	.372 **
11 Density Color IR Red	.432 **	-.029	-.600 -**	.656 **
12 Density Color IR Infrared	-.061	.113	.672 **	-.588 -**

TABLE 5.2. Continued.

	9 Density Color IR Neutral	10 Density Color IR Green	11 Density Color IR Red	12 Density Color IR Infrared
1 Gr. Soil Moist. Top 30.48 cm				
2 Soil Moist. Top 30.48 cm				
3 Soil Moist. Top 60.96 cm				
4 Soil Moist. Top 91.44 cm				
5 Soil Moist. Top 121.92 cm				
6 Density B&W #58 Green				
7 Density B&W #25A Red				
8 Density B&W #89B Infrared				
9 Density Color IR Neutral	1.000 **			
10 Density Color IR Green	.572 **	1.000 **		
11 Density Color IR Red	.615 **	.772 **	1.000 **	
12 Density Color IR Infrared	.698 **	-.001	-.127	1.000 **

* Significant at .05 level (> .140).

** Significant at .01 level (> .184).

TABLE 5.3. SEASONAL CORRELATION COEFFICIENTS FOR CORRECTED FILM DENSITIES FROM 610m (2,000 ft) agl AND SOIL MOISTURE ACCUMULATED DEPTHS TO 121.92 cm FOR GRAIN SORGHUM.

	1 Gravimetric Soil Moisture Top 30.48 cm	2 Neutron Soil Moisture Top 30.48 cm	3 Neutron Soil Moisture Top 60.96 cm	4 Neutron Soil Moisture Top 91.44 cm
1 Gr. Soil Moist. Top 30.48 cm	1.000 **			
2 Soil Moist. Top 30.48 cm	.647 **	1.000 **		
3 Soil Moist. Top 60.96 cm	.641 **	.946 **	1.000 **	
4 Soil Moist Top 91.44 cm	.611 **	.899 **	.987 **	1.000 **
5 Soil Moist. Top 121.92 cm	.579 **	.883 **	.972 **	.993 **
6 Cor. Den. B&W #58 Green	.198 **	.230 **	.323 **	.333 **
7 Cor. Den. B&W #25A Red	.230 **	.652 **	.735 **	.751 **
8 Cor. Den. B&W #89B Infrared	-.146 -*	.037	.026	.010
9 Cor. Den. Color IR Neutral	.277 **	.166 *	.174 *	.201 **
10 Cor. Den. Color IR Green	.154 *	.246 **	.295 **	.335 **
11 Cor. Den. Color IR Red	.354 **	.624 **	.646 **	.660 **
12 Cor. Den. Color IR Infrared	.031	.114	.032	.006

TABLE 5.3. Continued.

	5 Neutron Soil Moisture Top 121.92 cm	6 Corrected Density B&W #58 Green	7 Corrected Density B&W #25A Red	8 Corrected Density B&W #89B Infrared
1 Gr. Soil Moist. Top 30.48 cm				
2 Soil Moist. Top 30.48 cm				
3 Soil Moist. Top 60.96 cm				
4 Soil Moist. Top 91.44 cm				
5 Soil Moist. Top 121.92 cm	1.000 **			
6 Cor. Den. B&W #58 Green	.328 **	1.000 **		
7 Cor. Den. B&W #25A Red	.746 **	.511 **	1.000 **	
8 Cor. Den. B&W #89B Infrared	-.058	.311 **	.262 **	1.000 **
9 Cor. Den. Color IR Neutral	.218 **	.025	.025	-.243 -**
10 Cor. Den. Color IR Green	.363 **	.289 **	.254 **	-.207 -**
11 Cor. Den. Color IR Red	.654 **	.201 **	.678 **	-.068
12 Cor. Den. Color IR Infrared	-.043	-.088	-.029	.468 **

TABLE 5.3. Continued.

	9 Corrected Density Color IR Neutral	10 Corrected Density Color IR Green	11 Corrected Density Color IR Red	12 Corrected Density Color IR Infrared
1 Gr. Soil Moist. Top 30.48 cm				
2 Soil Moist. Top 30.48 cm				
3 Soil Moist. Top 60.96 cm				
4 Soil Moist. Top 91.44 cm				
5 Soil Moist. Top 121.92 cm				
6 Cor. Den. B&W #58 Green				
7 Cor. Den. B&W #25A Red				
8 Cor. Den. B&W #89B Infrared				
9 Cor. Den. Color IR Neutral	1.000 **			
10 Cor. Den. Color IR Green	.857 **	1.000 **		
11 Cor. Den. Color IR Red	.645 **	.643 **	1.000 **	
12 Cor. Den. Color IR Infrared	.515 **	.282 **	.445 **	1.000 **

* Significant at .05 level (> .140).

** Significant at .01 level (> .184).

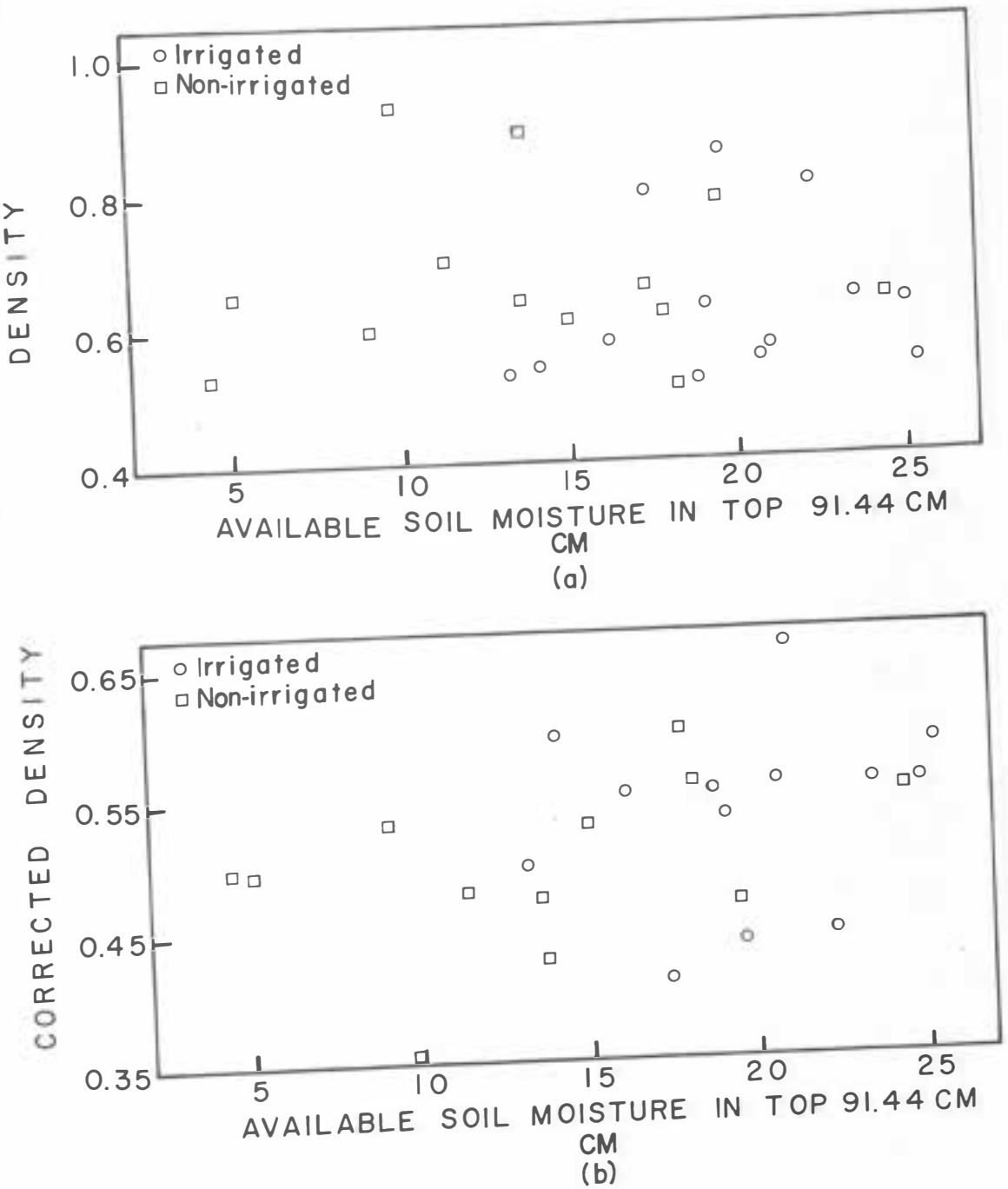

Figure 5.19 - Available soil moisture in 91.44 cm profile in the sorhum versus the green filtered black and white film for (a) film density, and (b) corrected film density.

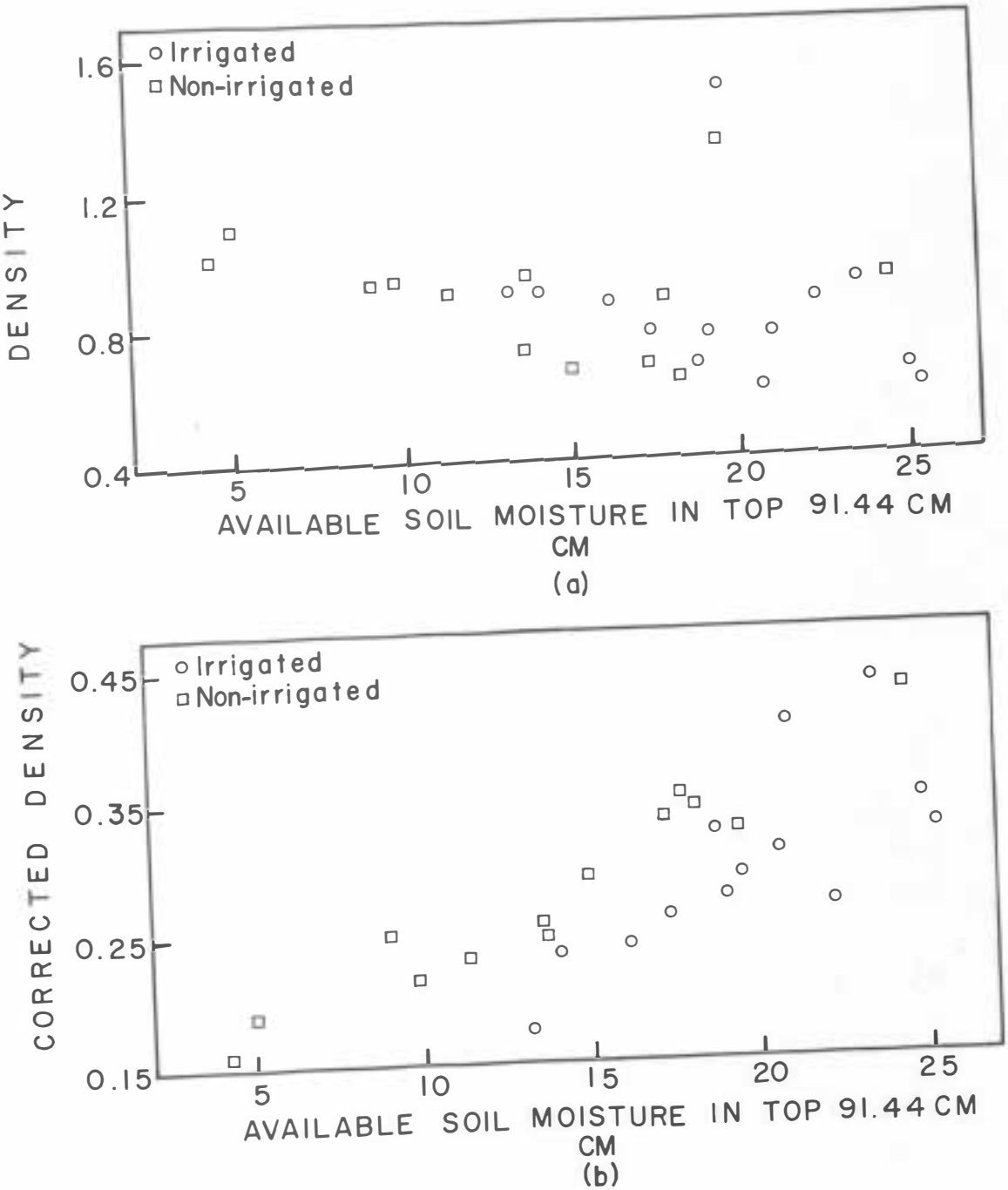

Figure 5.20 - Available soil moisture in 91.44 cm profile in the sorghum versus the red filtered black and white film for (a) film density, and (b) corrected film density.

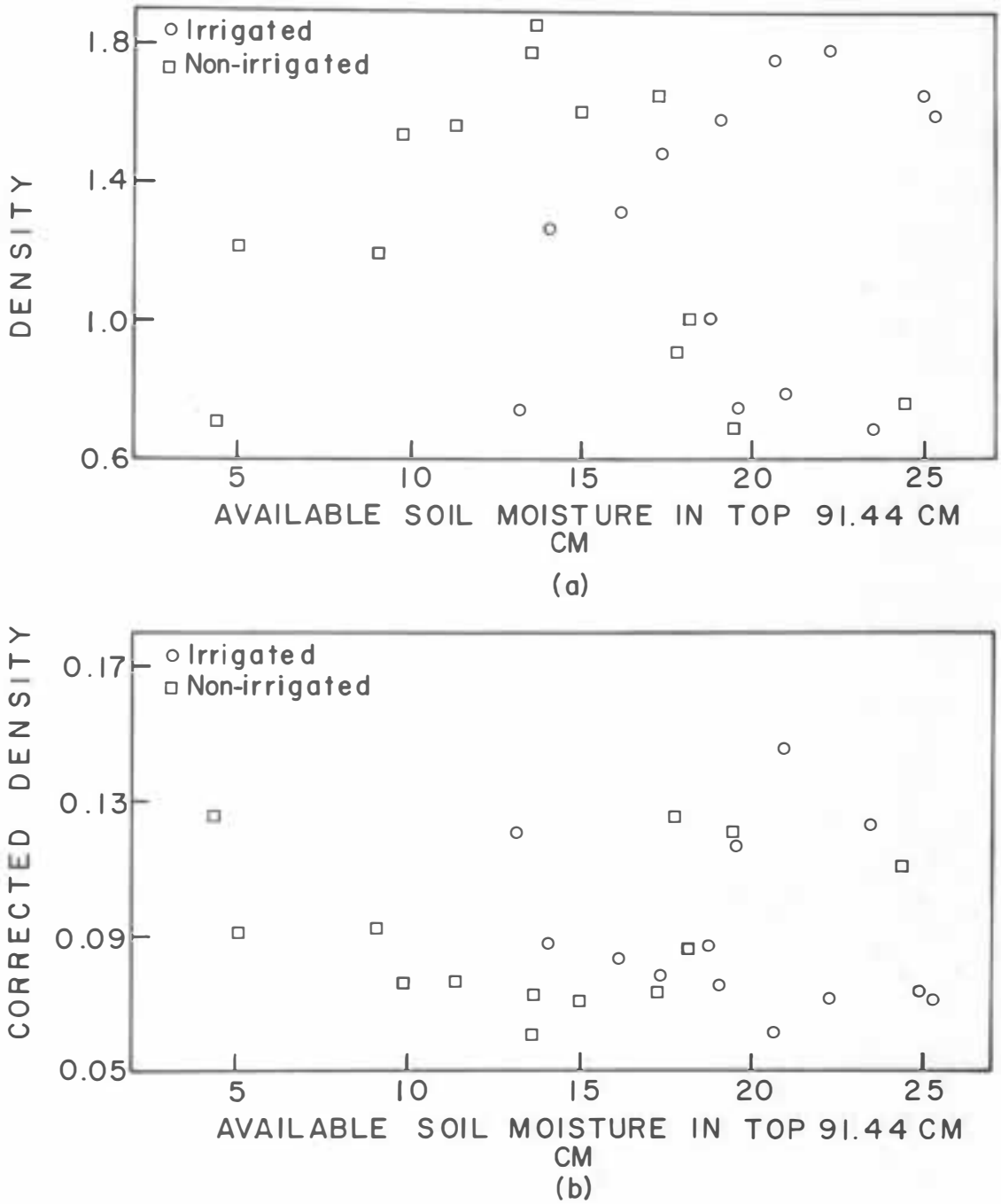

Figure 5.21 - Available soil moisture in 91.44 cm profile in the sorghum versus the infrared filtered black and white film for (a) film density, and (b) corrected film density.

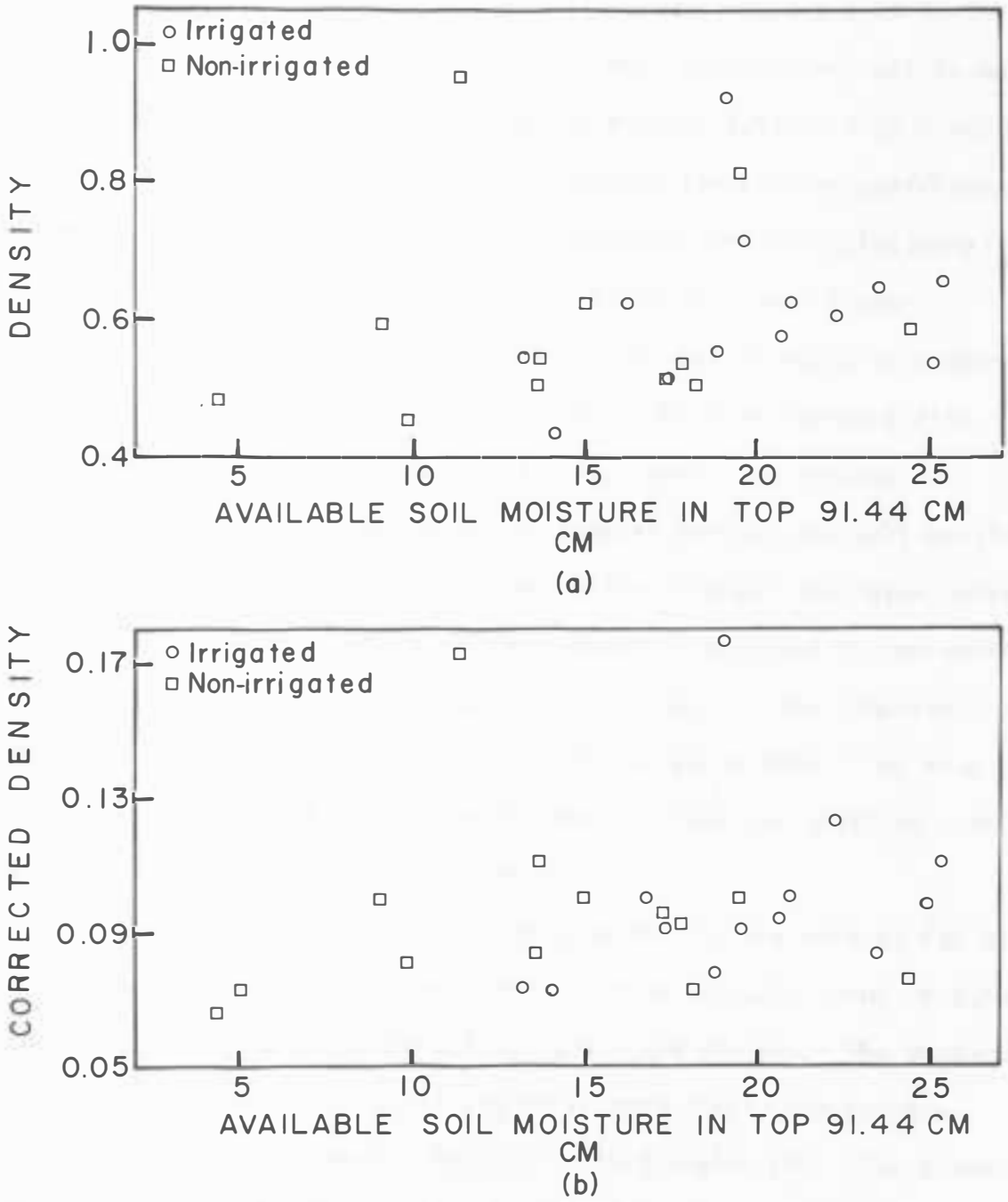

Figure 5.22 - Available soil moisture in 91.44 cm profile in the sorghum versus the color infrared film for neutral (a) film density, and (b) corrected film density.

green filtered film, 5.20 is the black and white red filtered film, 5.21 is the black and white infrared filtered film, and 5.22 is the neutral filtered color infrared film. The linearity that exists between soil moisture and film density shown on Figures 5.19 to 5.22 is closely associated to the value of the corresponding correlation coefficients from Tables 5.2 and 5.3. Correlation measures how variables vary together; therefore, high correlations indicate a good linear relationship between variables. The poorest relationship is between the available soil moisture and the black and white infrared film densities as plotted in Figure 5.21. The correction process definitely improves the relationship between density and soil moisture. For both the green filtered black and white film and the color infrared film, nearly the same degree of improvement is obtained by correcting the densities. The striking improvement is seen in the comparison of the two plots for the red filtered black and white film. The reverse in slope is caused by correcting the density from the negative type film into a positive corrected density.

In terms of spectral bands, the same results are evident for the corrected and noncorrected densities. The red spectral band produced the best correlation between soil moisture and density. The pigment absorption in the red spectral region is most likely the primary cause for the better overall results in that region (9). The pigment responds quicker to changes in plant condition than the cell structure responds to the same changes. Cell structure variation is caused by severe stress and is closely related to changes in near infrared

reflectance. This may explain why the near infrared reflectance did not relate differences between soil moisture treatments.

As shown previously, the soil moisture treatments did not cause moisture stress in the sorghum during the growing season. The yields were 8,432 kilograms per hectare (7,375 pounds per acre) for the irrigated sorghum and 6,592 kilograms per hectare (5,766 pounds per acre) for the non-irrigated sorghum. This is only 21.8 percent difference. The yield of 6,592 kilograms per hectare (103 bushels per acre) for dryland sorghum was very high for a semiarid region.

Chapter VI

SUMMARY AND CONCLUSIONS

A total of 16 ground truth missions were conducted for the remote sensing-soil moisture research in 1970. Soil moisture and crop-soil-weather conditions were collected on each of these missions. Thirteen aerial missions were flown concurrent with 13 of the ground truth missions. The missions were conducted approximately once per week throughout the growing season from June 17 to October 5, 1970. The grain sorghum ranged from seedling stage to complete maturity.

Three methods of data analysis, visual, laboratory, and statistical, were used in this study. The visual analysis primarily involved photographic interpretation. Spot film densitometers and a color encoding density analysis system were used in the laboratory analysis. The statistical analysis was performed on the film density and soil moisture data. In addition, corrected film densities were obtained and statistically analyzed.

The three methods of imagery analysis support the conclusion that soil moisture can best be detected by the visible red portion of the spectrum if grain sorghum is used as the indicator plant. The red band is within one region of plant pigment absorption by chlorophyll. The green spectral band also gave good results during the time of active plant growth. The near infrared region of the spectrum furnished little information about the soil moisture status and plant condition. Near infrared reflectance by plants is dependent upon the total physiological condition of the plant which is the result of many

factors including soil moisture, salinity, diseases and leaf geometry (16). The crop canopy infrared reflectance does relate the overall crop vigor and growth. However, it does not appear to relate, for sorghum, a change in reflectance that can be correlated to available soil moisture. The significant correlations obtained with the color infrared film (#8443) did not appear to be the result of the reflected infrared layer in the film, but rather seemed to be the result of the layers sensitive to the green and red spectral bands.

A film density correction process was developed to account for variations in incoming radiation and crop cover. Comparison of the correlations between densities and corrected densities illustrated that the corrected densities were considerably better for monitoring soil moisture. The corrected density correlations from the red spectral band were, in most cases, more than double the uncorrected densities.

The soil moisture in the sorghum was never low enough to seriously stress either the irrigated or non-irrigated sorghum. An accumulation of residual moisture in the lower portion of the root zone in the non-irrigated sorghum may have been the result of irrigation applications in previous years. Also, the rainfall during the season was received during critical periods in the growing season and provided good moisture conditions for dryland sorghum production. Therefore, differences in the total available soil moisture supplies between the irrigated and non-irrigated sorghum were smaller than normal. Soil moisture differences were substantial in the upper portion of the root

zone profile, but the differences tended to disappear with increasing depth in the profile. The conclusion on soil moisture stress sustained by the sorghum is substantiated by the yield results.

With reference to the objectives set forth at the beginning of this research, the conclusion can be made that remote sensing is feasible for soil moisture monitoring. The remote sensing data were able to reliably detect differences between soil moisture treatments in grain sorghum. Evaluation of plant stress conditions related to soil moisture should be possible by remote sensing. In this study, the visible red portion of the electromagnetic spectrum provided the best information about soil moisture conditions in grain sorghum.

Recommendations for Further Studies

The remote sensing soil moisture research has produced satisfactory preliminary results, but the project should be continued at least one more year. If possible, a sorghum field with the same treatment plots should be maintained at the same location. Another year of study may give larger soil moisture differences between the irrigated and non-irrigated treatments. The procedure of having concurrent ground truth and aerial missions should also be continued. The frequency of the flights in the 1970 study seemed sufficient for proper monitoring of the soil moisture status.

Future soil moisture research should include thermal infrared data collection. Application of equation 3.10 to analysis of the thermal data that is collected would contribute to the complete

analysis of the energy balance (equation 3.1). The limited thermal data that was collected in this effort indicates that the addition of thermal radiation data to supplement the reflected radiation data may provide improved results.

Procurement of certain additional data collection equipment and revision of the use of some equipment in operation may produce improved results. Many variables assumed constant or negligible should be measured. Either a spectrometer or a spectrophotometer is needed to determine spectral responses of given surfaces and materials. For soil moisture research, spectral studies should be conducted at various stages of plant maturity and soil surface condition. Filtered solameters should be placed on the upper surface of the aircraft or on the ground at the test site to supplement the solameter which measures total incoming shortwave radiation. These solameters should be filtered in the same bands as the multispectral photography. The filtered solameter reading divided by the total solameter reading would give the radiation correction term, R_{Sband}, for equation 3.8 and would also provide an inflight measurement of relative spectral radiance. Future remote sensing research of plants and crops should include measurements in the blue spectral band. The high pigment absorption by chlorophyll within this band might prove equally as useful as the red spectral band.

In future soil moisture research, flight missions should include higher altitudes. The higher altitude missions would help to provide a transition between space application and low altitude application.

At least two diurnal data collection missions should be flown to investigate whether the variation of sun angle and radiant intensity affects a remote sensing analysis of soil moisture. Flights should be at midmorning, noon, and late afternoon, on the same day. Another helpful expansion might be to add to the study another sorghum field near the same location. The field needs to have the same soil characteristics, but should not be irrigated. The additional field would provide essentially another soil moisture treatment. Expansion to an enlarged and more diversified area would provide additional insight for making recommendations on an operational system to be used by resource management agencies.

LIST OF REFERENCES

REFERENCES

1. "Climatological Summary", Station Summaries No. 1, No. 2, and No. 5, Climatography of the U. S. No. 20-39, U. S. Weather Bureau, U. S. Department of Commerce, Environmental Science Services Administration, South Dakota State University Agricultural Experiment Station, Brookings, South Dakota.

2. Colwell, Robert N., "Applications of Remote Sensing in Agriculture and Forestry", Chapter 4, Remote Sensing, National Academy of Sciences, Washington, D. C., 164-223, 1970.

3. "Decennial Census of United States Climate -- Monthly Normals of Temperature, Precipitation, and Heating Degree Days", South Dakota, Climatography of the United States No. 81-34, U. S. Weather Bureau, U. S. Department of Commerce, U. S. Government Printing Office, Washington, D. C., 1962.

4. Electromagnetic Spectrum, Chart MB-1937, Westinghouse Electric Corporation, Printing Division, Trafford, Pennsylvania, 1961.

5. Encyclopedia Britannica, Encyclopedia Britannica, Inc., William Benton, Publisher, Chicago, Illinois, Vol. 4, 17, 1968.

6. Gardner, W. R., "Soil-Water Relations in Arid and Semi-Arid Conditions", UNESCO: Reviews of Research.

7. Gates, David M., "Characteristics of Soil and Vegetated Surfaces to Reflected and Emitted Radiation", Proceedings of the Third Symposium on Remote Sensing of Environment, University of Michigan, Ann Arbor, Michigan, 573-600, 1966.

8. Gates, David M., "Physical and Physiological Properties of Plants", Chapter 5, Remote Sensing, National Academy of Sciences, Washington, D. C., 224-252, 1970.

9. Gates, David M., Keegan, Harry J., Schleter, John C., and Weidner, Victor R., "Spectral Properties of Plants", Applied Optics, Vol. 4, No. 1, 11-20, January 1965.

10. Hagan, Robert M., Haise, Howard R., and Edminster, Talcott W., Eds., Irrigation of Agricultural Lands, Agronomy Monograph No. 11, American Society of Agronomy, Madison, Wisconsin, 1967.

11. Halliday, David, and Resnick, Robert, Physics, Part II, John Wilen & Sons, Inc., New York, N. Y., 993, 1962.

12. Heller, Robert C., "Imaging with Photographic Sensors", Chapter 2, Remote Sensing, National Academy of Sciences, Washington, D. C., 35-72, 1970.

13. Hoffer, R. M., and Johannsen, C. J., "Ecological Potentials in Spectral Signature Analysis", Chapter 1, Remote Sensing in Ecology, University of Georgia Press, Athens, Georgia, 1-16, 1969.

14. Holter, Marvin R., "Imaging with Nonphotographic Sensors", Chapter 3, Remote Sensing, National Academy of Sciences, Washington, D. C., 73-163, 1970.

15. Hornbeck, George A., "Optical Methods of Temperature Measurements", Applied Optics, Vol. 5, No. 2, 179-186, 1966.

16. Knipling, Edward B., "Leaf Reflectance and Image Formation on Color Infrared Film", Chapter 2, Remote Sensing in Ecology, University of Georgia Press, Athens, Georgia, 17-29, 1969.

17. Luney, Percy R., and Dill, Henry W. Jr., "Uses, Potentialities, and Needs in Agriculture and Forestry", Chapter I, Remote Sensing, National Academy of Sciences, Washington, D. C., 1-34, 1970.

18. Morgan, Joseph, "Infrared Technology", Proceedings of the First Symposium on Remote Sensing of Environment, the University of Michigan, Ann Arbor, Michigan, 61-80, 1962.

19. Myers, Victor I., "Soil, Water and Plant Relations", Chapter 6, Remote Sensing, National Academy of Sciences, Washington, D. C., 253-297, 1970.

20. Myers, V. I., Wiegand, C. L., Heilman, M. D., and Thomas, J. R., "Remote Sensing in Soil and Water Conservation Research", Proceedings of the Fourth Symposium on Remote Sensing of Environment, University of Michigan, Ann Arbor, Michigan, 801-813, 1966.

21. Myers, Victor I., and Allen, William A., "Electroptical Remote Sensing Methods as Nondestructive Testing and Measuring Techniques in Agriculture", Applied Optics, Vol. 7, No. 9, 1819-1838, September 1968.

22. Parker, Dana, "Some Basic Considerations Related to the Problem of Remote Sensing", Proceedings of the First Symposium on Remote Sensing of Environment, University of Michigan, Ann Arbor, Michigan, 7-23, 1962.

23. Rose, C. W., Agricultural Physics, Pergamon Press, Long Island City, N. Y., 1-25, 1966.

24. Slatyer, R. O., "Absorption of Water by Plants", Botanical Review, Vol. 25, 331-392, 1960.

25. Steel, Robert G. D., and Torrie, James H., Principles and Procedures of Statistics, McGraw-Hill Book Company, Inc., New York, N. Y., 183-193, 453, 1960.

26. Sutton, O. G., Micrometeorology, McGraw-Hill Book Company, Inc., New York, N. Y., 1-25, 1966.

27. Van Lopik, J. R., Rambie, G. S., and Pressman, A. E., "Pollution Surveillance by Noncontact Infrared Techniques", Journal-Water Pollution Control Federation, Vol. 40, No. 3, Part 1, 425-438, March 1968.

28. Water Resources Council, "The Nation's Water Resources", U. S. Government Printing Office, Washington, D. C., 1968.

29. Wiegand, C. L., Heilman, M. D., and Gerbermann, A. H., "Detailed Soil and Plant Thermal Regime in Agronomy", Proceedings of the Fifth Symposium on Remote Sensing of Environment, University of Michigan, Ann Arbor, Michigan, 325-334, 1968.

30. Wisler, C. O., and Brater, E. F., Hydrology, John Wiley & Sons, Inc., New York, N. Y., 37, 1967.

31. Wolfe, William L., Ed., Handbook of Military Infrared Technology, Office of Naval Research, Department of the Navy, Washington, D. C., 7-10, 878, 1965.

APPENDICES

APPENDIX A

GLOSSARY

Absolute Temperature - the temperature in degrees above absolute zero.

Absorptance - fraction of the incoming radiation that is absorbed by the body.

Albedo - fractional reflectance of shortwave radiation.

Atmospheric Attenuation - absorption and scattering of the electromagnetic radiation by molecules and particles within the air.

Available Soil Moisture - the water in the soil that is available for consumptive use by the plants.

Band-pass Filter - a filter which permits a sensing device to detect electromagnetic radiation from only one band or portion of the spectrum.

Blackbody - a body which absorbs and emits all radiation falling upon it.

Convection - movement or transfer of air by turbulence or overturning due to temperature differences.

Correlation coefficient - statistical value relating how two variables vary together.

Diurnal - cycling within one given day.

Electromagnetic Spectrum - the composite of all types of radiant energy where the wavelength and frequency are inverse functions. The electromagnetic spectrum varies from the short gamma rays to long waves used for power and telephone transmission.

Emissive Power or Emissivity - the ratio of the emitted radiation of the body to the emitted radiation of a blackbody emitter.

Evapotranspiration - the combined process of evaporation from the soil and transpiration from the plant. Evapotranspiration relates the water used by the soil-plant system.

Film Density - the value given to the relative thickness or density of a film base after exposure. Density is equal to the common logarithm of the inverse of transmittance of the film and relates the amount of exposure. Low densities are light areas on the film and high densities are dark areas.

Gravimetric Soil Moisture - soil moisture expressed on a weight basis or weight of water per unit weight of dry soil.

Ground Truth - data collected from a ground or terrestrial location which is used to identify and interpret the features and phenomena that are recorded by remote sensing detectors.

Latent Energy - the heat that is exchanged in the evaporation or transpiration processes.

Longwave Radiation - generally considered to be terrestrial radiation or radiation from the earth's surface. Longwave radiation is between 3μm and 80μm.

Photosynthesis - the formation of carbohydrates in plants from water and carbon dioxide, by the action of sunlight on chlorophyll.

Radiant Flux - the flow of radiant energy passing a point at a given time.

Reflectance - the fraction or ratio of the amount of energy reflected from a surface to the total incoming radiation at the surface.

Remote Sensing - the detection of an existing condition or conditions from a distance or remote location.

Semiarid - geographical areas characterized by light rainfall, specifically, between 25 cm and 50 cm.

Sensible Energy - heat exchanged by conduction or convection to the surroundings.

Shortwave Radiation - considered to be solar radiation and is contained between 0.15μm and 4μm.

Thermal Radiation - heat radiation that is usually considered to be emitted or longwave radiation from the earth.

Transmittance - the fraction or ratio of the amount of energy transmitted through a layer or surface to the total incoming radiation at the surface.

Transpiration - the evaporation of water from the cells of a plant surface.

Volumetric Soil Moisture - soil moisture expressed on a volume basis or volume of water per unit volume of dry soil.

Wavelength - the distance, measured in the direction of progression of a wave, from any point to the next point characterized by the same wave.

APPENDIX B

SYMBOLS AND ABBREVIATIONS

A	angstroms (10^{-10} m)
agl	above ground level
BD_S	bulk density of the soil (grams per cubic centimeter)
BD_W	density of water (grams per cubic centimeter)
C	neutron counts
cal	calories
^oC	degrees centigrade
C_1	constant in Plank's Radiation Formula
C_2	constant in Plank's Radiation Formula
cds	central daylight savings time
cps	frequency (cycles per second)
cm	centimeters
$C_{,S}$	neutron standard counts
D	film density
DC	corrected film density
DW	dry weight of soil (grams)
E	energy
E_g	moisture evaporated or transpired at the soil surface (grams)
E_H	sensible energy gain or loss by the surface
E_ℓ	moisture transpired or condensed at the plant surface (grams)
E_S	energy stored by the surface

IR	infrared
f	fraction of exposed soil
F	functional relationship
ft	feet (30.48 cm)
^{o}K	degrees Kelvin (absolute temperature)
L	latent heat of vaporization of water (586 cal $gram^{-1}$)
m	meters
min	minutes
n	number of observations
r	correlation coefficient
R_a	downward longwave radiation from the atmosphere (cal cm^{-2} min^{-1})
RF	fraction of the total incoming shortwave radiation from a spectral band
R_L	net longwave radiation at the surface (cal cm^{-2} min^{-1})
R_{Lout}	outgoing longwave radiation from the surface (cal cm^{-2} min^{-1})
R_e	reflected shortwave radiation (cal cm^{-2} min^{-1})
R_S	total incoming shortwave radiation received by the surface (cal cm^{-2} min^{-1})
R_{Sband}	incoming shortwave radiation within a specific spectral band (cal cm^{-2} min^{-1})
T	absolute temperature (^{o}K)
T_c	absolute temperature of the crop (^{o}K)
T_g	absolute temperature of the soil (^{o}K)
WW	wet weight of the soil (grams)
X	value of the first variable
$\bar{x}$	mean of the first variable

Y	value of the second variable
$\bar{y}$	mean of the second variable
α	absorptance
ε	emissivity
ε_c	emissivity of the crop surface
ε_g	emissivity of the soil surface
λ	wavelength (m, cm or μm)
λ_{max}	wavelength at which radiance is maximum (m, cm or μm)
θ_g	gravimetric soil moisture (% or grams per gram)
θ_v	volumetric soil moisture (% or cm^3 per cm^3)
ρ	reflectance
ρ_c	fraction reflectance of the crop
ρ_g	fraction reflectance of the soil
σ	Stefan-Boltzmann universal constant (8.13×10^{-11} cal cm^{-2} min^{-1} $^oK^{-4}$)
τ	transmittance
μm	micrometers (10^{-6} m)
Σ	algebraic summation of terms
%	percent

APPENDIX C

GROUND TRUTH VARIABLE ANALYSIS

The codes enabled digital recording of these variables so that interpretation was simplified in the analysis. The code is comprised of two-digit numbers. The first digit relates a specific level or condition of the variable. The second digit either specifies another condition of the variable or relates varying levels or degrees of the first digit in the code.

CROP CONDITION

00	No Crop
10	Dead
20	Very Poor
30	Poor
40	Below Average
50	Average
60	Above Average
70	Good
80	Excellent
90	Outstanding

0 → 9 are varying degrees between each division.

PLANT MATURITY

00	No Crop
10	Planted
20	Seedling
30	Small Growth
40	Active Growth
50	Flower Stage
60	Production Development Stage
70	Maturing Production
80	Mature
90	Harvest

0 → 9 are varying degrees between each division.

SURFACE SOIL CONDITION

00 → 99	Moisture Condition
00	Oven Dry
10	Very Dry
20	Dry
30	Damp
40	Slightly Moist
50	Moist
60	Very Moist
70	Slightly Wet
80	Wet (Muddy)
90	Very Wet (Standing Water)

0 → 9	Aggregation
0	Very Fine
1	Fine
2	Medium
3	Coarse
4	Very Coarse
5	Cloddy
6	Large Clods
7	Gravel
8	Rocks
9	Large Rocks

CULTIVATION CONDITION

00 → 70	Method or Type	0 → 9	Condition
00	No Cultivation	0	Weeds and Trash
		↓	
10	Broadcast Seeding	9	Excellent Practice
20	Drill or Disk Plant		
30	Check Plant		
40	Surface Plant		
50	List or Furrow		
60	Minimum Tillage		
70	Fallow Cultivation		

HAZE CONDITION (VISIBILITY)

00	No Haze	0 → 9 are varying degrees between each division.
10	Very Light Haze	
20	Light Haze	
30	Below Average Haze	
40	Moderate Haze	
50	Above Average Haze	
60	Heavy Haze	
70	Very Heavy Haze	
80	Poor Visibility (heavy smoke, dust, moisture)	
90	No Visibility (fog)	

CLOUD CONDITION

00	No Clouds, Clear
10	Light Cirrus
20	Cirrus Overcast
30	Light Stratus
40	Stratus Overcast
50	Nimbostratus (rainy)
60	Light Cumulus
70	Cumulus Overcast
80	Cumulonimbus (thunderhead)
90	Tornado

0 → 9 are varying degrees between each division.

WEATHER CONDITION

00	Clear, Calm
10	Clear, Breeze
20	Clear, Strong Wind
30	Fog
40	Partly Cloudy, Calm
50	Partly Cloudy, Windy
60	Cloudy, Calm
70	Cloudy, Windy
80	Cloudy, Precipitation
90	Stormy and Turbulent

0 → 9 are varying degrees between each division.

APPENDIX D

EQUIPMENT AND INSTRUMENT DESIGNATION

Ground Truth Equipment

Soil moisture
- Soil Test Soil Probe - Model A-1
- Troxler Neutron Probe

Ground truth photography
- Stereo - two 35 mm Nikkormats
  - (1) Color Reversal Infrared Film - #8443
  - (2) High Speed Ektachrome Film

Soil tension - manometer tensiometers

Soil and air temperatures - thermocouples

Humidity - Honeywell Dew Probes

Wind speed and direction - cup anemometer and wind vane

Net radiation - Thornthwaite Miniature Net Radiometer - Model 601

Incoming radiation - Mark I-G Solameter

Evaporation - ESSA Standard Pan

Precipitation - U. S. Weather Bureau Gage

Aerial Equipment

Aircraft - Twin Engine Beechcraft - Model RC45J shown in Figure D.1

Cameras - four 70 mm format Hasselblads - 50 mm focal length
- Black and white film - #8403 - #58 green filter
- Black and white film - #8403 - #25A red filter
- Black and white film - #2424 - #89B infrared filter
- Color Reversal Infrared film - #8443 - Dark yellow filter - #15G + 30 magenta

Incoming radiation - Mark I-G Solameter

Figure D.1 Print of the Remote Sensing Institute aircraft, Twin Beechcraft RC45J.

Outgoing radiation - three filtered Mark I-RF Solameters
#58 green
#25A red
#89B infrared

Thermal infrared scanner - Daedalus
InSb detector - filtered 4.5μm to 5.5μm

Surface temperature - Precision Radiation Thermometer
Barnes PRT-5

Laboratory Equipment

Light table - Richards Model GFL-918X with magnifying stereo viewer

Film density - two MacBeth Model TD-404 Densitometers

Color encoding density analyzer - Spatial Data Datacolor Model 703

The Datacolor system is a useful instrument for interpreting overall density patterns within a field. The transparency is viewed by a black and white television camera, and the electronic signal from the camera is separated with respect to the various density levels of the transparency. The differential density levels are encoded into colors selected by the operator and displayed on the color television monitor. Up to 32 density levels or colors may be used on the instrument at one time. A print of the Model 703 is shown in Figure D.2.

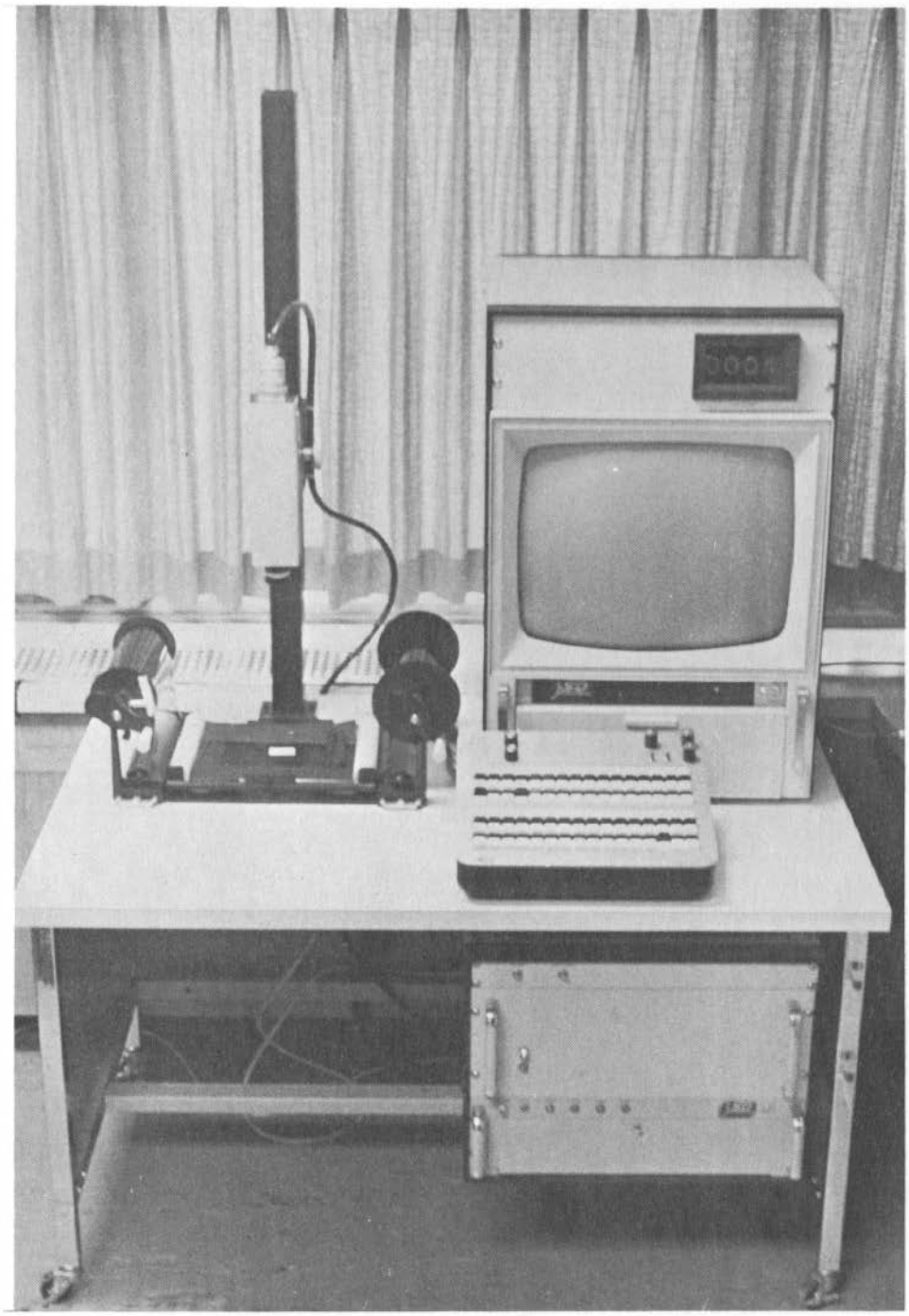

Figure D.2 Print showing the Spatial Data Datacolor Model 703.

APPENDIX E

BLACK AND WHITE AERIAL IMAGERY

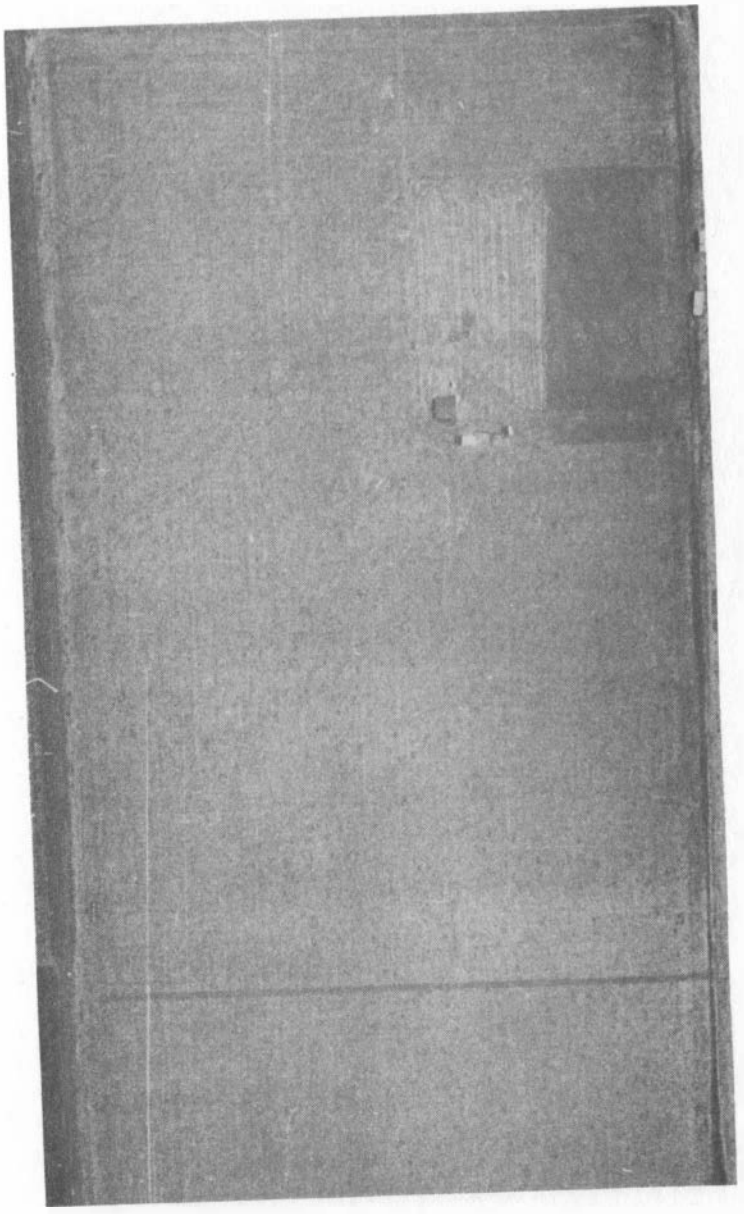

Figure E.1 Print from the green filtered black and white film, #8403 with #58 filter, showing the soil moisture plots for June 25, 1970, 610m (2,000 ft) agl, scale: 1 cm = 16m.

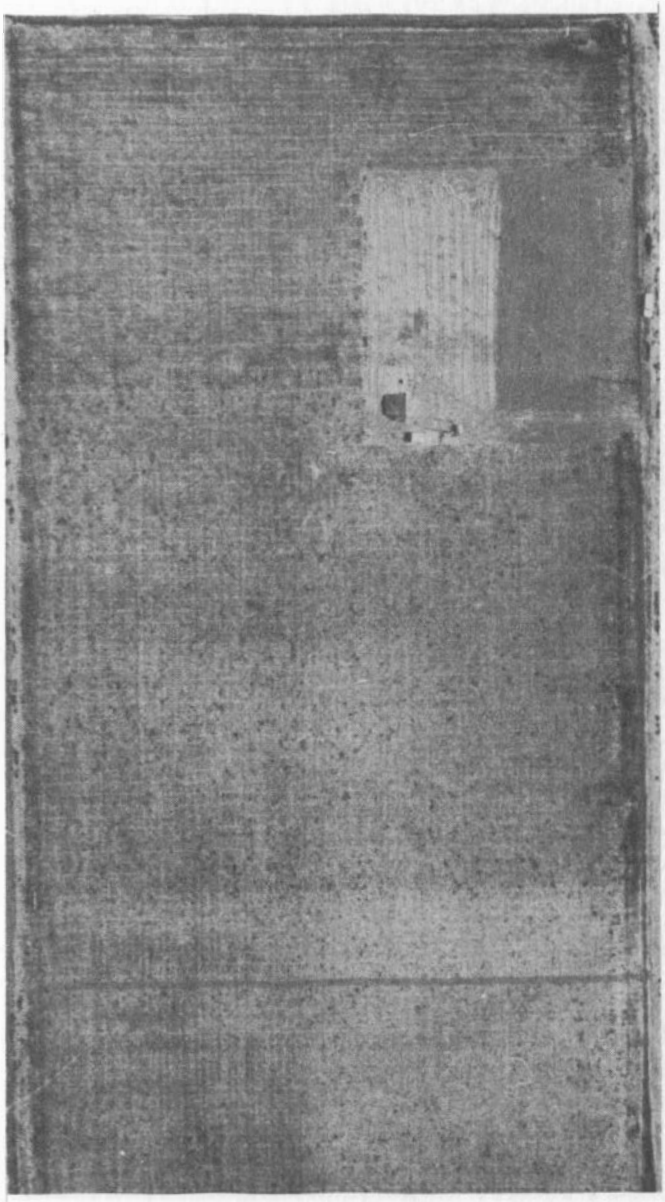

Figure E.2 Print from the red filtered black and white film, #8403 with #25A filter, showing the soil moisture plots for June 25, 1970, 610m (2,000 ft) agl, scale: 1 cm = 16.5m.

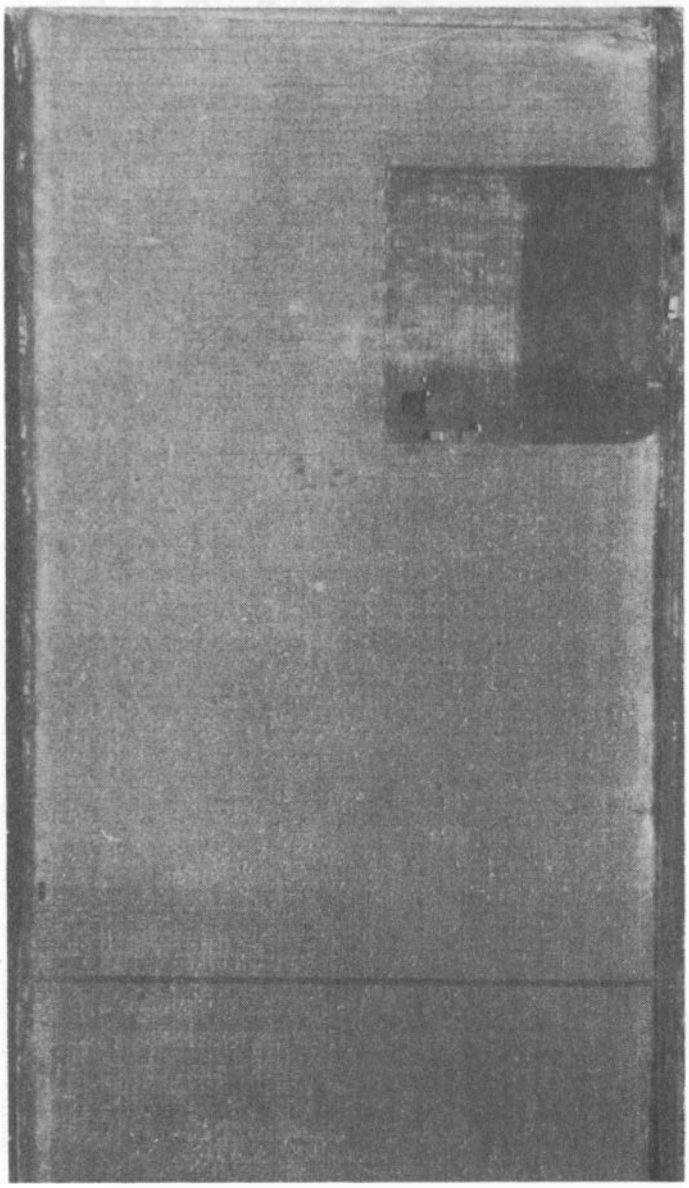

Figure E.3 Print from the infrared filtered black and white film, #2424 with #89B filter, showing the soil moisture plots for June 25, 1970, 610m (2,000 ft) agl, scale: 1 cm = 16.2m.

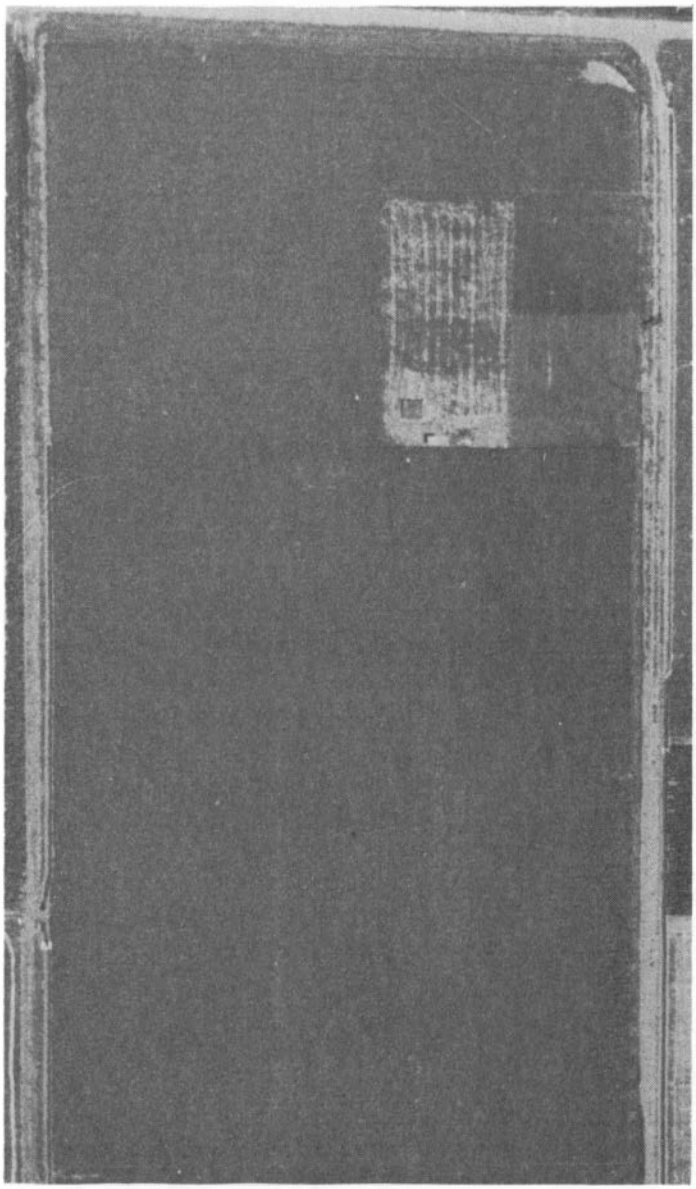

Figure E.4 Print from the green filtered black and white film, #8403 with #58 filter, showing the soil moisture plots for July 30, 1970, 610m (2,000 ft) agl, scale: 1 cm = 17.1m.

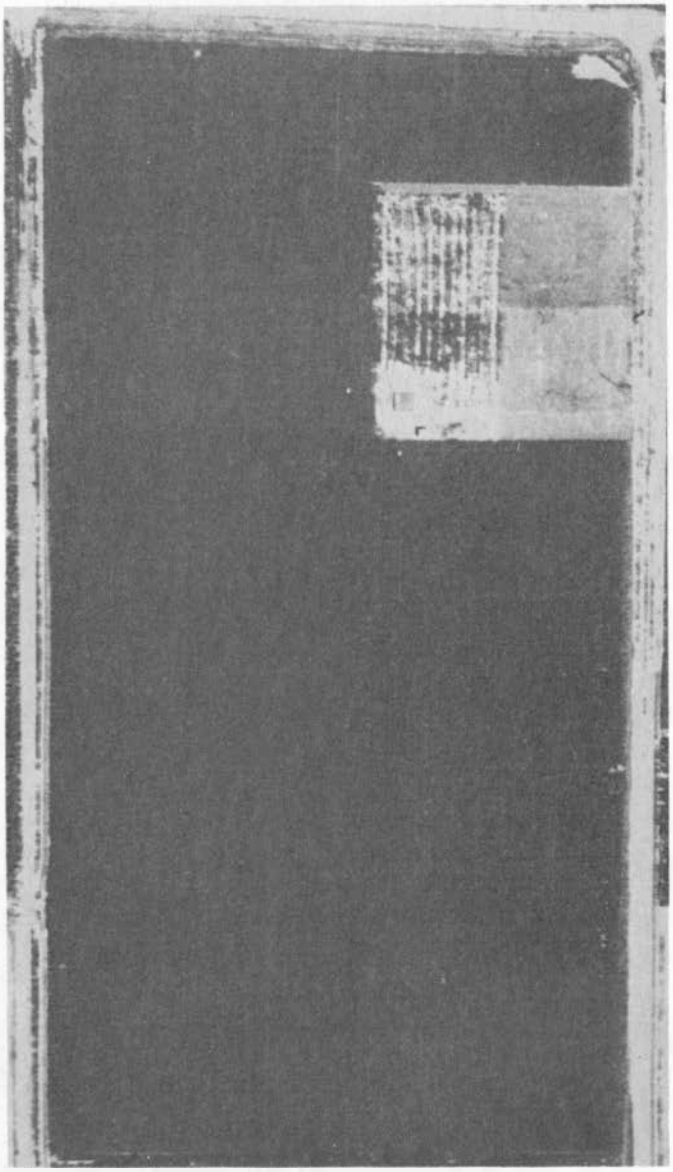

Figure E.5 Print from the red filtered black and white film, #8403 with #25A filter, showing the soil moisture plots for July 30, 1970, 610m (2,000 ft) agl, scale: 1 cm = 17.3m.

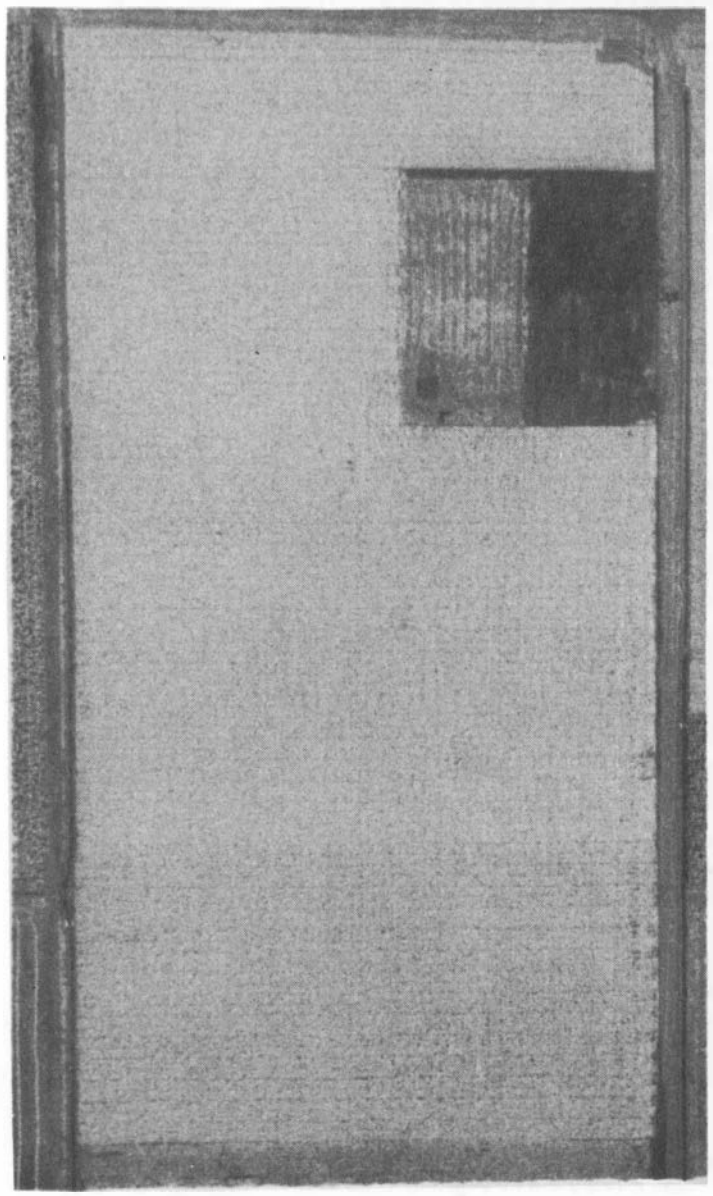

Figure E.6 Print from the infrared filtered black and white film, #2424 with #89B filter, showing the soil moisture plots for July 30, 1970, 610m (2,000 ft) agl, scale: 1 cm = 17.3m.

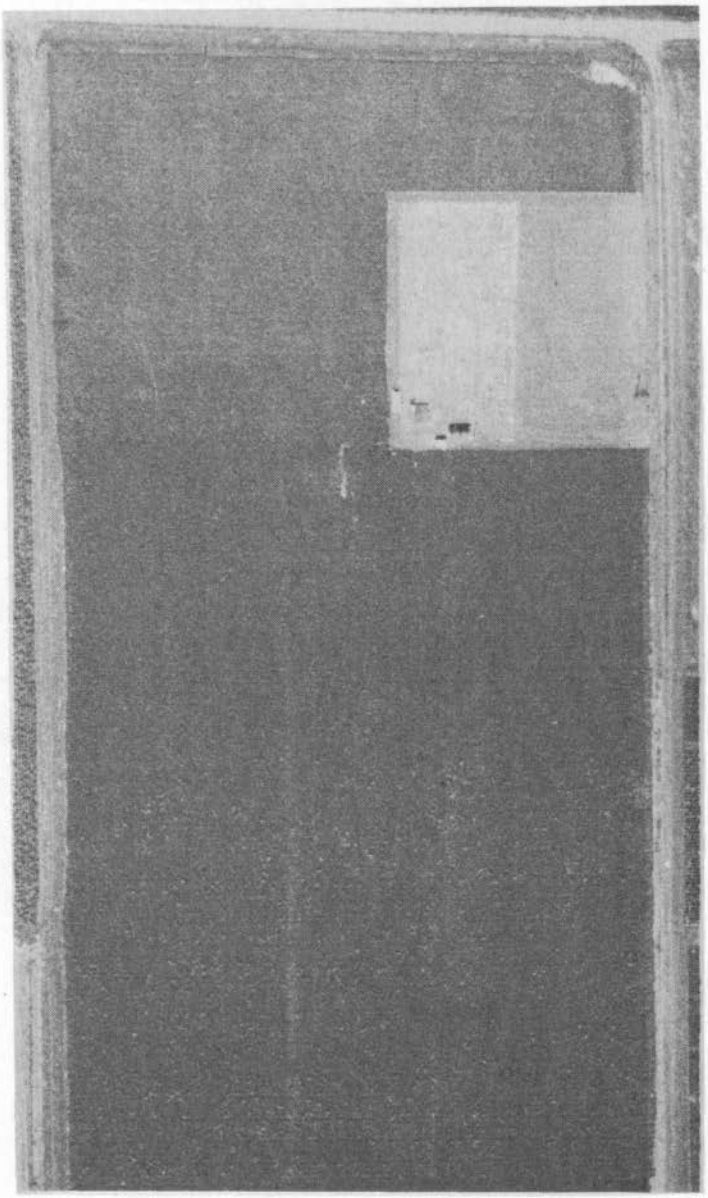

Figure E.7 Print from the green filtered black and white film, #8403 with #58 filter, showing the soil moisture plots for August 25, 1970, 610m (2,000 ft) agl, scale: 1 cm = 17.3m.

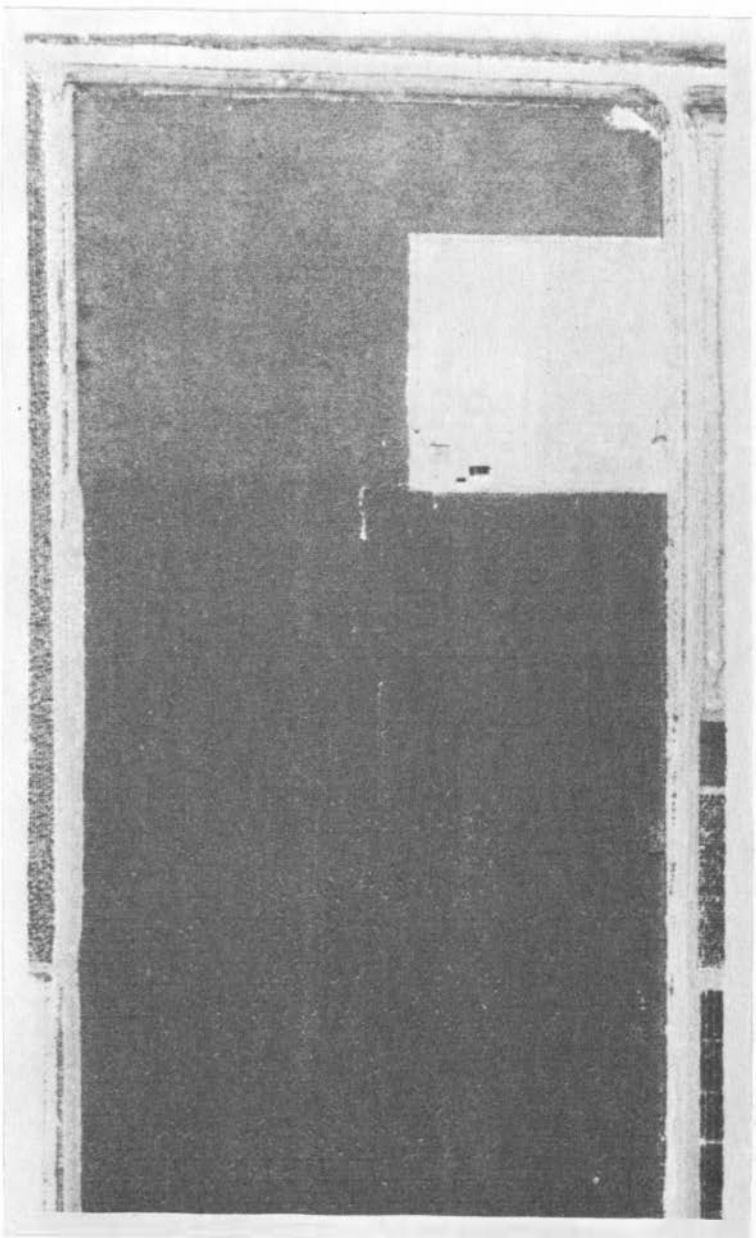

Figure E.8 Print from the red filtered black and white film, #8403 with #25A filter, showing the soil moisture plots for August 25, 1970, 610m (2,000 ft) agl, scale: 1 cm = 17.3m.

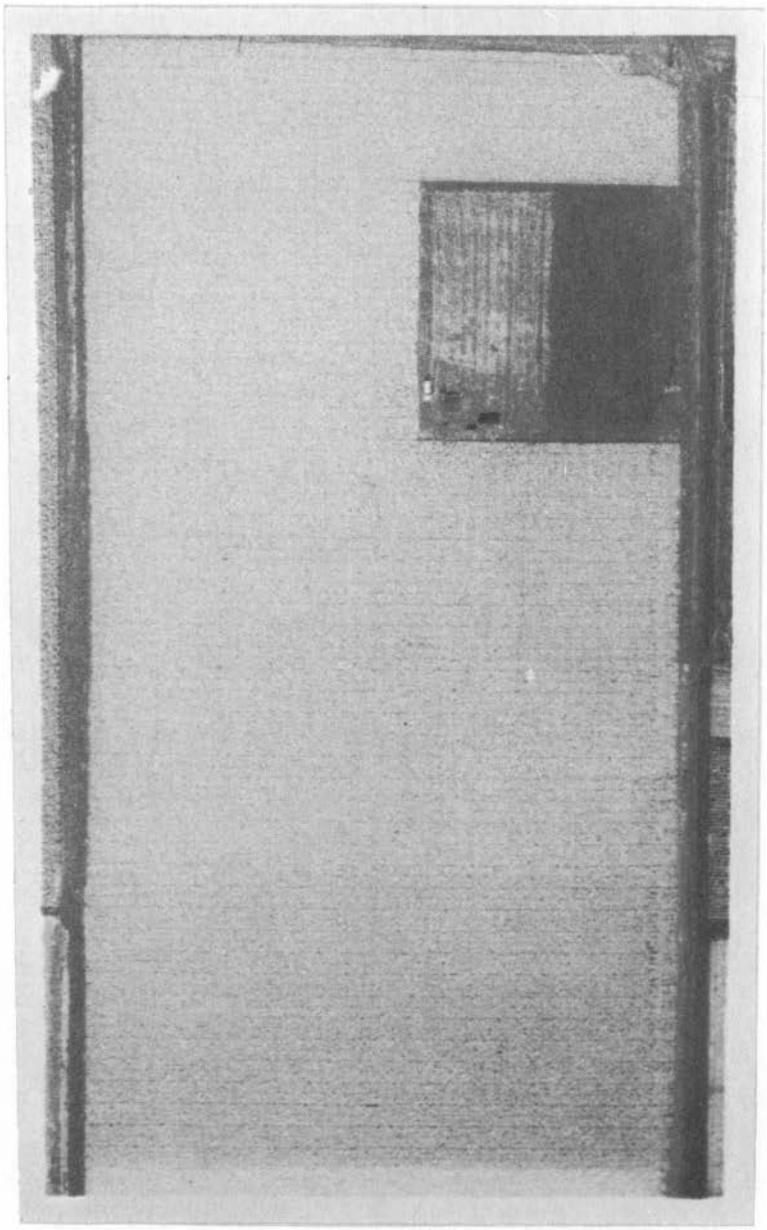

Figure E.9 Print from the infrared black and white film, #2424 with #89B filter, showing the soil moisture plots for August 25, 1970, 610m (2,000 ft) agl, scale: 1 cm = 17.1m.

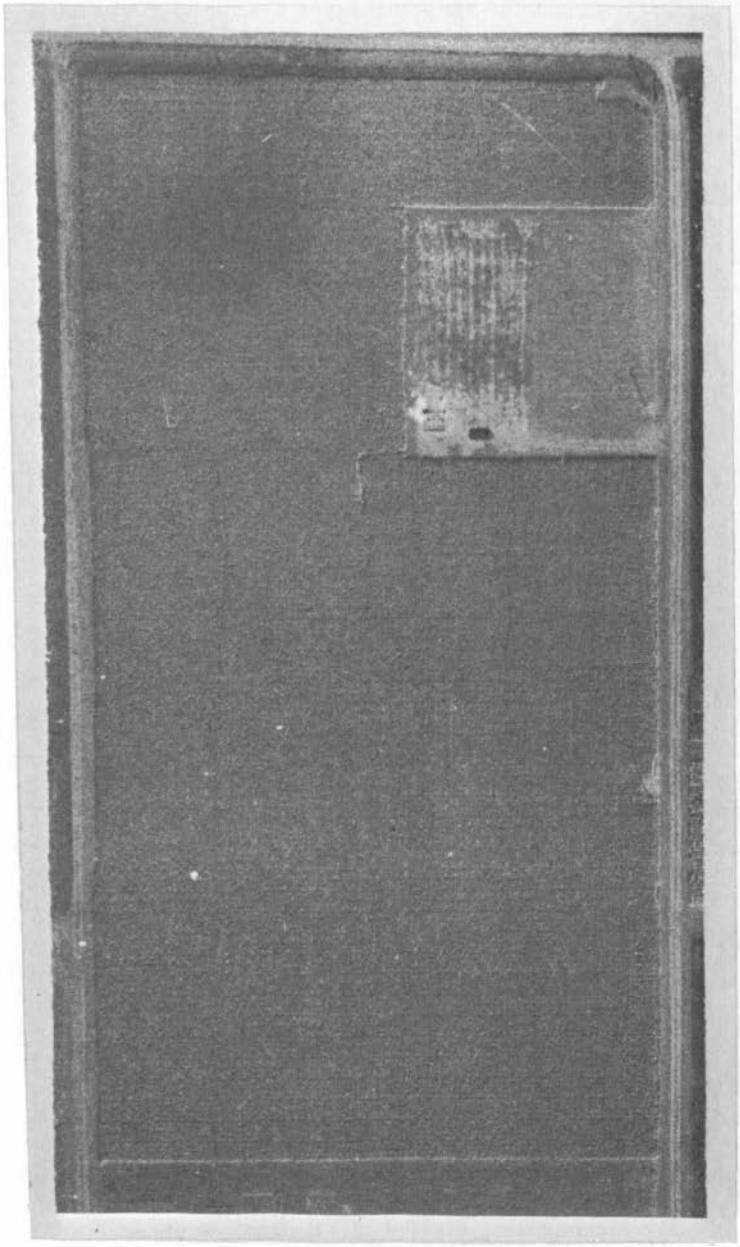

Figure E.10 Print from the green filtered black and white film, #8403 with #58 filter, showing the soil moisture plots for October 5, 1970, 610m (2,000 ft) agl, scale: 1 cm = 17.8m.

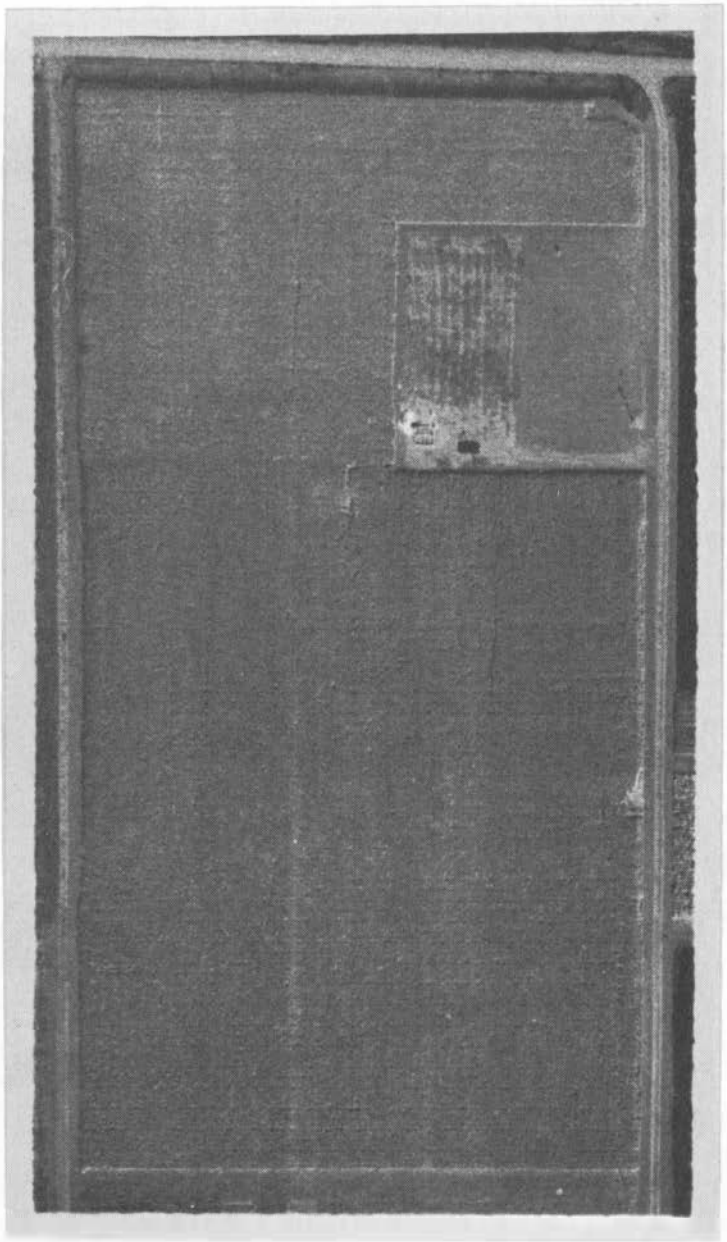

Figure E.11 Print from the red filtered black and white film, #8403 with #25A filter, showing the soil moisture plots for October 5, 1970, 610m (2,000 ft) agl, scale: 1 cm = 18.0m.

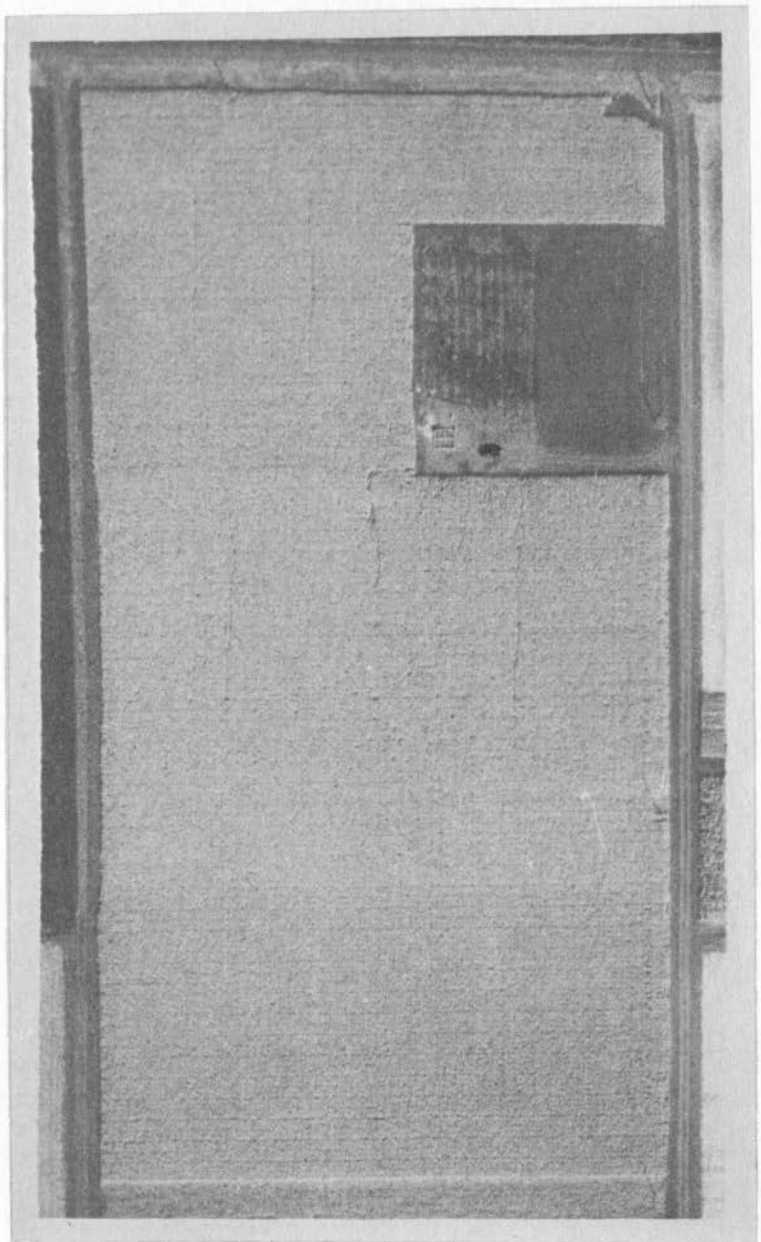

Figure E.12 Print from the infrared black and white film, #2424 with #89B filter, showing the soil moisture plots for October 5, 1970, 610m (2,000 ft) agl, scale: 1 cm = 17.6m.